ABSTRACT

DIXON, JENNIFER LOUISE. Seasonal Changes in Estuarine Dissolved Organic Matter due to Variable Flushing Time and Wind-Driven Mixing Events. (Under the direction of Dr. Christopher Osburn.)

Estuaries are highly productive habitats that transport and transform organic matter (OM), experience large changes in ionic composition and act as a transition zone between terrestrial and marine environments (Paerl et al. 1998; Markager et al. 2011; Osburn et al. 2012). OM source and matrix effects (such as salinity and pH) influence the chemical structure of DOM in estuaries and therefore affect its bioavailability, photo-reactivity, and its overall fate in these systems (Jaffé et al. 2004; Boyd et al. 2010; Pace et al. 2012; Osburn et al. 2012; Cawley et al. 2013). Within estuaries, dissolved organic matter (DOM) is a heterogeneous mixture of aromatic and aliphatic compounds, and its composition in aquatic systems varies spatially and temporally with source (Bauer and Bianchi 2011). However, the main source of DOM in estuaries, rivers and other aquatic systems, originates from vascular plant detritus, soil humus, older fossil (i.e., petrogenic) organic carbon, black carbon, marine OM and in situ production (Hedges 2002; Houghton 2007; Bauer and Bianchi 2011).

Chromophoric dissolved organic matter (CDOM), the light absorbing fraction of DOM, can be characterized using optical methods such as absorption and fluorescence spectroscopy (e.g. Coble, 1996; Stedmon and Markager, 2003). By analyzing the spatial and temporal variability of DOM and CDOM within estuaries, information pertaining to OM source and fate across the freshwater-marine continuum can be obtained. These methods offer an inexpensive, non-destructive means for obtaining sensitive measurements of a diverse group of organic compounds. By using this technology to analyze the spatial and temporal variability of CDOM within estuaries, information pertaining to OM source and

fate across the freshwater-marine continuum can be obtained (Fellman et al. 2011; Osburn et al. 2012; Murphy et al. 2014).

Chemical biomarkers are also routinely used to identify DOM sources in coastal waters. Examples are carbon stable isotopes (Bauer, 2002) and lignin (e.g., Benner and Opsahl, 2001; Harvey and Mannino, 2001). Marine DOM derived from phytoplankton typically has carbon stable isotope ($\delta^{13}C$) values that range from −20 to −22‰, while terrestrial DOM derived from C3 land plants typically have $\delta^{13}C$ values that range from −26 to −28‰ (Bauer, 2002). Lignin is an important component of vascular plants, thus making it a unique geochemical biomarker, which can be used to trace the fate of terrestrial DOM in coastal seawater (e.g., Hernes and Benner, 2003; Walker et al. 2009; Osburn and Stedmon, 2011). Further, the ratios of the different phenolic compounds derived from the oxidation of lignin can be used to distinguish between plant sources (e.g. angiosperm vs. gymnosperm, or woody vs. non-woody tissue) and the extent of exposure to degradation (Hedges et al. 1988).

The highly productive, eutrophic waters of the Neuse River Estuary (NRE), in eastern North Carolina, USA, serve as a transition zone for terrigenous DOM between the head of the Neuse River and Pamlico Sound. Previous studies have determined that the NRE is dominated by inputs from riverine discharge, yet very clear shifts in DOM quality are apparent as discharge varied (Paerl et al. 1998; Osburn et al. 2012). Furthermore, flushing times within the NRE will aid in determining whether DOM is primarily autochthonous or allochthonous and if it is processed internally or transported downstream to the Pamlico Sound (Paerl et al. 1998; Mari et al. 2007, Peierls et al. 2012). Therefore, the main sources of DOM and its composition can change throughout an estuary depending on the hydrodynamic conditions. For example, increases in flushing time may allow for the accumulation of

autochthonous DOM because of (1) planktonic communities within the water column having more time to utilize nutrients within the system, resulting in phytoplankton blooms and (2) lower inputs of allochthonous OM from the NRE's watershed (Dixon et al. accepted). Therefore, the main sources of DOM and its composition can change throughout an estuary depending on the hydrodynamic conditions.

Seasonal Changes in Estuarine Dissolved Organic Matter Due to Variations in Discharge, Flushing Times and Wind-driven Mixing Events

by
Jennifer Louise Dixon

A dissertation submitted to the Graduate Faculty of
North Carolina State University
in partial fulfillment of the
requirements for the Degree of
Doctor of Philosophy

Marine, Earth and Atmospheric Sciences

Raleigh, North Carolina

2014

APPROVED BY:

_____	_____
Dr. Christopher L. Osburn Committee Chair	Dr. G. Brooks Avery
_____	_____
Dr. Daniel L. Kamykowski	Dr. David J. DeMaster

Dedication

This dissertation is dedicated to my husband, Josh Dixon. There are no words to express the profound impact you have had on my life. You swept me away. I love you.

Biography

I found one of the deepest loves of my life, the ocean, at a very early age. I was born to two ocean loving people, how could I not have salt water in my veins? My father is a boat mechanic and lifelong fisherman. My mother loves to surf and would prefer driving a boat to a car any day. Looking back, it's pretty easy to see how I came to love the sea and coastal waters.

My childhood years were spent living in the coastal town of Morehead City, NC and I jumped at every opportunity to go down the beach with my family. As a little kid, if someone asked me what I was going to be when I grew up, I would have probably told him or her a mermaid. I simply couldn't get enough of the water. My sister and I would hold our breath underwater for as long as possible, just trying to take it all in. We would walk the beach looking for shells and shark teeth. Throughout the summer we would wake up at sunrise and go on walks called "dawn patrols". This entailed walking along the beach looking for the signs of new sea turtle nests and emerging hatchlings. I couldn't have been more than 10 years old when I got to excavate my first sea turtle nest and watch as the hatchlings make their way to the ocean. I spent the rest of my childhood fishing with my father and surfing with my mother.

Upon entering college I met Dr. Brooks Avery who introduced me to marine science and Jean Beasley who opened my eyes to environmental education and outreach. I quickly became enthralled with both of these topics and have spent the majority of my adult life trying to find ways to intertwine them.

It is impossible to say how my life would be different without the influence of my parents, Brooks and Jean. There are no words to express the profound impact they have had on my life as a mentors, teachers and above all friends. They changed my life.

Lastly, I spent my final year of graduate school with this as my mantra-

“I get up every morning determined to both change the world and have one hell of a good time. Sometimes this makes planning my day difficult.”

— E.B. White

I think it says it all.

Table of Contents

List of Tables

Chapter 1: Seasonal changes in estuarine dissolved organic matter due to variable flushing time and wind-driven mixing events.

Chapter 2: Characterizing the quality and quantity of chromophoric dissolved organic matter (CDOM) in the Neuse River Estuary, eastern North Carolina: a preliminary study using PARAFAC modeling.

List of Figures

Chapter 1: Seasonal changes in estuarine dissolved organic matter due to variable flushing time and wind-driven mixing events.

Chapter 2: Characterizing the quality and quantity of chromophoric dissolved organic matter (CDOM) in the Neuse River Estuary, eastern North Carolina: a preliminary study using PARAFAC modeling.

Overall Introduction

Organic matter (OM) is present in all natural aquatic environments. For example, estuaries are highly productive habitats that transport and transform OM and act as a transition zone between terrestrial and marine environments (Paerl et al. 1998; Markager et al. 2011; Osburn et al. 2012). Additionally, within estuaries dissolved organic matter (DOM) consists of a complex mixture of organic molecules that vary greatly in molecular weight (Bauer and Bianchi 2011). The heterogeneity of OM is a product of its wide variety of sources and its reactivity to physical, chemical, and microbial degradation processes. The major sources of OM are (1) dissolution of soil organic matter, (2) extracellular release of organic matter by algae, (3) release via grazing and excretion by zooplankton, (4) viral lysis of bacteria and algae cells, (5) degradation and exudation of macrophytes, and (6) release from sediments (Hedges 2002; Houghton 2007; Bianchi 2011; Bauer and Bianchi 2011).

Chromophoric dissolved organic matter (CDOM) is the light absorbing fraction of DOM in natural waters. Specifically, CDOM absorbs light over a broad range of light wavelengths. For example, CDOM absorption is strongest in the ultraviolet (UV) region (200-380nm) and diminishes to near zero in the visible light red region (380-780nm) and near infrared (IR) region (780-800nm). CDOM can be characterized using optical methods such as absorption and fluorescence spectroscopy (e.g. Stedmon and Markager, 2003). By analyzing the spatial and temporal variability of DOM and CDOM within estuaries, information pertaining to OM source and fate can be obtained. These methods offer an inexpensive, non-destructive means for obtaining sensitive measurements of a diverse group of organic compounds. By using this technology to analyze the spatial and temporal

variability of CDOM within estuaries, information pertaining to OM source and fate across the freshwater-marine continuum can be obtained (Fellman et al. 2011; Osburn et al. 2012; Murphy et al. 2014).

Chemical biomarkers are also routinely used to identify DOM sources in coastal waters. Examples include carbon stable isotopes (Bauer, 2002) and lignin (e.g., Benner and Opsahl, 2001; Harvey and Mannino, 2001). Marine DOM derived from phytoplankton typically has carbon stable isotope ($\delta^{13}C$) values that range from −20 to −22‰, while terrestrial DOM derived from C3 land plants typically have $\delta^{13}C$ values that range from −26 to −28‰ (Bauer, 2002). Lignin is an important component of vascular plants, thus making it a unique geochemical biomarker, which can be used to trace the fate of terrestrial DOM in coastal seawater (e.g., Hernes and Benner, 2003; Walker et al. 2009; Osburn and Stedmon, 2011). Further, the ratios of the different phenolic compounds derived from the oxidation of lignin can be used to distinguish between plant sources (e.g. angiosperm vs. gymnosperm, or woody vs. non-woody tissue) and the extent of exposure to degradation (Hedges et al. 1988).

The highly productive, eutrophic waters of the Neuse River Estuary (NRE), in eastern North Carolina, USA, serve as a reaction zone for terrigenous DOM between the head of the Neuse River and Pamlico Sound. Previous studies have determined that the NRE is dominated by inputs from riverine discharge, yet very clear shifts in DOM quality were apparent as discharge varies (Paerl et al. 1998; Osburn et al. 2012). Furthermore, flushing times within the NRE aids in determining whether DOM is primarily autochthonous or allochthonous and if it is processed internally or transported downstream to the Pamlico Sound (Paerl et al. 1998; Mari et al. 2007; Peierls et al. 2012). For example, increases in

flushing time may allow for the accumulation of autochthonous DOM because of (1) planktonic communities within the water column having more time to utilize nutrients within the system, resulting in phytoplankton blooms and (2) lower inputs of allochthonous OM from the NRE's watershed (Dixon et al. accepted). Therefore, the main sources of DOM and its composition can change throughout an estuary depending on the hydrodynamic conditions.

The objectives and hypothesis of this study are:

1. Examine the monthly and seasonal cycling and alteration of DOM and CDOM quality within the Neuse River in order to understand larger physical mixing controls on estuarine DOM. We hypothesize that the quality of DOM in the NRE reflects allochthonous sources driven by increased discharge and shorter flushing time. In addition, reduced discharge and longer flushing times within the NRE allows for extensive autochthonous production to modify the quality of the DOM pool.
2. Examine DOM quality and production/destruction along the freshwater to marine continuum using statistical analysis of DOM fluorescence. We hypothesize that our PARAFAC model will demonstrate variations in CDOM composition within the NRE.
3. Examine geochemical measurements on DOM such as carbon stable isotopes and lignin content within the NRE. We hypothesize that our geochemical data will reflect variations in CDOM composition as discharge varies within the NRE.

Chapter 1: Seasonal changes in estuarine dissolved organic matter due to variable flushing time and wind-driven mixing events.

1.1 Introduction

Estuaries are highly productive habitats that transport and transform organic matter (OM), experience large changes in ionic composition and act as a transition zone between terrestrial and marine environments (Paerl et al. 1998; Markager et al. 2011; Osburn et al. 2012). Within estuaries, dissolved organic matter (DOM) is a heterogeneous mixture of aromatic and aliphatic compounds, and its composition in aquatic systems varies spatially and temporally with source (Bauer and Bianchi 2011). However, the main source of DOM in estuaries, rivers and other aquatic systems, originates from vascular plant detritus, soil humus, older fossil (i.e., petrogenic) organic carbon, black carbon (e.g. kerogen, soil organic charcoals), marine OM and *in situ* production (Hedges 2002; Houghton 2007; Bianchi 2011; Bauer and Bianchi 2011). Chromophoric dissolved organic matter (CDOM), the light absorbing fraction of DOM in natural waters, can be characterized using optical methods such as absorption and fluorescence spectroscopy (e.g. Coble, 1996; Stedmon and Markager, 2003). By analyzing the spatial and temporal variability of DOM and CDOM within estuaries, information pertaining to OM source and fate across the freshwater-marine continuum can be obtained.

In many estuarine systems OM dynamics are often driven by inherent complex physical dynamics such as river discharge, wind speed, and wind direction. For example, variations in river discharge directly impact flushing and residence time and are a major determinant of OM transformations (Paerl et al. 1998; Peierls et al. 2012; Dixon et al.

accepted). In cases of long residence time or flushing time the DOM pool is subjected to degradation processes and *in situ* production (Paerl et al. 1998; Mari et al. 2007, Peierls et al. 2012). Thus, long residence time and flushing time should lead to prolonged bacterial and photochemical degradation of OM (Mari et al. 2007; Osburn et al. 2009) as well as increased light penetration, the latter resulting in marine algae, such as phytoplankton, utilizing inorganic nutrients and transforming them into autochthonous OM (Paerl et al. 1998). When inputs of OM match hydrodynamically-driven removal rates (i.e. shorter residence times and fast flushing times), DOM will be controlled to a greater extent by physical rather than by biogeochemical processes (Mari et al. 2007). For example, at increased discharge rates and fast flushing times, *in-situ* production may not occur because phytoplankton may not reside long enough in a system to accumulate, despite an abundance of nutrients (Peierls et al. 2012). Therefore, the main sources of DOM and its composition can change throughout an estuary depending on the hydrodynamic conditions.

Although variations in hydrodynamic conditions, (e.g. discharge) often drive the mixing regime within estuarine systems, winds can play an important additional role within shallow-water systems, such as the Neuse River Estuary (NRE), in eastern North Carolina, USA. The mixing regime of the NRE can vary from a strongly stratified estuary to a well-mixed estuary depending on wind direction and speed. For example, winds directed down estuary (primarily from the southwest (toward the northeast) enhance downstream fresh water surface flow, thus enhancing stratification (Luettich et al. 2002). In the upper NRE (above the bend) (Fig. 1.1), winds blowing from the southwest (toward the northeast) also have the effect of developing cross-river seiches, which can cause bottom water upwelling on

the southern shore of the NRE (Reynolds-Fleming and Luettich 2004). Furthermore, if the winds are strong enough, stratification can be broken down.

Therefore, winds oriented down estuary would produce faster flushing time and shorter residence time, while the opposite effect is true for winds that are oriented up estuary (from the east). Winds blowing from the northeast (toward the southwest) would result in slower flushing times and longer residence times within the NRE (Luettich et al. 2002). The Chesapeake Bay has experienced similar mixing regimes driven by wind direction, where winds can both destratify the water column and lead to enhanced stratification (Goodrich et al. 1987; Valle-Levinson et al. 1998).

In this study, we examined the monthly cycling and alteration of DOM and CDOM within the NRE based on mean surface and bottom DOM measurements in order to understand larger physical mixing controls on DOM in the estuary from March 2010 through February 2011. We described how mean discharge, mean wind speed, and wind direction affect the variability of mean concentrations of DOM and CDOM within the NRE. We then investigated the seasonal changes in mean DOM quality using various CDOM quality parameters. We hypothesized that the quality of DOM in the NRE reflects allochthonous sources driven by increased discharge and shorter flushing time. Furthermore, reduced discharge and longer flushing times within the NRE allows for extensive autochthonous production to modify the quality of the DOM pool. Finally, our data suggest that variations in wind speed and direction local to the NRE can cause the resuspension of surficial sediments, which contain heavily reworked, algal derived OM.

1.2 Methods

1.2.1 Study Site

The NRE is a drowned river valley and a major tributary of the second largest estuarine complex (by area) in the United States, the Albemarle-Pamlico Sound (Steel, 1991) (Fig. 1.1). The watershed is approximately 16,108 km^2, and the estuary has an average surface area of 455 km^2 with an average depth is about 2.7 m (Paerl et al. 2010). River discharge rates range from 50 to 1000 m^3s^{-1}, resulting in flushing times that range from 20 to 200 days (Luettich et al. 2002; Crosswell et al. 2012). The limited oceanic exchange of the NRE contributes to the long residence and slower flushing times, which aid in extensive recycling of nutrients in the water column (Christian et al. 1991; Steel, 1991). Furthermore, over the past few decades, accelerated eutrophication and OM loading, driven by urban development and expanding agricultural operations in the NRE watershed, have resulted in annual fish kills, harmful algal blooms, and poor water quality in the NRE (Paerl et al. 1998, 2010; Burkholder et al., 2006). The flow regime in the mesohaline estuary is surface outflow and bottom-water inflow with minimal tidal influence (Reed et al., 2004; Null et al. 2011). Winds are an important mixing force in this shallow system and play a significant role in sediment resuspension, influencing OM and nutrient release from the benthic environment (Reed et al., 2004; Corbett, 2010; Null et al. 2011).

1.2.2 Meteorological Data, River Discharge and Flushing Time Calculations

Meteorological data was collected from the CRONOS database of the State Climate Office of North Carolina. For winds pertaining to the Neuse River, site Cherry Point Marine Corps Air Station (MCAS) (Station ID- KNKT) located in Craven County was used. Data

from this location were chosen for our study because of its central location and proximity to the NRE. These data consist of hourly and daily values of wind speed and direction. Total precipitation data for the Neuse River were obtained from Kinston, NC (Station ID-KINS). Data from this location were used for our study because of its upstream location of Fort Barnwell, NC. River discharge data were downloaded using the USGS National Water Information System web interface. For the Neuse River, this was Fort Barnwell (USGS site #02091814), which is 24 km upstream of station NR0. Discharge data were divided by the ratio of gauged to total watershed area (0.69 for the NRE) as a correction for un-gauged watershed discharge (Peierls et al. 2012). Flushing time for the lower NRE was calculated by dividing the volume of the NRE by the average discharge over each month.

1.2.3 Sample Collection

Samples were collected monthly between March 2010 and February 2011 during the NRE modeling and monitoring (ModMon: see; http://www.unc.edu/ims/neuse/modmon/index.htm) sampling cruises which spanned the main axis of the estuary (Fig. 1.1). Physical and chemical properties of the water column were sampled along the river during each sampling cruise and vertical profiles of salinity, temperature, dissolved oxygen (DO), *in vivo* fluorescence (chl), photosynthetically active radiation (PAR, 400-700 nm) and pH were obtained with a YSI 6600 multiparameter water quality sonde (Yellow Springs Inc., Yellow Springs, OH, USA) (Table 1.1). Diffuse light attenuation coefficients, k (m^{-1}), were computed by:

$$k = (\ln I_0 - \ln I_z) / z$$

Where z is the water column depth (m), I_0 is surface irradiance and I_z is irradiance at depth z. I_0 was measured just below the surface and z is 0.5 m above the bottom at each sampling site (Kirk 2004).

At each site, water samples were collected near the water surface and at roughly 0.5 meters above the bottom, transferred to acid-cleaned 1 liter HDPE bottles, and kept cool and shaded during transport to the laboratory. All samples were stored in the dark at 4 °C until shipped to N.C. State University, where they were vacuum-filtered through Sterivex-GP 0.22 μm filters into pre-cleaned glass vials with Teflon coated lids. All glassware in contact with samples was soaked in a detergent solution for a minimum of six hours, rinsed with ultrapure (18.2 MΩ resistivity) water, air-dried, and then combusted in an oven at 550°C for at least six hours.

1.2.4 Dissolved Organic Carbon (DOC) and Dissolved Organic Nitrogen (DON)

Dissolved organic carbon (DOC) and dissolved organic nitrogen (DON) samples were transported in carboys to the Institute of Marine Sciences (IMS) and either refrigerated before filtration or immediately pressure filtered through a pre-combusted, 142 mm Whatman GF/F filter and a 142 mm Millipore Express Plus 0.22 μm effective particle removal size polyethersulfone membrane filter arranged in series. DOC measurements were made using high temperature combustion techniques on a Shimadzu model TOC5000, equipped with an ASI-5000A autosampler (Benner & Strom 1993). Acidified (HCl, pH < 2) samples were sparged for 8 min with air to drive off DIC. Background checks revealed complete removal of DIC by this treatment. Reported values represented the average of 3 injections. DON was calculated as the difference between total dissolved N (TDN) and total

dissolved inorganic N (DIN: sum of nitrite, nitrate, and ammonium) measured on a Lachat QuikChem 8000 flow injection analyzer (Lachat, Milwaukee,WI, USA). C:N values, the molar ratio of DOC to DON, were calculated and used as an indicator of DOM source, e.g., terrestrial or vascular plant derived C:N values are generally greater than 15 and C:N values less than 8 suggest marine (or more broadly autochthonous) sources of DOM (Premuzic et al. 1982).

1.2.5 Absorption Spectra of DOM

Absorbance spectra of DOM were measured from 240 to 800 nm using a 1-cm quartz cell (relative to air) on a Varian 300 UV spectrophotometer. Samples were allowed to warm to room temperature prior to measurement. Absorption spectra were blank-corrected by subtracting the absorbance of Milli-Q water from each sample. Blank-corrected absorbance values were converted to Napierian absorption coefficients (a_λ, m^{-1}) at each wavelength (λ):

$$a_\lambda = 2.303 / A_\lambda * l$$

where A_λ is the blank corrected spectrophotometer absorbance reading at wavelength λ and l is the optical pathlength in meters (Kirk 1994). CDOM was quantified as the absorption coefficient at 350 nm (a350). The spectral slope ratio, S_R, of the absorption curve was calculated over the wavelength ranges 275–295 nm ($S_{275–295}$) and 350–400 nm ($S_{350–400}$) and was obtained using log-transformed absorption spectra (Helms et al. 2008). S_R is defined as the ratio of the slope of the shorter wavelength interval (275–295 nm) to that of the longer wavelength interval (350–400 nm). S_R values were used to characterize DOM source and molecular weight. S_R values less than 1.0 have been reported for fresh and estuarine waters and are indicative of predominantly terrestrial OM that is of a high molecular weight

(HMW), while S_R values greater than 1.0 have been reported for coastal and open ocean water and are indicative autochthonous OM of low molecular weight (LMW) (Helms et al. 2009). The specific UV absorbance (*a*254/DOC), $SUVA_{254}$, was used as an index of DOM aromaticity, with increases in $SUVA_{254}$ corresponding to DOM with a higher aromatic content and lower values corresponding to DOM with a reduced aromatic content.

1.2.6 Fluorescence Spectra of DOM

Fluorescence spectra of NRE DOM were acquired on a Varian Eclipse spectrofluorometer. Excitation (Ex) wavelengths were sampled from 240 to 450 at 5-nm intervals, whereas emission (Em) wavelengths were sampled every 2-nm from 300 to 600 nm. The excitation lamp was set at 600 or 800 volts, with an Ex/Em slit width of 5-nm for both, a scan rate of 9600 nm/min and an integration time of 0.0125 seconds. The instrument measured fluorescence intensity in arbitrary units (A.U.), which were transformed to Raman units (R.U.) and then converted and reported as quinine sulfate equivalents (ppb QSE) (Laewetz and Stedmon 2009). Excitation emission matrix (EEM) fluorescence intensities were corrected for Rayleigh and Raman (natural scattering properties of pure water after it absorbs light) scattering by Milli-Q water blank subtraction and for instrument bias prior to correction for any inner-filtering effect (Stedmon and Bro 2008). Smoothing of the data was also necessary to remove instrument noise and scatter, and to remove an area of the EEM where signal to noise ratio was low. All data processing and corrections were performed using in-house scripts written for Matlab (Mathworks, Inc., Natick, MA). The fluorescence maximum (FMax), reported in QSE, was determined by identifying the maximum fluorescence value at its associated excitation-emission wavelength. The autochthonous

index (BIX) is a fluorescence index used to assess the relative contribution of autochthonous DOM in water samples (Huguet et al., 2009). BIX is calculated from the ratio of emission intensities at a shorter (Em 380 nm) and longer (Em 430 nm) wavelength using a fixed excitation (Ex 310 nm). High BIX values (0.8 to 1.0) correspond to freshly produced DOM of biological or microbial origin, whereas BIX values below ~0.6 are considered to contain little autochthonous OM (Huguet et al. 2009). HIX is a fluorescence index used to determine the degree of DOM humification and recalcitrance within a natural system (Zsolnay et al.1999; Huguet et al. 2009). HIX was calculated as the ratio of two integrated emission ranges, the first from 435–480 nm and the second integrated emission range from 300–345 nm at a set excitation wavelength of 255 nm. Highly humified OM is resistant to degradation and often persists in environments longer than OM with a lower degree of humification. Low HIX values (<5) represent fresh OM and high values of HIX (10–16) represent the presence of condensed humic OM usually of terrestrial origin.

*1.2.7 Statistical Analysi*s

All statistical tests were performed using Matlab v.R2009a software. Nonparametric tests were applied when assumptions of parametric tests could not be met with either non-transformed or transformed data. A one-way analysis of variance (ANOVA) or a Kruskal-Wallis test was used to examine the individual effects of season and spatial location on physical and chemical variables at a 95% confidence interval (i.e., $P<0.05$) unless otherwise specified. Significant differences between seasons and spatial location were determined using either a Tukey or Dunn post-hoc test.

1.3 Results

1.3.1 Physical Mixing Patterns

Regional climate trends for the area can be described as a wet period, which began in the late autumn of 2009 and extended through April 2010 (Peierls et al. 2012). In late September/early October 2010, the remnants of Tropical Storm Nicole combined with a stationary low pressure system to produce record rainfall over the region (National Climatic Data Center 2010). This was reflected in the freshwater runoff to the NRE, which was highest in spring and autumn, with peak monthly mean discharge values of 266 $m^3 s^{-1}$ and 179 $m^3 s^{-1}$ in March and April 2010 and 245 $m^3 s^{-1}$ in October 2010. Increases in discharge within the NRE were due to increases in precipitation (Fig. 1.2). Furthermore, the late September/early October 2010 rain event produced record discharge for the Neuse River. This result was similar to previous findings that illustrate how overland flow and discharge are responsive to precipitation events, and influence the large inputs of dissolved materials via runoff that the NRE receives (Mallin et al. 1993; Paerl et al. 1998; Fellman et al. 2011). The mean flushing time of water within the NRE ranged between 23 and 250 days, similar to the range reported by Crosswell et al. (2012). Specifically, the shortest mean flushing times were reported during months when average discharge was the highest (March 2010, average flushing time=23 days; October 2010, average flushing time=25 days). The longest mean flushing time in the NRE was 250 days in July 2010, which also exhibited the lowest average water discharge. Salinity increased from NR0 (mean 0.07±0.02) at the head of the NRE into estuarine water, NR160 (mean 14.4±4.22), and ranged from 0.1 to 20.8.

The monthly mean wind speed measured at Cherry Point MCAS near New Bern, NC ranged from 1.7 to 3.9 m s^{-1}, with a yearly mean wind speed of 2.5 ± 0.8 m s^{-1} (Table 1.1). The prevailing wind direction in March of 2010 was out of the WSW, with maximum wind speeds of 5.7 m s^{-1} (Table 1.1). From April to September 2010 the prevailing wind direction varied and maximum wind speeds were lower and ranged from 4.6 to 6.2 m s^{-1} (Table 1.1). In October and November, the prevailing wind direction was out of the SSW and SW and maximum wind speeds increased, ranging from 5.7 m s^{-1} in October 2010 to 6.7 m s^{-1} in November 2010. In following months, the prevailing wind direction varied and maximum wind speeds ranged from 5.1 to 9.8 m s^{-1} (Table 1.1).

1.3.2 Dissolved Oxygen, Chlorophyll, and Diffuse Attenuation Coefficients

Mean DO concentrations in the NRE changed with variations in discharge, chl and temperature. From March to May 2010, mean DO concentrations decreased from 11.3 mg L^{-1} to 7.5 mg L^{-1} as discharge decreased in the spring. From May through September 2010 mean DO values for the water column were the lowest measured during the study and corresponded to lower discharge (Table 1.2). In November 2010 through February 2011, mean DO values increased following increased freshwater discharge in October 2010, although the correlation between mean DO and mean temperature was quite significant (R^2 = -0.89, $P<0.05$). The increase in mean DO values also corresponded to an increase in observed mean chl concentrations as high as 25.3 µg L^{-1} in the winter of 2011(Table 1.2). Furthermore, a significant and positive correlation (R^2 = 0.56, $P<0.05$) between mean monthly DO values and mean monthly chl values was observed, with increases in mean DO values corresponding to increases in chl values. Mean attenuation coefficients, *k*, did not show a clear pattern with

variation in discharge and ranged from 0.94 to 1.53 m^{-1} during the duration of this study (Table 1.3).

1.3.3 Spatial and Temporal Distributions of DOC, DON and CDOM

Upon further examination of the effects of sampling depth and sampling month, varying trends in monthly estuarine-averaged surface and bottom DOC, DON, *a*350, and FMax values emerged (Table 1.2). First, neither monthly mean DOC nor monthly mean DON values were statistically different ($P>0.05$) between surface and bottom waters (Figs. 1.3A-D). However, CDOM values, represented by mean *a*350 and mean FMax values, were statistically different between surface and bottom waters ($P<0.05$), illustrating that CDOM dynamics in the NRE vary with depth (Fig. 1.4A-D). More specifically, mean *a*350 and mean FMax values were lower in bottom waters regardless of discharge within the NRE. Second, the NRE exhibited variations in DOC, DON, *a*350, and FMax values in relation to freshwater discharge. Pulses of DOC, DON and CDOM were closely associated with runoff events, which were most commonly observed in the spring and late autumn. For example, in the spring and autumn, both mean DOC values and mean FMax values were significantly higher than their corresponding mean summer values ($P<0.05$) (Fig. 1.3A,B). These differences occurred during peaks in riverine discharge at Fort Barnwell, NC. Furthermore, mean DON values were significantly higher in autumn compared to all other seasons ($P<0.05$), while mean *a*350 values were significantly higher in the spring compared to all other seasons ($P<0.05$) (Fig. 1.4A,B). Overall, these trends suggest that throughout the year, increases in discharge in the Neuse River proper flush terrestrial DOC, DON and CDOM into the estuary.

1.3.4 Monthly Trends in Dissolved Organic Matter Quality

The monthly averages of various DOM qualitative parameters (i.e. C:N, HIX, $SUVA_{254}$, S_R and BIX) were examined to explore DOM characteristics within the NRE over a range of flow regimes (Table 1.2). Mean C:N values in the estuary ranged from 18.9 to 29.4, indicating the predominantly terrestrial nature of DOM, although differences in C:N values associated with discharge were apparent (Fig. 1.5). Lower discharge in the summer corresponded to lower mean C:N values in surface and bottom waters. Mean C:N values in surface and bottom waters during the winter of 2011 were also lower than the previous fall but not as low as those values reported for the summer of 2010. Increases in discharge in the spring (March and April 2010) corresponded to higher mean C:N values in bottom waters and lower mean C:N values in surface waters. Increases in discharge in autumn (October 2010) were simultaneous with increases in mean C:N values in bottom waters but decreases in mean C:N values in surface waters (Fig. 1.5). Surface and bottom waters were significantly different ($P<0.05$) during this time.

Changes in DOM C:N ratios were reflected in the mean HIX and mean $SUVA_{254}$ values, which ranged from 6.8 to 12.5 and from 2.8 to 3.8, respectively (Table 1.2). Increases in both parameters in surface waters were observed with increasing discharge, suggesting DOM in the NRE increased in aromaticity and humification (Fig. 1.6A,C). Consequently, the months of lowest discharge also had the lowest mean HIX and $SUVA_{254}$ values in surface and bottom waters, indicating less humified and lower aromatic DOM within the NRE during periods of base flow in the river (Fig. 1.6A,C). It is important to note that in October 2010 surface and bottom mean HIX values were significantly different ($P<0.05$). This result

indicated that on average the bottom waters of the NRE during this time were not as humified as surface waters, although increases in mean HIX values were observed in the summer. Moreover, in October 2010 mean $SUVA_{254}$ values in bottom waters were lower and significantly different from mean surface values ($P<0.05$), corresponding to less aromatic DOM (Fig. 1.6C). Overall, mean HIX and mean $SUVA_{254}$ values were not correlated in bottom waters of the NRE during peak discharge events in the river at Ft. Barnwell, with DOM exhibiting increased humification but less aromaticity.

Lastly, mean S_R and mean BIX values showed nearly identical trends with discharge (Fig. 1.6B,D). Both parameters decreased as discharge increased within the estuary (while HIX increased), illustrating a shift towards HMW, terrestrial OM with a smaller autochthonous component (Fig. 1.6B,D). As discharge decreased, increases in both parameters were observed, illustrating a shift towards autochthonous OM, with LMW DOM being the main source of DOM during base flow (Fig. 1.6B,D). Mean surface and mean bottom S_R and BIX values were not significantly different from each other regardless of changes in discharge ($P>0.05$). The lack of difference between surface and bottom mean S_R and BIX values indicates that the NRE was well-mixed with respect to these two parameters.

1.4 Discussion

1.4.1 Discharge as a control on DOM concentrations and quality in the NRE

Within the micro-tidal NRE, freshwater discharge and flushing time influenced CDOM and DOM sources throughout the sampling year. The mean flushing times of water in the NRE during this study ranged between 23 and 250 days and was similar to Crosswell et al. (2012). These findings are similar to a previous study by Paerl et al. (2010), who

reported freshwater flushing times that ranged between 7-200 days in the NRE over varying hydrological regimes. Increases in discharge and faster/shorter flushing times within the NRE resulted in increases in DOC, DON and CDOM concentrations in the estuary. This was most noticeable during the high discharge events measured at Ft. Barnwell, NC, in 2010 (Fig. 1.2). Moreover, decreases in mean discharge and longer flushing times in the late spring and summer months resulted in declining DOC, DON, *a*350 and FMax concentrations within the NRE. The quality of DOM during periods of peak discharge is discussed below and indicated a terrestrial source (Mallin et al. 1993; Pinckney et al. 1999; Fellman et al. 2011).

Primary productivity leads to algal biomass accumulation throughout the estuary and is further enhanced during periods of increased water flushing time (Rudek et al.1991; Mallin et al. 1993; Paerl et al. 2006; Osburn et al. 2012). During downstream transit, there must be sufficient time for primary production and degradation processes to occur in order for autochthonous DOM to influence the allochthonous DOM signal that is most prevalent in the NRE. For example, increased residence time as seen in the summer of 2010, allowed for substantial degradation of DOM (via bacterial respiration or photochemical processes) and/or autochthonous production of new DOM to occur (Paerl et al. 1998; Markager et al. 2011; Peierls et al. 2012). This was expressed in increases in the mean S_R and BIX values, which reflected LMW DOM of autochthonous (and/or microbial) origin during the summer of 2010. As flow at Fort Barnwell increased in the spring and autumn, shorter flushing times occurred in the NRE and mean S_R and BIX values exhibited a shift in DOM quality that were indicative of HMW DOM of a terrestrial origin. Mean HIX values exhibited the opposite trend, with the lowest mean HIX values seen in summer of 2010, indicating less humified

DOM autochthonous-like and higher mean HIX values were seen during and immediately after peaks in discharge, thus resembling more humified, allochthonous DOM. The shorter flushing times reduced the time for biological and/or chemical processes to significantly impact the allochthonous DOM pool, effectively allowing unaltered allochthonous OM to be flushed through the NRE and into the Pamlico Sound (e.g., Paerl et al. 1998; Peierls et al. 2012).

1.4.2 DOM cycling within the NRE

DOM quality as described by C:N ratios in the NRE varied under different flow regimes and flushing times and likely reflected the extent of DOM cycling within the NRE. During periods of high discharge, mean C:N values indicated the dominance of terrestrial-like DOM within the NRE. This was expected because high discharge and low flushing time favors rapid transport of DOM through the system. In other words, freshwater-saltwater mixing in the estuary (i.e., conservative mixing) dominates over in situ processing. As discharge decreased, mean C:N values decreased, reflecting a shift towards autochthonous DOM. Although decreases in mean C:N values were seen during this time, they were never low enough to be considered solely autochthonous (C:N values less than ~8). Previously reported C:N ratios for the NRE ranged from 17.5 to 30.0, similar to our results in this study (Vähätalo et al. 2005). Within the NRE, as discharge at Ft. Barnwell increased, mean surface C:N values for DOM exhibited marked decreases, implying that there was DON enrichment relative to DOC.

Within the NRE, the source of DON enrichment in surface waters could be due to overland flow (Paerl et al. 1998; Osburn et al. 2012). For example, Osburn et al. (2012)

found increased inputs of terrestrial DON into the NRE after the passage of Hurricane Irene. Therefore, nutrients, specifically the biologically available fraction of DON, can be carried into the NRE from the surrounding terrestrial environment during precipitation events, which create new and redirect existing hydrologic flow paths (Salmon et al. 2001; Meixner et al. 2007; Corbett 2010). Osburn et al. (2012) hypothesized that land use in the Neuse River basin could be driving exacerbated fluxes of DON during storm events. Moreover, there is an opportunity for nutrient exchange between surface waters and the sediments of cypress swamps that can occur when streams flood and water overflows into the surrounding swamps resulting in runoff into the surrounding reservoir (Brinson et al.1981). Therefore, precipitation events in March and October 2010 could potentially flush organic nutrients into the surface waters of the NRE, resulting in N-enriched DOM in surface waters as evidenced by reduced mean C:N values.

During periods of low river discharge the shifts in DOM quality observed in CDOM and FDOM properties support the replacement of terrestrial DOM with planktonic DOM in the NRE. First, regardless of depth, mean HIX and mean $SUVA_{254}$ values decreased during the summer months, while both mean BIX and mean S_R values increased. It appeared that during periods of low discharge at Fort Barnwell, DOM in the NRE shifted toward a LMW and more autochthonous-like source of OM. Conversely, regardless of depth, both mean BIX and mean S_R values decreased in the NRE during the autumn months, while mean HIX and mean surface $SUVA_{254}$ values increased as discharge increased above base flow values. This result suggested that DOM in the surface waters NRE was shifting back towards HMW, terrestrial sources, likely derived from the watershed (Paerl et al. 1998; 2006). These findings

are similar to prior work on the loading of degradable OM in the NRE, which fuels low oxygen conditions in the bottom waters (Paerl et al. 1998). Furthermore, mean $SUVA_{254}$ and mean HIX values in the NRE behaved in a similar manner to those values reported in a variety of aquatic systems. In several studies, increases in overland flow due to precipitation events flushed terrestrial OM into the system resulting in higher mean HIX and mean $SUVA_{254}$ values in surface waters (Hood et al. 2006; Huguet et al. 2009; Saraceno et al. 2009; Spencer et al. 2009; 2010). Based on the conclusions of Luettich et al. (2000), groundwater flow was not significant in the center of the NRE. Therefore, this suggests that OM sourced from groundwater flow through the upper soil horizon into the middle of the NRE is not a significant source of OM within this system.

1.4.3 NRE Mixing Regimes and Benthic Resuspension Events

DOM within estuaries is supplied by external sources as well as *in situ* regeneration and recycling. A major component of this internal recycling is exchange at the benthic boundary layer (Corbett et al. 2010). In the shallow waters of the NRE, exchanges between surface sediments and the overlying water are enhanced by local winds, specifically as a function of wind speed and wind direction. Thus, the recycling process (remineralization and regeneration of OM) that occurs due to the interaction between the benthic environment and the overlying waters is extremely important for understanding OM dynamics (Corbett et al. 2010). Previous studies conducted in the lower NRE have shown near bottom currents as high as 20 cm s^{-1} (average current at or below 5 cm s^{-1}), which indicate that resuspension may be prevalent throughout the year in the NRE (Corbett et al. 2007). This is specifically important within the mesotrophic to eutrophic regions of NRE, where a main source of POM

(particulate organic matter) that reaches the sediment surface after settling out of the water column is derived from phytoplankton (Osburn et al. 2012).

In October of 2010, a likely source for the humified, less aromatic DOM observed in the bottom waters of the NRE was from resuspension events. Autochthonous derived DOM in bottom waters was likely resuspended due to a shift in wind direction and increased wind speeds blowing out of the SSE rather than precipitation driven discharge. Although increases in rainfall were recorded at the end of September and beginning of October, little to no rain was reported within two weeks of the actual sampling date in October 2010. Additionally, Corbett (2010) stated that the dominant process causing resuspension of sediments in the NRE was wind-induced waves, due to shifts in wind direction and increases in wind speed, producing orbital movement in the water column. Three days prior to the sampling date of October 18, 2010, winds were blowing out of the SSW to W until the wind direction shifted to the SSE on October 17, 2010. Furthermore, mean and maximum wind speeds on October 18, 2010 (mean 2.6 m s^{-1} and maximum- 5.7 m s^{-1}) were not quite high enough to cause major resuspension events alone, based on the Corbett et al. (2007) findings. Therefore, it is possible that a combination of increased wind speed (several days prior to sampling) as well as shifts in wind direction resulted in the development of sufficient wave energy to generate orbital velocities capable of resuspending sediment within the NRE. Moreover, mean bottom water HIX values in October 2010 indicated DOM that was more humified than surface waters, whereas mean bottom water $SUVA_{254}$ values reflected less aromatic DOM. These findings illustrate that after the summer of 2010, when mean S_R and mean BIX values reflected DOM quality of an autochthonous origin, the following autumn experienced a

resuspension event of heavily reworked, algal-derived DOM due to local winds. Furthermore, Bianchi et al. (2009) observed similar wind-driven mixing mechanisms in Mississippi River shelf waters. During their April 2008 cruise, strong wind speed and northerly direction resulted in an increase in the flux of water and material from the bay seaward into the Gulf, while weaker southerly winds in July reduced the flux from the bay into the Gulf.

During the spring and winter, resuspension of bottom sediments did not result in the same heavily reworked, algal-derived DOM that was seen in October 2010. A possible explanation for this may be that during the spring and winter the estuary was dominated by terrestrial inputs from precipitation events and increased overland flow. The flux of freshwater and terrestrial OM following precipitation events was evident due to an increase in the allochthonous quality of both DOM and CDOM as well as increases in their concentrations compared to times of minimal rainfall. For example, Avery et al. (2003) found that external DOC fluxing into coastal waters at the base of the Cape Fear River (CFR) in North Carolina is sourced from riverine and rainwater DOC. Specifically, they found that rainwater fluxes roughly 21 x 10^9 $gCyr^{-1}$ on an annual basis within the CFR, which is roughly 4x less than the riverine DOC flux of 77 x 10^9 $gCyr^{-1}$. Additionally, Osburn et al. (2012) found increased inputs of terrestrial OM into the NRE after rain events due to overland flow. Furthermore, the increase in discharge in the NRE led to reduced flushing times, which would likely flush a portion of the phytoplankton population out of the NRE (Peierls et al. 2012; Osburn et al. 2012). Thus, the removal of phytoplankton and increased terrestrial OM

loading would result in a loss of autochthonous POM being deposited onto the surface sediments, which was reflected in DOM and CDOM indices.

Lastly, the increase in mean DOM bottom water C:N values in October 2010 indicated that the resuspension of DOM was relatively depleted in organic nitrogen. Ammonification of DON to NH_4^+ in sedimentary pore waters in the NRE could facilitate the loss of organic N, resulting in C:N ratios of pore waters being relatively high and resembling terrestrial OM sources. This process would explain the increase in mean bottom water NH_4^+ concentrations seen in the NRE during October 2010, when we propose that resuspension of surface sediments mixes DON-depleted (and NH_4^+-enriched) pore waters into the overlying water column (Fig.1.7). Corbett et al. (2007) also found that the concentrations of NH_4^+ in porewater and bottom waters of the NRE increased during resuspension events and attributed those increases to ammonification and release of NH_4^+ to overlying waters. In addition, Null et al. (2012) found advective NH_4^+ fluxes from sediments to the water column within the NRE, which they attributed to submarine groundwater discharge. Lastly, Keiber et al. (2006) and Southwell et al. (2010) results suggest that photoproduction of dissolved nutrients from resuspended sediments could be an episodically significant source of dissolved organic and inorganic nutrients to coastal ecosystems. They also suggest that this process may be especially important for continental margins where episodic resuspension events occur, as well as in regions experiencing high riverine sediment fluxes resulting from erosion associated with deforestation and desertification. Thus, it appears that DOM quality in shallow-microtidal estuaries like the Neuse can change rapidly in response to physical mixing processes in a matter of days.

1.4.4 Autochthonous DOM Production within the NRE

Planktonic DOM in the NRE could be a potential source of the NH_4^+ released in October 2010. Paerl et al. (1998) found that large rainfall events and elevated runoff supported phytoplankton blooms within the NRE due to the flushing of nutrients into the estuary from the watershed and precipitation into the basin. Avery et al. (2003) also found that rainwater contributes less DOC overall but deposits more bioavailable DOC relative to Cape Fear River. Therefore, rain DOC appears to be an important source of carbon for secondary productivity resulting in autochthonous DOM production and increased concentrations of chl and DO in surface waters, similar to what was seen after the October 2010 discharge event (Table 1.2). Although a more autochthonous signature in the DOM was seen following the autumn discharge event, mean values for HIX, $SUVA_{254}$, S_R and BIX did not indicate a strong autochthonous signal to the DOM as did those mean values measured during the summer of 2010 (Fig. 1.6A-D). The mixing of autochthonous OM formed in the estuary with terrestrial OM supplied during overland flow is not surprising for this system given its historical eutrophication problem (Paerl et al. 1998; Paerl et al. 1999). Therefore, primary production of algal DOM may be a persistent background signal within the NRE. For example, chl concentrations were relatively low throughout the estuary except following peaks in discharge in the winter of 2011 (Table 1.2). This result suggested that autochthonous DOM derived from planktonic sources forms due to nutrients being flushed in to the NRE during high discharge, but then it is either rapidly degraded or overwhelmed by increased inputs of terrestrial DOM. Typically, autochthonous estuarine DOM is consumed and

respired rapidly by microbial activity as well as altered photochemically (Tulonen et al. 1992; Søndergaard et al. 2000; Amon et al. 2001; Stedmon and Markager 2005).

Photochemical degradation of autochthonous and allochthonous DOM depends on sufficient light exposure (Stedmon and Markager 2005; Osburn et al. 2009). However, in the NRE light is attenuated rapidly in the upper water column as seen by the high PAR attenuation coefficients (Table 1.3) (Mallin and Paerl 1992). Due to the strong light attenuation, photo-degradation likely is restricted to the uppermost layer (just below the surface) of the water column of the NRE, affecting only a small portion of the estuary on a volume basis (Osburn et al. 2009). As DOC concentrations decreased in the NRE from April to September 2010, DOM quality became less humified and less aromatic, but mean chl concentrations remained relatively constant during this period. The patterns observed in DOM indicated a shift in relative abundance of allochthonous to autochthonous DOM, but overall *a*350 and DOC concentrations remained relatively large. Thus, photo-degradation is not a primary removal mechanism of autochthonous DOM within the NRE due to the tremendous amounts of allochthonous DOM detected in the estuary and the near constant mean chl values. Rather, it is likely that autochthonous DOM in the NRE is removed rapidly by microbial activity (Peierls and Paerl 2010).

If autochthonous DOM is degraded within the NRE via microbial activity, it ultimately will be remineralized to CO_2. Overall, the fate of carbon in the NRE is dependent on the rate of transport and primary production, which is primarily influenced by river discharge and wind-driven mixing (Crosswell et al. 2012). More specifically, Crosswell et al. (2012) found that during high river flow conditions, pCO_2 generally decreased from the river

mouth to the Pamlico Sound and resembled a well-mixed system. This trend was not observed during warm, low-flow conditions, where surface water pCO_2 distributions were spatially variable. For example, pCO_2 variability in the lower estuary corresponded to seasonal trends in respiration rates and thermal forcings (Crosswell et al. 2012). Furthermore, Crosswell et al. (2012) found that pCO_2 was maximal during warm, low discharge conditions in the NRE. Additionally, Crosswell et al. (2012) found that net air-water CO_2 fluxes showed high spatial and temporal variability, with a maximum (release) of 271 mmol C $m^{-2}d^{-1}$ during high river flow conditions and a minimum (uptake) of -38 mmol C $m^{-2}d^{-1}$ during wind-driven, high primary productivity conditions. In addition, they determined that the annual air-water CO_2 efflux from the NRE was 4.7 mol C $m^{-2}yr^{-1}$ (Crosswell et al. 2012). These findings coincided with the autochthonous nature of DOM during times of low discharge measured in this study. Thus, we suggest that meso- to eutrophic estuaries such as the NRE can modulate sea-air CO_2 fluxes, in part due to the lability of DOM produced within a given system. Abril and Borges (2004) noted that large spatial and temporal variability in CO_2 emissions within estuaries results from complex interactions of river carbon inputs, sedimentation and resuspension processes, microbial degradation, and tidal exchange. We have shown that these processes can control DOM quality in the NRE. Detailed analysis of these processes within the NRE is necessary in order to shed light on variability of estuarine CO_2 fluxes that may be coupled to estuarine DOM dynamics.

1.5 Conclusions

Our finding suggest that a synergy exists between wind-driven mixing, flushing time, autochthonous POM and DOM production, and resuspension that can result in the re-

introduction of substantial amounts of autochthonous OM and nutrients to shallow, microtidal estuaries on episodic timescales. Using monthly trends in mean DOM properties for the entire reach of the NRE, it was determined that this estuary is dominated by inputs from riverine discharge, yet very clear shifts in DOM quality were apparent as discharge varied. Flushing time estimates will aid in determining whether DOM is autochthonous or allochthonous and if it is processed internally or swept downstream to the Pamlico Sound. More specifically, we found that increases in flushing time may have allowed for the accumulation of autochthonous DOM and could be coupled to a lower input of allochthonous OM from the NRE's watershed. These observations indicate that shallow, microtidal estuaries can generate substantial DOM internally, which can possibly dominate the loadings from land when discharge is low.

Shifts in wind direction and increases in wind speed were important in the resuspension of surface sediments and porewaters in the NRE. Moreover, when resuspension events occurred in October 2010, they resulted in a release of nutrients, specifically NH_4^+, and highly humified, low aromatic DOM—likely originating from algal POM that accumulated over the summer when DOM quality was more autochthonous in origin and flushing time was long. Bottom water conditions with elevated NH_4^+ levels indicated that nutrients stored in the sediments and released during wind-driven mixing play an important role in overall water quality within the NRE.

These findings for the NRE are likely important for other shallow, micro-tidal estuaries that are experiencing accelerating eutrophication. The role of DOM in C and N cycles in estuaries continues to be critical for estuarine biogeochemistry. Thus, understanding

the hydrography and mixing mechanisms of shallow estuaries will be critical to understanding the impacts and fate of anthropogenic and natural OM and nutrient inputs into the NRE and similar systems stressed by eutrophication.

1.6 References

Abril G. and Borges A.V., 2004. Carbon dioxide and methane emissions from estuaries. In Greenhouse Gas Emissions: Fluxes and Processes. Hydroelecrtic Reservoirs and Natural Environments. A. Tremblay, L. Varfalvy, C. Roehm and M. Garneau (Eds.), Environmental Science Series, Springer-Verlag, Berlin, Heidelberg, New York, 187-207.

Amon, R.M.W., Fitznar, H.-P., Benner, R., 2001. Linkages among the bioreactivity, chemicalcomposition, and diagenetic state of marine dissolved organic matter. Limnology and Oceanography, 46: 287-297.

Avery, G. B., Jr., Willey, J.D., Kieber, R.J., Shank, G.C. and Whitehead, R.F., 2003. Flux and bioavailability of Cape Fear River and rainwater dissolved organic carbon to Long Bay, southeastern United States, Global Biogeochemical Cycles, 17(2), 1042, doi:10.1029/ 2002GB001964.

Bauer J.E. and Bianchi T.S., 2011. Dissolved Organic Carbon Cycling and Transformation. In: Wolanski E and McLusky DS (eds.) Treatise on Estuarine and Coastal Science, Vol 5, pp. 7–67. Waltham: Academic Press.

Benner, R., 2002. Chemical composition and reactivity. D.A. Hansell, C.A. Carlson (Eds.), Biogeochemistry of Marine Dissolved Organic Matter, Academic Press, USA, pp. 59–90.

Benner, R. and Strom, M. 1993. A critical evaluation of the analytical black associated with DOC measurements by high-temperature catalytic oxidation. Marine Chemistry, 41(1-3): 153-160.

Bianchi, T.S., 2011. The role of terrestrially derived organic carbon in the coastal ocean: A changing paradigm and the priming effect. Proceedings of the National Academy of Sciences of the United States of America, 108(49): 19473-19481

Borges, A. V., Delille, B., and Frankignoulle, M., 2005. Budgeting sinks and sources of CO2 in the coastal ocean: Diversity of ecosystems counts, Geophysical Research Letter., 32, L14601, doi:10.1029/2005GL023053.

Brinson, M.M., Bradshaw, D.H., and Kane, E.S., 1981. Nitrogen Cycling and Assimilative Capacity of Nitrogen and Phosphorus by Riverine Wetland Forests, UNC-WRRI-81-167.

Burdige, D.J., Kline, S.W. and Chen, W.H., 2004. Fluorescent dissolved organic matter in marine sediment pore waters. Marine Chemistry, 89(1-4).

Burdige, D.J. 2006. Geochemistry of marine sediments. Princeton Univ. Press

Burkholder, J.M. et al., 2006. Comprehensive trend analysis of nutrients and related variables in a large eutrophic estuary: A decadal study of anthropogenic and climatic influences. Limnology and Oceanography, 51(1): 463-487.

Christian, R.R., Boyer, J.N. and Stanley, D.W., 1991. Multiyear distribution patterns of nutrients within the Neuse River Estuary, North Carolina. Marine Ecology Progress Series, 71(3): 259-274.

Coble, P.G., 1996. Characterization of marine and terrestrial DOM in seawater using excitation emission matrix spectroscopy. Marine Chemistry, 51(4): 325-346

Corbett, D.R., Riggs, S. and Giffin, D., 2007. Sediment Resuspension in the Pamlico and Neuse River Estuaries an Additional Source of Nutrients and Contaminants. UNC-WRRI Report No. 363, 1-106.

Corbett, D.R., 2010. Resuspension and estuarine nutrient cycling: insights from the Neuse River Estuary. Biogeosciences, 7(10): 3289-3300.

Crosswell, J. R., M. S. Wetz, B. Hales, and Paerl., H. W., 2012. Air-water CO2 fluxes in the microtidal Neuse River Estuary, North Carolina, Journal Geophysical Research, 117, C08017, doi:10.1029/2012JC007925.

Crusius, J., Berg, P., Koopmans, D.J. and Erban, L., 2008. Eddy correlation measurements of submarine groundwater discharge. Marine Chemistry, 109(1-2): 77-85.

Dillard, S., 2008. Resuspension events and seabed dynamics in the Neuse River Estuary, NC. MSc. Thesis, East Carolina University.

Fellman, J.B., Petrone, K.C. and Grierson, P.F., 2011. Source, biogeochemical cycling, and fluorescence characteristics of dissolved organic matter in an agro-urban estuary. Limnology and Oceanography, 56(1): 243-256.

Goodrich, D. M., Boicourt, W. C., Hamilton, D., and Pritchard, D.W. 1987. Wind-Induced Destratification in Chesapeake Bay. Journal of Physical Oceanography, 17, 2232-2240.

Guo, W.D., Yang, L., Hong, H., Stedmon, C.A., Wang, F., Xu, J., and Yuyuan, X. 2011. Assessing the dynamics of chromophoric dissolved organic matter in a subtropical estuary using parallel factor analysis. Marine Chemistry, 124(1-4): 125-133.

Hedges, J.I, 1992. Global biogeochemical cycles- progress and problems. Marine Chemistry, 39(1-3): 67-93.

Helms, J.R., Stubbins, A., Ritchie, J.D., Minor, E.C., Kieber, D.J., and Mopper, K. 2008. Absorption spectral slopes and slope ratios as indicators of molecular weight, source, and photobleaching of chromophoric dissolved organic matter. Limnology and Oceanography, 53(3): 955-969.

Hood, E., Gooseff, M.N. and Johnson, S.L., 2006. Changes in the character of stream water dissolved organic carbon during flushing in three small watersheds, Oregon. Journal of Geophysical Research-Biogeosciences, 111(G1): 8.

Houghton, R.A., 2007. Balancing the global carbon budget. Annual Review of Earth and Planetary Sciences, 35: 313-347.

Huguet, A., Vacher, L., Relexans, S., Saubusse, S., Froidefond, J.M., and Parlanti, E. 2009. Properties of fluorescent dissolved organic matter in the Gironde Estuary. Organic Geochemistry, 40(6): 706-719.

Kieber R.J., Whitehead R.F., Skrabal S.A., 2006. Photochemical production of dissolved organic carbon from resuspended sediments. Limnol Oceanogr 51:2187–2195.

Kirk, J. T. O., 1994. Light and Photosynthesis in Aquatic Ecosystem. Cambridge University Press.

Köhler, H., Mean, B., Gordeev, V.V., Spitzy, A., and Amon, R.M.W., 2003. Dissolved organic matter (DOM) in the estuaries of the Ob and Yenisei and the adjacent Kara Sea, Russia. Proceedings in Marine Science, 6: 281-310.

Kowalczuk, P., Stedmon, C.A. and Markager, S., 2006. Modeling absorption by CDOM in the Baltic Sea from season, salinity and chlorophyll. Marine Chemistry, 101(1-2): 1-11.

Langenheder, S., Kisand, V., Wikner, J. and Tranvik, L.J., 2003. Salinity as a structuring factor for the composition and performance of bacterioplankton degrading riverine DOC. Fems Microbiology Ecology, 45(2): 189-202.

Lawaetz, A.J. and Stedmon, C.A., 2009. Fluorescence Intensity Calibration Using the Raman Scatter Peak of Water. Applied Spectroscopy, 63(8): 936-940.

Lubben, A., Dellwig, O., Koch, S., Beck, M., Badewien, T.H., Fischer, S., and Reuter. R. 2009. Distributions and characteristics of dissolved organic matter in temperate coastal waters (Southern North Sea). Ocean Dynamics, 59(2): 263-275.

Luettich, R. A. J., S. D. Carr, J. V. Reynolds-Fleming, C. W. Fulcher, and J. E. Mcninch. 2002. Semi-diurnal seiching in a shallow, micro-tidal lagoonal estuary. Continental Shelf Research, 22: 1669–1681.

Maier, C., Hegeman, J.,Weinbauer, M. G., and Gattuso, J.-P., 2009. Calcification of the cold-water coral Lophelia pertusa, under ambient and reduced pH, Biogeosciences, 6, 1671–1680

Mallin, M.A. and Paerl. H.W., 1992. Effects of variable irradiance on phytoplankton productivity in shallow estuaries, Limnology and Oceanopgraphy, 37(1): 54-62.

Mallin, M.A., Paerl, H.W., Rudek, J. and Bates, P.W., 1993. Regulation of estuarine primary production by watershed rainfall and river flow. Marine Ecology-Progress Series, 93(1-2): 199-203.

Mari, X., Rochelle-Newall, E., Torréton, J.P., Pringault, O., Jouon, A., and Migon, C., 2007. Water residence time: A regulatory factor of the DOM to POM transfer efficiency. Limnology and Oceanography, 52(2): 808-819.

Markager, S., Stedmon, C.A. and Sondergaard, M., 2011. Seasonal dynamics and conservative mixing of dissolved organic matter in the temperate eutrophic estuary Horsens Fjord. Estuarine Coastal and Shelf Science, 92(3): 376-388.

Matson, E. A., Brinson, M. M,, Cahoon, D. D.. Davis, G. J.,1983. Biogeochemistry of the sediments of the Pamlico and Neuse River Estuaries, North Carolina. Water Resources Research Institute Report No. 191. Univ. of North Carolina, Raleigh.Null, K.A. et al., 2011. Porewater advection of ammonium into the Neuse River Estuary, North Carolina, USA. Estuarine Coastal and Shelf Science, 95(2-3).

Meixner, T., Huth, A. K., Brooks, P. D., Conklin, M. H., Grimm, N. B., Bales, R. C., Haas, P. A, and Petti, J. R., 2007. Influence of shifting flow paths on nitrogen concentrations during monsoon floods, San Pedro River, Arizona, J. Geophys. Res., 112, G03S03.

Null, K.A., Corbett, D.R., DeMaster, D.J., Burkholder, J.M., Thomas, C.J., and Reed, R.E. 2011. Porewater advection of ammonium into the Neuse River Estuary, North Carolina, USA. Estuarine, Coastal and Shelf Science, 95: 314-325.

Osburn, C. L., Retamal, L., & Vincent, W. F., 2009. Photoreactivity of chromophoric dissolved organic matter transported by the Mackenzie River to the Beaufort Sea. Marine Chemistry, 115(1), 10-20.

Osburn C.L., Handsel L.T., Mikan M.P., Paerl H.W., and Montgomery M.T., (2012). Fluorescence tracking of dissolved and particulate organic matter quality in a river-dominated estuary. Environ. Sci. Technol. 46,8628-36.

Paerl, H.W., Pinckney, J.L., Fear, J.M. and Peierls, B.L., 1998. Ecosystem responses to internal and watershed organic matter loading: consequences for hypoxia in the eutrophying Neuse river estuary, North Carolina, USA. Marine Ecology-Progress Series, 166: 17-25.

Paerl, H.W., Pinckney, J.L., Fear, J.M. and Peierls, B.L., 1999. Fish kills and bottom-water hypoxia in the Neuse River and Estuary: reply to Burkholder et al. Marine Ecology-Progress Series, 186: 307-309.

Paerl, H.W., Valdes, L.M., Peierls, B.L., Adolf, J.E., and Harding, Jr. L.W., 2006. Anthropogenic and climatic influences on the eutrophication of large estuarine ecosystems. Limnology and Oceanography, 52(1, part 2): 448-462.

Paerl, H.W., Rossignol, K.L., Hall, N.S., Peierls, B.L., and Wetz, M.S., 2010. Phytoplankton Community Indicators of Short- and Long- term Ecological Change in the Anthropogenically and Climatically Impacted Neuse River Estuary, North Carolina, USA, 33: 485-497.

Peierls, B.L., Hall, N.S., and Paerl, H.W., 2012. Non-monotonic Responses of Phytoplankton Biomass Accumulation to Hydrologic Variability: A Comparison of Two Coastal Plain North Carolina Estuaries, 35: 1376-1392.

Premuzic, E.T., Benkovitz, C.M., Gaffney, J.S., and Walsh, J.J., 1982. The nature and distribution of organic matter in the surface sediments of world oceans and seas. Org. Geochem., 4:63-77.

Reed, R.E., Glasgow, H.B., Burkholder, J.M. and Brownie, C., 2004. Seasonal physical-chemical structure and acoustic Doppler current profiler flow patterns over multiple years in a shallow, stratified estuary, with implications for lateral variability. Estuarine Coastal and Shelf Science, 60(4): 549-566.

Reynolds-Fleming, J., and R. Luettich. 2004. Wind-driven lateral variability in a partially mixed estuary. Estuarine Coastal and Shelf Science, 60: 395–407.

Rudek, J., Paerl, H.W., Mallin, M.A. and Bates, P.W., 1991. Seasonal and hydrological control of phytoplankton nutrient limitation in the lower Neuse River Estuary, North Carolina. Marine Ecology-Progress Series, 75(2-3): 133-142.

Salmon, C. D., Walter, M. T., Hedin, L. O., and Brown, M. G., 2001. Hydrological controls on chemical export from an undisturbed oldgrowth Chilean forest, J. Hydrol., 253, 69–80.

Saraceno, J.F., Pellerin, B.A., Downing, B.D., Boss, E., Bachand, P.A.M., and Bergamaschi, B.A., 2009. High-frequency in situ optical measurements during storm event: Assessing relationships between dissolved organic matter, sediment concentrations and hydrologic processes, Journal of Geophysical Research, 114, G00F09, doi:10.1029/2009JG000989.

Søndergaard, M., Williams, P.J.B., Cauwet, G., Riemann, B., Robinson, C., Terzic, S., Woodward, E.M.S., and Worm,J., 2000. Net accumulation and flux of dissolved

organic carbon and dissolved organic nitrogen in marine plankton communities. Limnology and Oceanography, 45(5), 1097-1111.

Southwell, M.W., Kieber, R.J., Mead, R.N., Avery, G.B., and Skrabal, S.A., 2010. Effects of sunlight on the production of dissolved organic and inorganic nutrients from resuspended sediment. Biogeochemistry, 98:115-126.

Spencer, R.G.M., Ahad, J.M.E., Baker, A., Cowie, G.L., Ganeshram, R., Upstill-Goddard, R.C., and Uher, G., 2007. The estuarine mixing behaviour of peatland derived dissolved organic carbon and its relationship to chromophoric dissolved organic matter in two North Sea estuaries (UK). Estuarine Coastal and Shelf Science, 74(1-2): 131-144.

Spencer, R.G.M., Aiken, G.R., Butler, K.D., Dornblaser, M.M., Striegl, R.G., and Hernes, P.J., 2009. Utilizing chromophoric dissolved organic matter measurements to derive export and reactivity of dissolved organic carbon exported to the Arctic Ocean: A case study of the Yukon River, Alaska. Geophysical Research Letters, 36.

Spencer, R.G.M., Hernes, P.J., Ruf, R., Baker, A., Dyda, R.Y., Stubbins, A., and Six, J., 2010. Temporal controls on dissolved organic matter and lignin biogeochemistry in a pristine tropical river, Democratic Republic of Congo. Journal of Geophysical Research-Biogeosciences, 115.

Stedmon, C.A. and Markager, S., 2003. Behaviour of the optical properties of coloured dissolved organic matter under conservative mixing. Estuarine Coastal and Shelf Science, 57(5-6): 973-979.

Stedmon, C.A., Markager, S. and Bro, R., 2003. Tracing dissolved organic matter in aquatic environments using a new approach to fluorescence spectroscopy. Marine Chemistry, 82(3-4): 239-254.

Steel, J. 1991. Albemarle-Pamlico estuarine system: technical analysis of status and trends. Albemarle-Pamlico Estuarine Study Report No. 91-01. N.C. Department of Environment, Health, and Natural Resources, Albemarle-Pamlico Estuarine Study, Raleigh, NC.

Stepanauskas, R., Edling, H. and Tranvik, L.J., 1999. Differential dissolved organic nitrogen availability and bacterial aminopeptidase activity in limnic and marine waters. Microbial Ecology, 38(3): 264-272.

Tulonen, T., Salonen, K., and Arvola, L., 1992. Effects of different molecular weight fractions of dissolved organic matter on the growth of bacteria, algae and protozoa from a highly humic lake. Hydrobiologia, 229: 239-252.

Valle-Levinson, A., J. L. Miller and G. H. Wheless. 1998. Enhanced Stratification in the lower Chesapeake Bay following northeasterly winds. Continental Shelf Research, 18, 1631-1647.

Vähätalo. A.V., Wetzel, R.G., and Paerl, H.W., 2005. Light absorption by phytoplankton and chromophoric dissolved organic matter in the drainage basin and estuary of the Neuse River, North Carolina (U.S.A). Freshwater Biology, 50, 477-493.

Weishaar, J.L., Aiken, G.R., Bergamaschi, B.A., Fram, M.S., Fujii, R., and Mopper, K., 2003. Evaluation of specific ultraviolet absorbance as an indicator of the chemical

composition and reactivity of dissolved organic carbon. Environmental Science & Technology, 37(20): 4702-4708.

Zsolnay, A., Baigar, E., Jimenez, M., Steinweg, B. and Saccomandi, F., 1999. Differentiating with fluorescence spectroscopy the sources of dissolved organic matter in soils subjected to drying. Chemosphere, 38(1): 45-50.

1.7 Tables and Figures

Table 1.1: Meteorological data for the NRE during the study period. Data were collected from the CRONOS database of the State Climate Office of North Carolina (wind data- Station ID- KNKT and precipitation data - Station ID-KINS).

Date	Average Speed (m/s)	Max Wind Speed (m/s)	Prevailing Wind Direction (°)	Prevailing Wind Direction	Monthly Sum of Precipitation (mm)
Mar.2010	3.4	5.7	224	WSW	95
Apr.2010	1.7	6.2	58	ENE	18
May.2010	1.2	3.6	69	ENE	32
Jun.2010	2.6	5.7	177	S	184
Jul.2010	2.5	5.1	175	S	74
Aug.2010	1.8	6.2	118	ESE	158
Sept.2010	3.0	4.6	238	WSW	448
Oct.2010	2.6	5.7	168	SSE	20
Nov.2010	2.6	6.7	217	SW	36
Dec.2010	3.4	9.8	123	ESE	82
Jan.2011	3.9	5.7	258	WSW	84
Feb.2011	1.8	5.1	90	E	88

Table 1.2: Mean, minimum and maximum values for DOM and CDOM concentration and qualitative data for the NRE during the study.

Date		Salinity	Temp. (C°)	DO (mg L^{-1})	pH	Chl (μg L^{-1})	DOC (μM)	DON (μM)
Mar. 2010	**Mean**	6.1	7.0	11.3	7.5	15.1	567.2	19.5
	Min	0.1	6.5	8.8	6.7	3.5	446.3	13.2
	Max	17.3	7.9	13.6	8.4	41.4	610.8	22.2
Apr.2 010	**Mean**	3.8	19.9	6.9	7.2	10.0	804.0	30.9
	Min	0.1	18.4	1.6	6.2	5.0	539.3	19.3
	Max	17.4	22.3	12.4	8.6	15.7	1111.7	37.9
May. 2010	**Mean**	4.7	24.1	7.3	7.5	6.4	626.9	25.3
	Min	0.1	22.9	5.8	6.6	3.0	472.4	18.3
	Max	12.2	26.1	10.0	8.5	10.9	732.8	31.3
Jun.2 010	**Mean**	6.3	29.8	5.4	7.6	9.0	599.7	28.7
	Min	0.1	28.3	0.7	7.0	3.4	534.3	25.7
	Max	13.1	33.7	9.1	8.3	14.7	720.1	32.9
Jul.2 010	**Mean**	9.6	29.6	6.2	7.7	4.9	530.7	23.0
	Min	0.1	28.7	2.3	7.2	0.3	451.4	19.3
	Max	17.5	32.2	8.3	8.2	9.5	729.4	27.3
Aug.2 010	**Mean**	10.2	30.4	5.2	7.8	7.3	511.9	23.7
	Min	0.1	29.3	0.7	6.8	3.7	400.7	20.3
	Max	18.6	32.0	9.1	8.4	13.7	638.9	27.1

Table 1.2 Continued

Sept. 2010	**Mean**	9.1	26.1	6.3	7.7	9.6	557.2	29.5
	Min	0.1	24.9	0.6	6.9	3.9	468.4	27.1
	Max	15.8	27.2	9.4	8.2	35.6	718.6	33.4
Oct.2 010	**Mean**	11.5	19.8	4.9	7.4	7.1	668.2	34.6
	Min	0.1	17.8	0.5	6.8	3.5	389.0	24.1
	Max	20.8	21.6	8.9	7.8	13.2	908.8	45.2
Nov.2 010	**Mean**	7.5	13.9	9.1	7.8	8.5	682.5	34.0
	Min	0.1	12.9	7.8	7.4	4.5	589.5	27.5
	Max	13.5	14.8	10.5	8.0	14.0	755.9	42.8
Dec.2 010	**Mean**	9.5	3.7	12.1	7.9	9.0	599.0	27.8
	Min	0.1	2.6	10.9	7.4	4.1	517.6	23.4
	Max	16.1	5.5	13.0	8.6	13.7	654.9	31.1
Jan.2 011	**Mean**	10.4	4.8	12.9	8.0	25.3	530.7	21.6
	Min	0.1	3.6	11.1	7.5	4.5	445.0	18.8
	Max	17.5	6.0	14.2	9.2	70.4	609.7	24.4
Feb.2 011	**Mean**	7.4	8.4	11.2	8.1	20.7	599.3	23.7
	Min	0.1	7.4	8.6	7.3	7.4	496.5	16.4
	Max	15.1	9.1	13.5	8.7	50.3	691.7	28.8

Table 1.2 Continued

Date		a350 (m^{-1})	Max Fl (Q.S.U.)	C:N	SUVA (L mg^{-1} C m^{-1})	S_R	HIX	BIX
Mar. 2010	**Mean**	14.4	35.6	29.4	3.8	0.9	10.0	0.5
	Min	7.0	15.6	23.9	1.7	0.8	7.8	0.4
	Max	19.7	42.3	36.0	5.0	0.9	12.9	0.6
Apr. 2010	**Mean**	21.7	49.2	27.2	3.8	0.8	12.5	0.5
	Min	9.5	33.7	18.5	1.5	0.7	9.7	0.4
	Max	32.8	75.5	55.5	5.5	0.9	16.2	0.6
May .2010	**Mean**	13.0	40.4	25.5	3.4	0.9	9.1	0.6
	Min	8.2	27.0	15.1	2.5	0.8	7.4	0.5
	Max	18.4	51.0	36.5	4.3	1.0	10.3	0.6
Jun. 2010	**Mean**	10.6	39.4	20.9	2.9	0.9	9.4	0.6
	Min	6.7	31.3	17.2	2.3	0.8	7.8	0.5
	Max	16.7	54.1	23.0	3.8	1.0	12.1	0.7
Jul.2010	**Mean**	7.7	31.6	23.2	2.8	1.0	7.3	0.7
	Min	5.4	22.8	18.1	2.3	0.9	5.6	0.6
	Max	12.3	43.3	29.5	3.4	1.1	8.4	0.8
Aug. 2010	**Mean**	9.0	32.0	21.5	3.0	1.1	6.9	0.7
	Min	4.9	22.6	19.3	2.3	0.8	5.0	0.6
	Max	15.8	44.9	25.2	4.0	1.3	9.5	0.8

Table 1.2 Continued

Sept. 2010	**Mean**	10.0	40.6	18.9	3.2	1.0	6.8	0.7
	Min	5.4	24.2	15.0	2.4	0.8	4.4	0.6
	Max	20.4	68.2	22.2	4.6	1.2	10.2	0.8
Oct. 2010	**Mean**	16.2	45.3	20.3	3.5	0.9	10.0	0.6
	Min	4.3	17.7	11.3	1.2	0.7	5.8	0.5
	Max	31.3	84.9	32.4	7.6	1.1	14.1	0.7
Nov. 2010	**Mean**	12.6	47.5	20.4	3.0	0.9	9.6	0.6
	Min	7.9	36.5	17.0	1.6	0.7	8.4	0.5
	Max	14.8	57.5	25.2	4.4	1.0	11.4	0.6
Dec. 2010	**Mean**	12.1	35.3	21.6	3.3	0.9	8.5	0.6
	Min	7.7	24.9	17.9	2.4	0.7	6.2	0.5
	Max	19.1	45.4	24.4	4.2	1.0	11.0	0.7
Jan. 2011	**Mean**	9.2	30.1	24.7	3.0	0.9	7.8	0.6
	Min	6.2	23.0	19.1	2.5	0.8	6.1	0.5
	Max	12.3	35.4	29.0	3.7	1.0	9.6	0.7
Feb. 2011	**Mean**	12.6	34.2	25.7	3.2	0.9	8.4	0.6
	Min	6.8	23.0	20.6	2.8	0.8	6.8	0.5
	Max	18.0	44.2	33.3	4.0	1.1	11.1	0.7

Table 1.3: Monthly mean attenuation coefficients, *k* (in m^{-1}), during the study.

Date	Mean *k* (m^{-1})
Mar.10	1.53
Apr.10	1.33
May.10	1.44
June.10	1.36
July.10	1.13
Aug.10	1.39
Sept.10	1.23
Oct.10	1.28
Nov.10	1.12
Dec.10	0.94
Jan.11	1.06
Feb.11	1.00

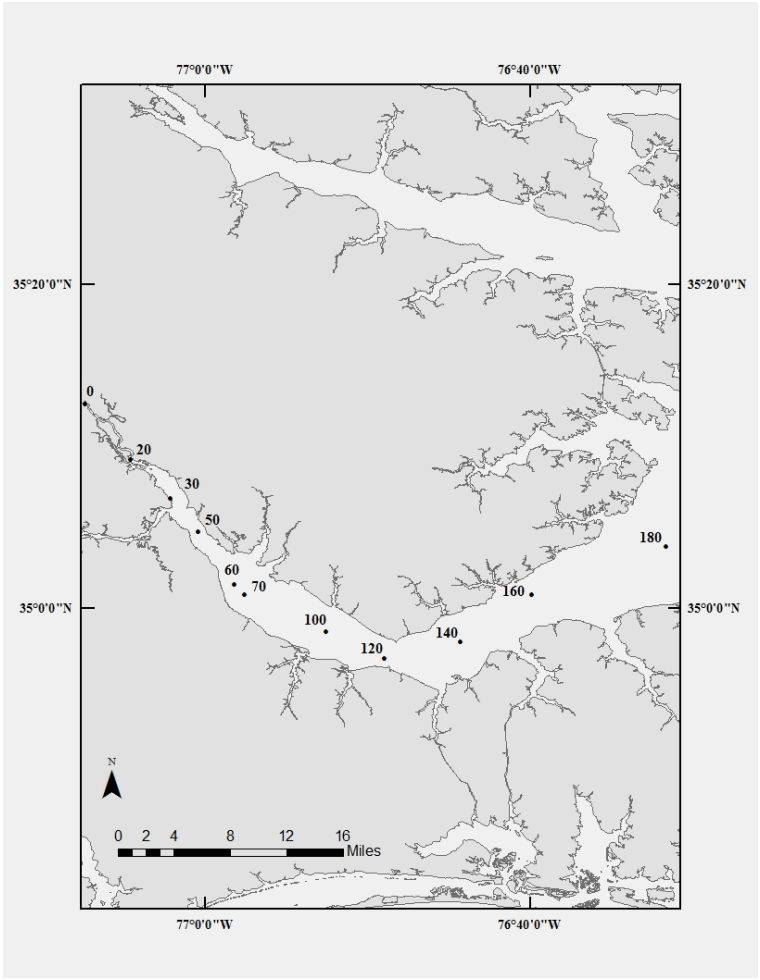

Figure1.1: Map of Neuse River Estuary including ModMon sampling sites (courtesy of Lauren Handsell).

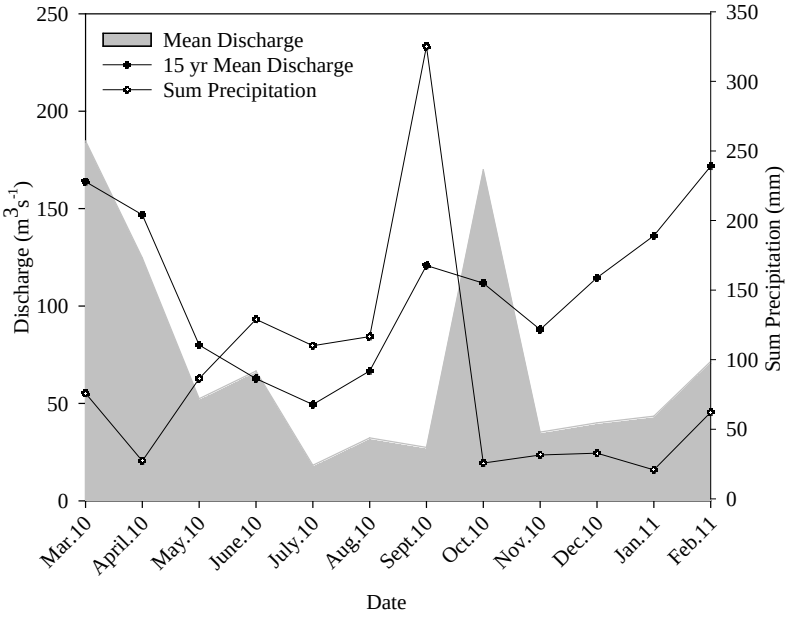

Figure 1.2: Mean discharge from March 2010 thru February 2011, monthly 15 year mean discharge from USGS Station Fort Barnwell and total precipitation from North Carolina Climate Office CRONOS database, Station KINS.

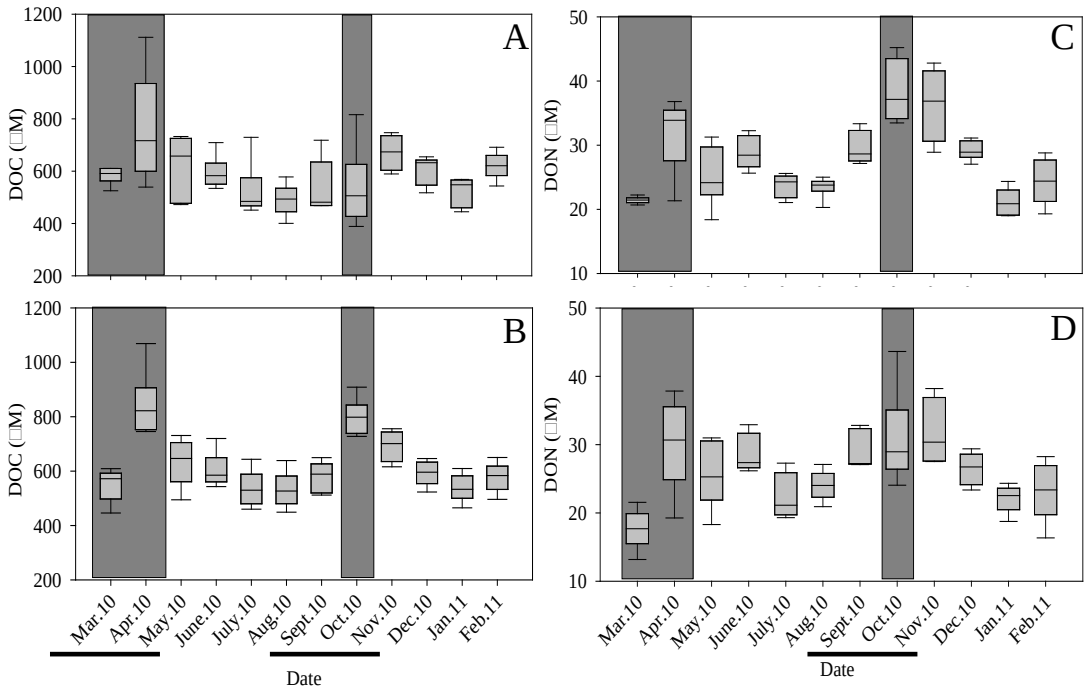

Figure 1.3: Range and mean of surface DOC (3A), mean bottom DOC (3B), mean surface DON (3C) and mean bottom DON (3D) concentrations within the NRE. Gray area represents peak discharge periods at Fort Barnwell. Black lines indicate significantly different seasons ($P<0.05$). Surface and bottom waters were not significantly different from each other ($P>0.05$).

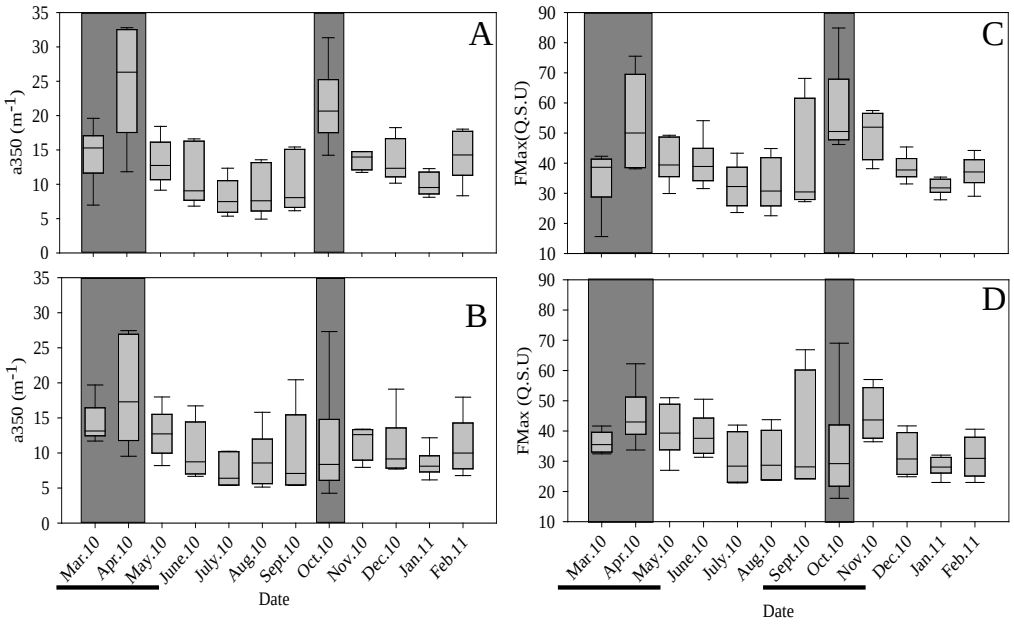

Figure 1.4: Range and mean of surface *a*350 (4A), mean bottom *a*350 (4B), surface FMax (4C), mean bottom FMax (4D) concentrations within the NRE Gray area represent peak discharge periods at Fort Barnwell within the NRE. Black lines indicate significantly different seasons ($P<0.05$). Surface and bottom waters were significantly different from each other ($P<0.05$).

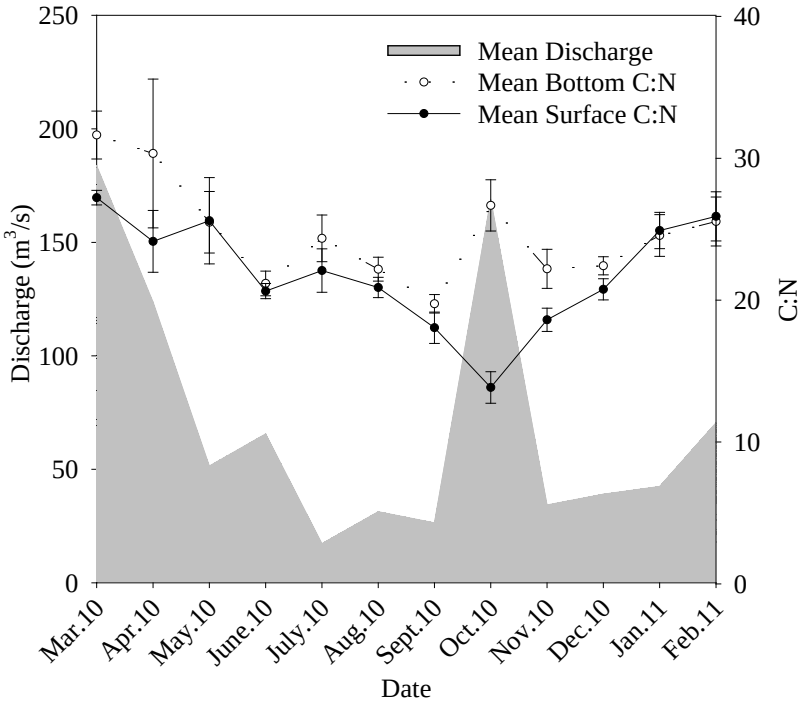

Figure 1.5: Mean surface and bottom C:N values compared to discharge at Fort Barnwell, NC.

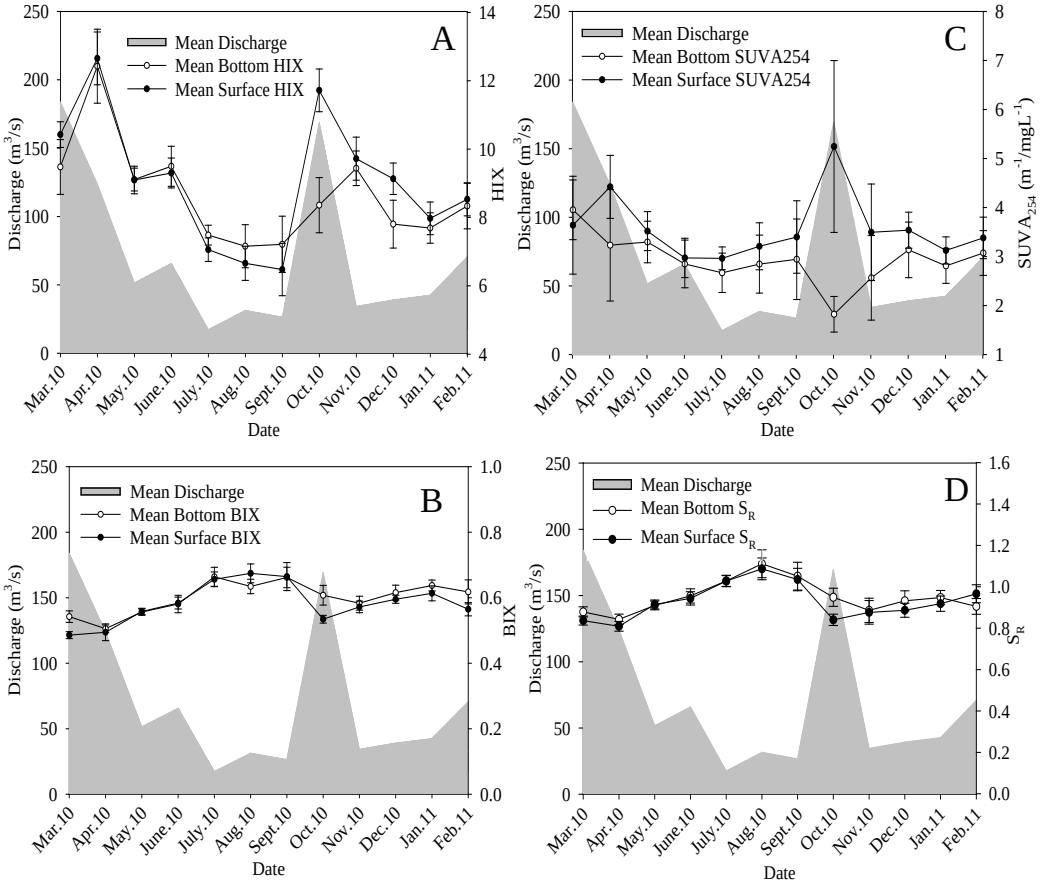

Figure 1.6: Mean surface and bottom HIX (6A), BIX (6B), $SUVA_{254}$ (6C) and S_R (6D) compared to discharge at Fort Barnwell, NC.

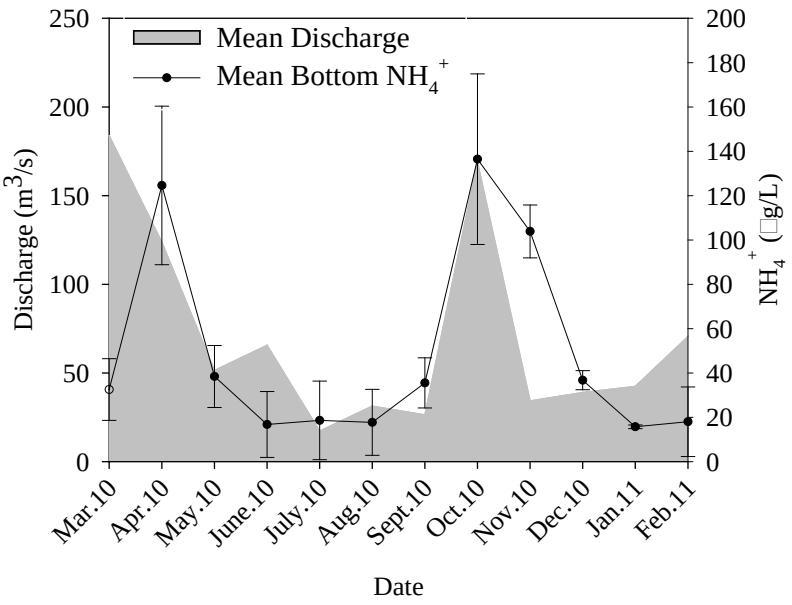

Figure 1.7: Mean bottom ammonium (NH_4^+) concentrations compared to discharge at Fort Barnwell, NC.

Chapter 2: Characterizing the quality and source of chromophoric dissolved organic matter (CDOM) in the Neuse River Estuary, eastern North Carolina: a preliminary study using PARAFAC modeling.

2.1 Introduction

Dissolved organic matter (DOM), in coastal rivers and estuaries is a heterogeneous mixture of aromatic and aliphatic compounds, and its composition varies spatially and temporally with source (Bauer and Bianchi 2011). Primary and secondary production in these systems can be quite high, and thus coastal rivers and estuaries transport and transform DOM as they act as transition zones between terrestrial and marine environments (Paerl et al. 1998; Markager et al. 2011; Osburn et al. 2012). Organic matter (OM) source (whether terrestrial or planktonic) and matrix effects (such as salinity and pH) influence the chemical structure of DOM in estuaries, and therefore, affects its bioavailability, photo-reactivity, and its overall fate in these systems (Jaffé et al. 2004; Boyd et al. 2010; Pace et al. 2012; Osburn et al. 2012; Cawley et al. 2013).

Chromophoric dissolved organic matter (CDOM), the light absorbing fraction of DOM in natural waters, can be used to quantify dissolved organic carbon (DOC) concentrations and to characterize DOM sources in natural waters. CDOM absorbs light over a broad range of light wavelengths, the strongest in the ultraviolet (UV) region (200-380nm) and diminishes to near zero in the visible light red region (380-780nm) and near infrared (IR) region (780-800nm).Previous studies in varying coastal waters have shown a generally strong correlation between absorption coefficients and DOC. Overall, CDOM contributes approximately 20% to the total DOC pool in the open ocean and can contribute up to 70% to

the total DOC pool in coastal waters (Coble 2007). The fraction of DOC that is CDOM varies both temporally and spatially as a consequence of the variability in (1) inputs of terrigenous OM, (2) sediments/detritus OM inputs and (3) autochthonous OM inputs from *in-situ* processes (Del Vecchio and Blough, 2004). Furthermore, the average concentration of the non-CDOM DOC fraction ranged from 230-280 μM within the Baltic Sea (Ferrari et al. 1996; Kowalczuk et al. 2010a). Additionally, previous work in other oceanic coastal regions (Middle Atlantic Bight, Delaware Bay and Chesapeake Bay) has found that the average concentration of non-CDOM DOC fraction (determined at an absorption wavelength at 355 nm) ranges from 50–100 μM (Rochelle-Newall and Fisher, 2002; Del Vecchio and Blough, 2004; Mannino et al. 2008).

CDOM can be used to characterize the source of DOM using two optical methods: UV-visible absorbance and fluorescence spectroscopy (e.g. Coble, 1996; Stedmon and Markager, 2003). For example, CDOM absorbs light in the ultraviolet (UV) region (200-380nm), the visible light region (380-780nm) and near infrared (IR) region (780-800nm). The absorbance and fluorescence of CDOM offers a cheap and sensitive means for obtaining information on a diverse group of organic compounds. By using this technology to analyze the spatial and temporal variability of CDOM within estuaries, information pertaining to OM source and fate across the freshwater-marine continuum can be obtained (Fellman et al. 2011; Osburn et al. 2012; Murphy et al. 2014). Specifically, by measuring the emission spectra of DOM at several excitation wavelengths, an excitation-emission matrix (EEM) can be obtained, which represents the total fluorescence from an unknown number of fluorophores. Previous studies have revealed several EEM peaks, originally designated A and C (terrestrial

humic acids and fulvic acids), T (protein resembling the amino acid tryptophan), and M (microbial humic material). Over the past decade, it has become common practice to resolve EEM datasets mathematically using parallel factor analysis (PARAFAC). PARAFAC provides a statistical means to analyze the data by reducing the EEM dataset into smaller building blocks, referred to as spectral components (Ohno and Bro 2006; Stedmon et al. 2003; Murphy et al. 2014). Each EEM within the dataset is modeled, based on the same building blocks or validated components. Thus, all EEMs are composed of varying amounts of the same building blocks, reflecting variable contributions of each component.

A previous study on the Neuse River Estuary (NRE) conducted by Osburn et al. (2012) used a combined POM-DOM (particulate and dissolved OM) PARAFAC model and principal components analysis (PCA) to determine that the source of OM within the NRE varies with discharge and is comprised of allochthonous and autochthonous material. They determined these changes over a short time period (ca. 2 weeks) after flood waters entered the estuary from a Category 1 hurricane. In addition, they found that the advection of pore water DOM from surface sediments into overlying waters could increase the planktonic quality of DOM in the NRE. Similarly to Osburn et al. (2012), Dixon et al. (submitted) also determined that the NRE is dominated by inputs from riverine discharge, yet very clear shifts in DOM quality were apparent as discharge varied. Moreover, Dixon et al. (submitted) found that a synergy exists between wind-driven mixing and flushing time within the NRE. Their findings suggest that resuspension events caused by these two mechanisms result in the re-introduction of substantial amounts of autochthonous OM and nutrients to NRE on episodic timescales. The observations of both studies further indicated that shallow, microtidal

estuaries generate substantial amounts of DOM internally, which can possibly dominate the loadings from land when discharge is low.

In this study we build upon previous work by Osburn et al. (2012) and Dixon et al. (submitted) to further examine DOM dynamics along the freshwater to marine contiuum. PARAFAC statistical analysis of DOM fluorescence was combined with a PCA to provide insight on the overall change in DOM quality within the NRE over varying hydrological conditions. We hypothesized that our PARAFAC model will demonstrate variations in CDOM composition within the NRE. Specifically, we suggest that our PARAFAC model will identify multiple, unique pools of riverine and planktonic inputs. Additionally, this information will shed light on how CDOM composition can influence CDOM quality within the NRE. Lastly, the ultimate goal of this study was to further assess OM sources and how OM is transformed within the NRE.

2.2 Methods

2.2.1 Study Station

The NRE is a drowned river valley and a major tributary of the second largest estuarine complex and lagoonal environment in the United States, Albemarle-Pamlico Sound (Steel, 1991) (Fig. 2.1). The watershed is approximately 16,108 km^2, and the estuary/sound complex has an average surface area of 455 km^2 and an average depth is about 2.7 m (Paerl et al. 2010). River discharge rates vary from 50 to 1000 m^3s^{-1} resulting in flushing times that range from 20 to 200 days (Luettich et al. 2002; Crosswell et al. 2012). The limited oceanic exchange of the NRE contributes to the long residence and slower flushing times, which aid in extensive recycling of nutrients in the water column (Christian et al. 1991; Steel, 1991).

Furthermore, over the past few decades, accelerated eutrophication and OM loading driven by urban development and expanding agricultural operations in the NRE watershed have resulted in annual fish kills, harmful algal blooms, and poor water quality in the NRE (Paerl et al. 1998, 2010; Burkholder et al., 2006). The flow regime in the mesohaline estuary is surface outflow and bottom-water inflow with minimal tidal influence (Reed et al., 2004; Null et al. 2011). Winds are an important mixing force in this shallow system and play a significant role in sediment resuspension, influencing OM and nutrient release from the benthic environment (Reed et al., 2004; Corbett, 2010; Null et al. 2011).

2.2.2 River Discharge at Fort Barnwell, NC

River discharge data were downloaded using the USGS National Water Information System web interface. For the Neuse River, this was Fort Barnwell (USGS station #02091814), which is 24 km upstream of station NR0. Discharge data were divided by the ratio of gauged to total watershed area (0.69 for the NRE) as a correction for un-gauged watershed discharge (Peierls et al. 2012). Flushing time for the lower NRE was calculated by dividing the volume of the NRE by the average discharge over each month.

2.2.3 Sample Collection

Samples were collected monthly between March 2010 and February 2011 during the NRE modeling and monitoring (ModMon: http://www.unc.edu/ims/neuse/modmon/index.htm) sampling cruises that spanned the main axis of the estuary (Fig. 2.1). Physical and chemical properties of the water column were sampled spanning freshwater, oligohaline and mesohaline segments of the NRE. Samplings consisted of vertical profiles of physical, chemical and irradiance conditions (salinity,

dissolved oxygen (DO), in vivo fluorescence (chl), photosynthetically active radiation (PAR, 400-700 nm) and pH) in the water column and were obtained with a YSI 6600 multi-parameter water quality sonde (Yellow Springs Inc., Yellow Springs, OH, USA) (Table 2.1).

Water was collected at the surface and at roughly 0.5 meters above the bottom, stored in acid-cleaned 1 liter HDPE bottles, and kept cool and shaded during transport to the Institute of Marine Science (IMS). Additionally, samples were stored in the dark at 4 °C until shipped to N.C. State University. Samples were vacuum-filtered through Sterivex-GP 0.22 μm filters into pre-cleaned glass vials (combusted in an oven at 550°C for at least six hours) with Teflon coated lids.

2.2.4 Dissolved Organic Carbon (DOC) and Dissolved Organic Nitrogen (DON)

Dissolved organic carbon (DOC) and dissolved organic nitrogen (DON) samples, collected by UNC-IMS investigators, were pressure filtered through a pre-combusted, 142 mm Whatman GF/F filter and a 142 mm Millipore Express Plus 0.22 μm effective particle size removal polyethersulfone membrane filter arranged in series. DOC measurements were made using high temperature combustion techniques on a Shimadzu model TOC5000, equipped with an ASI-5000A autosampler (Benner & Strom 1993). Acidified (HCl, pH < 2) samples were sparged for 8 min with air to drive off DIC. Background checks revealed complete removal of DIC by this treatment. Reported values represent the average of 3 injections. Dissolved organic nitrogen (DON) was calculated as the difference between total dissolved N (TDN) and total dissolved inorganic N (DIN: sum of nitrite, nitrate, and ammonium) measured on a Lachat QuikChem 8000 flow injection analyzer (Lachat, Milwaukee,WI, USA). C:N values, the molar ratio of DOC to DON, were calculated and

used as an indicator of DOM source, i.e., terrestrial or vascular plant derived C:N values are generally greater than 15 and C:N values less than 8 favor marine (or more broadly autochthonous) sources of DOM (Premuzic et al. 1982).

2.2.5 Absorption and Fluorescence Spectra of DOM

Before analysis the samples were allowed to warm to room temperature. The absorption coefficients were measured in a 1 cm quartz cuvette over the 240– 800 nm on a Varian 300 UV spectrophotometer and referenced to air. Absorption spectra were blank-corrected by subtracting the absorbance of Milli-Q water from each sample and converted to Napierian absorption coefficients (a_λ, m^{-1}) at each wavelength (λ):

$$a_\lambda = 2.303/A_\lambda * L$$

where A_λ is the blank corrected spectrophotometer absorbance reading at wavelength λ and *L* is the optical pathlength in meters (Kirk 1994).

A Varian Eclipse spectrofluorometer was used to obtain excitation emission matrix (EEM) fluorescence spectra of NRE DOM. Although higher resolution is possible, EEMs were constructed by concatenating emission (Em) wavelengths sampled every 2-nm from 300 to 600 nm using excitation (Ex) wavelengths from 240 to 450 at 5-nm intervals. The excitation lamp was set at 600 or 800 volts, with an Ex/Em slit width of 5-nm for both, a scan rate of 9600 nm/min and an integration time of 0.0125 seconds. Scans were corrected for primary and secondary Rayleigh and Raman (natural scattering properties of pure water after it absorbs light) scattering by Milli-Q water blank subtraction and for instrument bias prior to correction for any inner-filtering effect (Stedmon and Bro 2008). Smoothing of the data was also necessary to remove instrument noise and scatter, and to remove an area of the EEM

where signal to noise ratio was low. Following spectra correction, the data were converted from arbitrary units (A.U.) to Raman units (R.U.) and then converted and reported as quinine sulfate equivalents (ppb QSE) (Laewetz and Stedmon 2009). All data processing and corrections were performed using in-house scripts written for Matlab (Mathworks, Inc., Natick, MA).

2.2.6 Parallel Factor Analysis (PARAFAC)

A parallel factor analysis (PARAFAC) model was built using the DOMFluor and N-way toolbox (Stedmon and Bro 2008). 231 EEMS from the NRE were used for the NR-PARAFAC model and an additional 33 EEMs from the Trent River were used for the NRTR-PARAFAC model. PARAFAC statistically decomposes multi-way data into a set of three linear terms and a residual array to produce robust, non-biased models. In this approach X_{ijk} is the intensity of fluorescence for the *i*th sample at emission wavelength *j* and excitation wavelength *k*. F defines the number of components in the model and parameter *a* is directly proportional to the concentration of the *f*th analyte in the *i*th sample. Due to the wide range in fluorescent intensity of DOM samples, all EEMs were normalized to their maximum fluorescence intensity prior to PARAFAC modeling. Normalizing each EEM to its maximum signal gives high and low concentration samples similar weightings, thus allowing the model to focus on the chemical variations between samples rather than the magnitude of total signals. Moreover, normalization to the maximum fluorescence sets all EEMs between 0 and 1, so the most variability in the Ex and Em loadings can be modeled. This also increases the chance that minor peaks will be revealed. Data normalization can be reversed after validating the model, by simply multiplying the scores of each component by the mean fluorescence

intensity (Fmax**)** of the sample. For both models, five components, referred to as C1 through C5, were split-half validated from each data set under non-negativity constraints. A single EEM was identified as an outlier and removed from the NR-PARAFAC model and four EEMs were identified as outliers and removed from NRTR-PARAFAC model.

2.2.7 OpenFluor Analysis

In order to quantitatively compare fluorescence spectra among studies, the open-access spectral database established by Murphy et al. (2014), OpenFluor spectral database, was used. A search query was implemented on the validated PARAFAC spectra from this study and quantitatively similar spectra were retrieved from the database. OpenFluor spectral database identified similar spectra as having Tucker (θ) congruence exceeding 0.95 on the excitation and emission simultaneously. PARAFAC models in the OpenFluor database are accompanied by a synopsis of the study that generated the data, a short methodological description and an active link to the published record. Furthermore, matched data can be downloaded from the OpenFluor website.

2.2.8 Statistical Analysis

All statistical tests were performed using Excel and Matlab v.R2009a software. Nonparametric tests were applied when assumptions of parametric tests could not be met with either non-transformed or transformed data. A one-way analysis of variance (ANOVA) or a Kruskal-Wallis test was used to examine the individual effects of season and spatial location on physical and chemical variables at a 95% confidence interval (i.e., $P<0.05$) unless otherwise specified. Significant differences between seasons and spatial location were determined using either a Tukey or Dunn post-hoc test. A principal component analysis

(PCA) was run on the correlation matrix of 231 samples and eigenvalues greater than one were retained. The PCA scores show the extent of the variance in the data, and are plotted as a cluster diagram on the basis of the two biggest causes of variance, PC1 and PC2.

2.4 Results

2.3.1 Physical Mixing Patterns & Water Quality Parameters

Regional climate trends for the area can be described as a wet period beginning in the late fall of 2009 that extended through April 2010 (Peierls et al. 2012). Additionally, in late September/early October 2010, the remnants of Tropical Storm Nicole combined with a stationary low-pressure system to produce record rainfall and discharge in the region (National Climatic Data Center 2010). This was observed in the peaks in riverine discharge, which were the highest in spring and autumn, with peak monthly mean discharge values of 266 $m^3 s^{-1}$ and 179 $m^3 s^{-1}$ in March and April 2010 and 245 $m^3 s^{-1}$ in October 2010 (Table 2.1). Previous findings illustrate how overland flow and discharge are responsive to precipitation events and influence the large inputs of dissolved materials via runoff that the NRE received (Mallin et al. 1993; Paerl et al. 1998; Fellman et al. 2011).

Within the NRE, DO concentrations, discharge, chl and temperature varied between stations head of the NR (NR)), the historic chlorophyll maximum (NR70) and the mouth of the NR (NR180) (Table 2.1). At all three stations, mean DO concentrations reached a maximum of 11.5 mg L^{-1} in March 2010 and decreased to a minimum of 5.6 mg L^{-1} in May 2010 as discharge decreased during the spring. From the late spring and early autumn (May through September 2010) DO concentrations were the lowest measured at all three stations, and corresponded to lower discharge. In October 2010 through February 2011, DO

concentrations increased from 8.6 mg L^{-1} to 13.4 mg L^{-1} following increases in riverine discharge in October 2010. In addition to this, DO concentrations were positively correlated with pH ($R^2 = 0.25$, $P<0.05$). Furthermore, the relationship between DO and temperature was highly correlated ($R^2 = 0.80$, $P<0.05$). Increases in DO values also corresponded to increases in observed mean chl concentrations at all three sampling stations. For instance, at station NR0, in the winter of 2011, chl concentrations increased to 9.6 mg L^{-1} as DO concentrations increased to 12.5 mg L^{-1}. Additionally, at station NR70 chl concentrations increased to 76.8 mg L^{-1} in the winter of 2011 as DO concentrations peaked at 14.2 mg L^{-1}. Lastly at station NR180 DO values peaked at 12.5 mg L^{-1} and corresponded to increases in chl concentration of 28.1 mg L^{-1} during the spring of 2010. Furthermore, at NR70, the historic chl maximum, a significant and positive correlation ($R^2 = 0.45$, $P<0.05$) between DO values and chl concentrations was observed, with increases in DO values corresponding to increases in chl values.

2.3.2 NR-PARAFAC Components

Our NR-PARAFAC model of DOM fluorescence in the NRE produced five spectral components of allochthonous and autochthonous OM origin. Contour plots of each component, the excitation and emission loadings, and their split half validations are shown in Figure 2.2. For comparison to PARAFAC models from a variety of aquatic systems, the OpenFluor spectral database was used to identify similar PARAFAC spectra at a 95% confidence interval to those identified in the NRE (Table 2.3; Murphy et al. 2014). OpenFluor is a new database, and therefore, our evaluation was limited to the existing PARAFAC models contributed to OpenFluor. When less than three statistical matches were

made for any one component using the OpenFluor spectral database, visual evaluations of the PARAFAC components validated in this study were made against other PARAFAC models from a variety of environments.

Component 1 (C1) was characterized as a ubiquitous terrestrial humic-like fluorophore group, closely resembling humic acids. Four other sources in the OpenFluor spectral database also confirm this description (Stedmon et al. 2007; Yamashita et al. 2010; Jørgenson et al. 2011; Murphy et al. 2011). Components similar to our C1 were identified in a range of PARAFAC models fit to EEMs measured on a range of environments such as the Baltic Sea to wastewater treatment plants (Stedmon et al. 2007; Jørgenson et al. 2011; Murphy et al. 2011). Additionally, Stedmon and Markager (2005) found a similar component, C1 (ex/em maximum <250 nm/448 nm), in their PARAFAC model of the Horsens Estuary in Denmark. In this study, they determined that this component was from a UVC (ultraviolet C, short wavelength) humic fraction that closely resembled terrestrially derived humic acids.

Component 2 (C2) was characterized as a planktonic derived component and was statistically similar to six spectra in the OpenFluor spectral database. Murphy et al. (2011) identified a component similar to C2 in four recycled water treatment plants located in Australia. In one of the water treatment plants sampled by Murphy et al. (2011) C2 was also characterized as a wastewater/nutrient enrichment tracer. Yamashita et al. (2010) characterized C2 as a microbial-like component in the Florida Everglades. Visual comparison to the PARAFAC model validated by Fellman et al. (2011) suggested that C2 is similar to their C6, which they associated with humic-like material having less aromaticity than

terrestrial sources. Furthermore, Fellman et al. (2011) found that the fluorescence intensity of C6 was strongly correlated with both particulate nitrogen (PN) and total chlorophyll, thus suggesting phytoplankton production was contributing to this component. Lastly, Stedmon et al. (2007) characterized a similar component to C2 in the Baltic Sea as a humic-like component that was susceptible to photodegradation.

Component 3 (C3) can be described as a terrestrial humic-like component, whose origin has been attributed to soil fulvic-like material. Visual comparison of the excitation/emission spectra of C3 to the excitation/emission spectra of soils and soil related material by Senesi (1990) also confirm this description. Based on the results from the OpenFluor spectral database, C3 matched eight other terrestrial-like spectra modeled in DOM from a wide range of aquatic systems such as the South Atlantic Bight, tropical rivers in Venezuela and boreal lakes (Kowalczuk et al. 2009; Yamashita et al. 2010; Kothawala et al. 2013).

The spectral features of component 4 (C4) suggested that it is sourced from the amino acid tryptophan, likely due to recent biological production. C4 matched the OpenFluor spectral database in a single study of boreal lakes by Kothawala et al. (2013). Visual comparison to the combined POM-DOM PARAFAC model for the NRE validated by Osburn et al. (2012) suggested that C4 is similar to their C5, which was associated with protein-like material, specifically ubiquitous tryptophan. Moreover, Fellman et al. (2011) validated two components in the eutrophic Swan-Canning estuary in Australia as protein-like with fluorescence characteristics similar to tryptophan and tyrosine. They also determined that protein-like components could be an indicator of DOM lability and bacterial production.

It was difficult to classify component 5 (C5) statistically because it did not match any PARAFAC model in the OpenFluor spectral database (accessed in March 2014). Visual comparison to the combined POM-DOM PARAFAC model validated by Osburn et al. (2012) for the NRE suggest that this component strongly resembles possible molecular components of aquatic fulvic acids as well as constituents of tannins (e.g, gallic acid, Maie et al. 2007). C5 had an ex/em maximum of 335 nm/438 nm and is slightly blue-shifted relative to component 6 (ex/em maximum 350 nm/444 nm) as reported by Osburn et al. (2012) for both POM and DOM in the NRE. In addition, Stedmon and Markager (2005) identified similar components, C2 (ex/em maximum 385 nm/504 nm) and C4 (ex/em maximum 360 nm/440 nm), in their PARAFAC model of the Horsens Estuary in Denmark. They determined that these components were a UVA (ultraviolet A, long wavelengths) humic fraction that closely resembled terrestrially derived fulvic acids. Furthermore, Lochmuller and Saavedra (1986) found that a soil fulvic acid extract had an excitation maximum at 390 nm and an emission maximum at 509 nm. Lastly, Senesi (1990) observed fulvic acid excitation and emission spectra originating from estuarine waters and sediments generally have maximum emission intensities within a lower range of wavelengths (410-450). These studies suggest that component 5 in this study, is likely derived from terrestrial material, specifically soil leachate fulvic acids.

2.3.3 NR-TR PARAFAC Components

The Neuse River and Trent River (NR-TR) combined PARAFAF model of DOM fluorescence produced five-components of allochthonous and autochthonous OM origin (Table 2.5). This model was statistically compared to the NR PARAFAC model using the

Tucker Congruence Coefficient test, and compared to a variety of aquatic systems using the OpenFluor spectral database at a 95% confidence interval (Murphy et al. 2014). Visual evaluations of PARAFAC models were made when less than three statistical matches were made for any one component using the OpenFluor spectral database.

In the NR-TR PARAFAC model, both planktonic- and protein-like components, C3 and C5, were not statistically different from NR PARAFAC planktonic- and protein-like components, C2 and C4 ($P>0.05$). Component C3 can be described as a planktonic derived component, which was statistically similar to component C2 in the NR PARAFAC model and to seven spectra in the OpenFluor spectral database. Additionally, component C5 has been identified as being sourced from the amino acid tryptophan, likely due to recent biological production. C5 was statistically similar to component C4 in the NR PARAFAC model and matched the OpenFluor spectral database in four other studies.

The remaining three components, on the other hand, were statistically different ($P<0.05$). Component C2 in the NR-TR PARAFAC model matched fourteen studies in the OpenFluor spectral database and can be described as a terrestrial humic-like material, which is likely derived from soil fulvic-like component. Based on the OpenFluor spectral database, this component has been seen in a wide range of environments, such as: trans-oceanic cruises, tropical rivers in Venezuela and in the Brandenburg (North German plains, Germany) (Murphy et al. 2008; Yamashita et al. 2010; Graeber et al. 2012). Visual comparison of the excitation/emission spectra of C2 to the excitation/emission spectra of soils and soil related material by Senesi (1990) also confirm this description.

Component C1 matched two studies in the OpenFluor spectral database and can be described as terrestrial humic-like material (Walker et al. 2009; Murphy et al. 2014a). Additionally, Walker et al. (2009) reported that this component was positively correlated with lignin concentrations in Arctic surface waters. Visual comparison to Stedmon and Markager (2005) confirmed this description and found that this component is indicative of humic-like material and ubiquitous to a wide range of environments.

Component C4 was identified in twelve studies in the OpenFluor spectral database and closely resembles terrestrial material. C4 fluorescence characteristics are very similar to UVC humic-like fractions and have been referred to as the "A" peak in EEMs (Stedmon et al. 2003;Walker et al 2009; Yamashita et al. 2010). In addition to this, Stedmon et al. (2003) suggest that the observed emission at longer wavelengths indicate that C4 contains more conjugated fluorescent molecules, is more aromatic in nature and contains more functional groups. Lastly, visual comparison to Klapper et al. (2002), indicates that component C4 (ex/em- 240/440 nm) also resembles fresh fulvic acid-like fluorescence (shorter peak ex/em- 250-271/447-504 nm and longer peak ex/em- 323-329/441-448 nm) extracted from sediments in the San Diego Bay. Klapper et al. (2002) also found that fresh fulvic acid material from the Lake Fryxell has a short ex/em peak at 241/427 nm and a longer ex/em peak at 305/414 nm.

2.3.4 NR PARAFAC PCA Results

A PCA was conducted on the FMax values of fluorescent PARAFAC components and accounted for a total of 89% of the variance in the data (Fig. 2.3). PC1 accounted for 78% of the variance. Sample scores along PC1 were discriminated by salinity and discharge.

For example, sample scores along PC1 versus salinity had a negative linear relationship (R^2= 0.42; P<0.05; N=231), while sample scores along PC1 had a positive linear relationship with discharge (R^2= 0.31; P<0.05; N=231). Thus, positive loadings on PC1 should indicate freshwater sources. Furthermore, the PCA loadings plot showed that along PC1, the PARAFAC components were distributed such that terrestrial components (C1, C3 and C5) all had positive loadings and contributed roughly equally to PC1 (Fig. 2.3). The inverse relationship with salinity and positive relationship with discharge indicates that these components are terrestrial markers. Scores for planktonic and protein-like components (C2 and C4) covary together (R^2= 0.71; P<0.05; N=231) and had negative loadings on PC1 (Fig. 2.3).

PC2 explained 11% of the variance in the data set. Along PC2 the loadings for component C1 were negative, while components C2, C3, C4 and C5 exhibited positive loadings (Fig. 2.3). Additionally, the loadings of planktonic-like C2 and C4 were slightly lower than the loadings of terrestrial-like C3 and C5. C1 is the ubiquitous terrestrial-like component, which matched a variety of PARAFAC models ranging from inland freshwater to coastal seawater, and is likely representative of degraded DOM comprised of humic acids. Moreover, terrestrial-like C3 and C5 both exhibit emission peaks at longer wavelengths than C1, and possibly are sourced from fulvic acids (Senesi 1990). Thus, C3 and C5 likely also are indicative of less degraded or fresher terrestrial OM. Furthermore, planktonic and protein-like components C2 and C4 are related to *in situ* production and likely represent fresh or less degraded OM. Therefore, PC2 appears to be related to the degree of OM degradation,

with negative loadings representing degraded or refractory DOM and positive loadings on PC2 representing less degraded or fresher OM.

2.3.5 Spatial and Seasonal Distributions of DOM PARAFAC Components

The relative contribution of each PARAFAC component (%FMax) was used to examine spatial and seasonal trends in CDOM characteristics within the NRE. Of interest here was determining: (1) if the relative abundance of PARAFAC components changed between NR0 (head of the estuary); NR70 (historic chlorophyll maximum); and NR180 (mouth of the NR) throughout the year (Fig. 2.4A-D); and (2) if the relative abundance of the five PARAFAC components varied over season (Fig. 2.5A-E). The PCA results provided a guide to this interpretation. Stronger relative fluorescence from C1, C3, and C5 suggested more of a terrestrial nature to CDOM, while stronger relative fluorescence from C2 and C4 suggested planktonic CDOM.

The relative contribution (%FMax) of PARAFAC fluorescence components varied seasonally throughout the NRE (Fig. 2.4A-D, Table 2.3). Of the terrestrial-like components, C1 explained the largest amount of the fluorescence in the data set, ca. 50%, followed by C5 (up to 15%), then by C3 (at most ca. 9%) (Table 2.2). Regardless of season, the relative fluorescence contribution of C1 at stations NR0, NR70, and NR180 ranged from 44.5 to 57.7%, but did not change significantly from station to station ($P>0.05$) (Fig.2. 4A-D, Table 2.2). However, the %FMax for soil fulvic-like C3 did show a significant decrease from 9.3 to 4.5% between station NR0 to NR180 during the winter ($P<0.05$), though only being a small contribution to the total fluorescence relative to C1. The %FMax for the final terrestrial-like component we identified in NRE DOM, soil leachate fulvic-like C5, decreased significantly

between stations NR0 to NR180 and during all seasons ($P<0.05$) (Fig. 2.4A-D, Table 2.2). The highest %FMax values for C5 ranged from 5.0 to 16.4% while the lowest values were less than 1% for all seasons within the NRE.

Conversely, planktonic-like and protein-like components (C2 and C4) exhibited increases in their %FMax values from the low salinity to high salinity regions of the NRE (Fig. 2.4A-D). During all seasons, the %FMax values for planktonic-like C2 increased from NR0 to NR180 ranging between minima of 24.7 to 29.1% to maxima of 35.3 to 42.7% ($P<0.05$; Table 2.3). In a similar fashion, the fluorescence contribution of protein-like C4 also increased from NR0 to NR180 during all seasons. Minimum fluorescence contributions of protein-like C4 ranged from 3.0 to 5.8% and increased to maximum values ranging between 8.2 to 16.4% ($P<0.05$) from station NR0 to NR180 (Fig. 2.4A-D, Table2. 4).

2.3.6 Correlation of DOM quality in the NRE to Freshwater Discharge to the NRE

Prior work in estuaries has shown that the magnitude of DOM fluorescence and its terrestrial characteristics are influenced by river discharge to an estuary (Kowalczuk et al. 2010; Fellman et al. 2011; Osburn et al. 2012). Additionally, previous findings in southeastern North Carolina in the NRE and Cape Fear River estuary, as well as the Swan-Canning estuary in Australia have all observed a link between overland flow, precipitation and discharge (Kowalczuk et al. 2010; Fellman et al. 2011; Osburn et al. 2012). These processes combined can result in substantial inputs of dissolved materials via runoff into aquatic systems, such as the NRE (Mallin et al. 1993; Paerl et al. 1998; Fellman et al. 2011). Therefore, OM quality within the NRE was examined over a range of flow regimes to better assess variations in DOM characteristics and source.

The estuarine dynamics of DOM fluorescence differed throughout the sampling year, and was strongly influenced by seasonal changes in riverine discharge at Fort Barnwell, NC (Fig. 2.5A-E). Overall, increases in the relative fluorescence contributions of terrestrial-like OM were closely associated with runoff events, which were most commonly observed as discharge increased within the NRE. Conversely, the relative fluorescence contributions planktonic-like and protein-like OM increased as discharge decreased. In the spring of 2010, %Fmax values of terrestrial-like OM (C1, C3 and C5) were significantly greater than their corresponding mean summer 2010 values ($P<0.05$) (Fig. 2.5A, 2.5C, 2.5E, Table 2.3). Additionally, %Fmax values of planktonic-like and protein-like OM (C2 and C4) within the NRE were significantly greater in the summer 2010 compared to the spring of 2010 ($P<0.05$) (Fig. 2.5B, 2.5D, Table 2.3). %Fmax values of protein-like C4 were also greater in the winter 2010-2011 compared to the spring 2010 ($P<0.05$) (Fig. 2.5D, Table 2.3).

2.3.7 Correlations to DOC and DON

Previous studies in estuarine systems have shown that a linear relationship exists between DOM fluorescence and DOM concentration data (Kowalczuk et al. 2010; Osburn et al. 2012). For example, Kowalczuk et al. (2010) established that five out of six PARAFAC components were significantly correlated with DOC concentrations in the South Atlantic Bight. Furthermore, Osburn et al. (2012) observed a strong linear relationship between DON concentrations and a single PARAFAC component in the NRE. Therefore, it is worth examining the relationship between DOM quantity (DOC and DON concentrations) and DOM quality (DOM fluorescence) seasonally within the NRE.

Linear regression analysis was used to examine the overall relationship between the

fluorescence intensities of a subset of data (N=133) for which DOC and DON concentrations within the NRE also were measured (Table 2.6). When the entire data set was analyzed, positive linear relationships between DOC concentrations and FMax values for each of the terrestrial-like components C1, C3 and C5 were found but generally explained less than 30% of the variation ($P<0.05$ for all; Table 2.6). In addition, planktonic-like C2 and protein-like C4 exhibited significant negative linear relationships with DOC concentrations that generally explained less than 25% of the variation ($P<0.05$ for all) (Table 2.6). The data was further scaled down to determine if R^2 values calculated seasonally between DOC concentrations and FMax values improved. Overall, there was little difference in the R^2 values of the DOC concentrations vs. terrestrial-like FMax values and in most cases correlations were not significant (Table 2.6). These results indicate that NRE DOM fluorescence quality was mostly independent of DOC concentration when samples were grouped annually or seasonally.

A slightly different trend between DON concentrations and FMax values was observed when the entire data set was analyzed. For instance, positive relationships were observed for terrestrial-like components (C3 and C5). However, correlations between FMax values for terrestrial-like OM (C3 and C5) vs. DON concentrations generally explained less than 40% of the variation ($P<0.05$ for all: Table 2.6). In addition, FMax values for planktonic-like C2 and protein-like C4 exhibited significant negative relationships with DON concentrations and generally explained less than 25% of the variation, very similar to the result for DOC (Table 2.6). The data were further scaled down to determine if R^2 values calculated seasonally between DON concentrations and FMax values improved (Table 2.6).

Overall, seasonal correlations between FMax values and DON concentrations improved and for all components over all seasons with the exception of terrestrial-like OM (C1 and C3) in the winter ($P>0.05$).

More importantly, it appears that the relationship between PARAFAC component FMax values and DON concentrations responded to the timing of freshwater discharge events within the NRE. For example, as discharge increased in the spring and autumn of 2010 all five linear regressions between PARAFAC component FMax values and DON concentrations were significant ($P<0.05$) (Table 2.6). Furthermore, the R^2 values in the spring and autumn were significantly greater than R^2 values in the summer and winter ($P<0.05$). Although these findings are significant, it is important to note some seasonal differences occur between the spring and autumn within the NRE. As discharge increased in the spring of 2010, soil fulvic-like C3, protein-like C4 and soil leachate fulvic-like C5 exhibited the highest R^2 values relative to DON, while the R^2 values relative to DON of terrestrial humic-like C1 and planktonic-like C2 were the lowest reported. Increases in discharge in the autumn of 2010 resulted in some unique patterns that were not observed in the spring. Overall the correlations between the five PARAFAC component FMax values and DON concentrations were higher compared to the spring. Furthermore, in the autumn, the R^2 value of planktonic-like C2 was the highest reported and coincided with a peak in observed chlorophyll within the NRE at this time (Table 2.3).

2.3.8 Correlations Between PARAFAC component FMax and pH

Fluorescent DOM quality in aquatic systems reflects DOM reactivity, provenance and redox state (Larsen et al. 2010). In addition to this, fluorescent DOM properties are related to

parameters such as pH and DO concentrations. For example, DOM containing both humic and fulvic acids consists of acidic functional groups (such as carboxylic and phenolic groups) that can protonate and deprotonate depending on the pH of the aquatic environments (Chen et al. 2011). In addition to this, the molecular structural differences between humic and fulvic acids could also reflect different correlations with pH (Chen and Zheng, 2012). Furthermore, both linear and non-linear correlations between pH and DOM fluorescence have been observed in river systems (Chen et al. 2011). A number of studies have also suggested that correlations between DO and PARAFAC components indicate the presence or absence of oxidized quinone-like moieties in DOM molecular structures that contribute to DOM fluorescence (Cory and McKnight, 2005; Chen and Zheng, 2012). Therefore, the relationship between DO, pH and DOM fluorescence is worth verifying within the NRE.

Linear regression analysis was used to examine the overall relationship between the fluorescence intensities of a subset of data (N=133) for which pH and DO concentrations within the NRE also were measured. When the entire data set was analyzed, there was no significant relationship between pH, DO and DOM fluorescence ($P>0.05$). The data were further scaled down to determine if R^2 values calculated seasonally between DO, pH and FMax values improved. Overall, there was no significant correlation between DO and fluorescent DOM within the NRE. Seasonal correlations between FMax values and pH improved, but in most cases correlations were not significant ($P>0.05$). Of the terrestrial-like components that did exhibit significant trends; soil-like C3 was negatively correlated with pH in the summer ($P<0.05$) ($R^2=0.23$) and soil leachate fulvic-like C5 was negatively correlated in the summer ($R^2=0.22$) and winter ($R^2=0.36$) ($P<0.05$).

2.4 Discussion

2.4.1 Terrestrial DOM Fluorescence in the NRE

Land use change in the Neuse River basin has converted part of the natural landscape into urban and agricultural land (Paerl et al. 1998; Paerl et al. 2006; Osburn et al. 2012). Specifically, land use categories as a percentage of the total Neuse River basin area (16,000 km^2) are as followed: urban land accounts for 16%, agricultural land (crop and animal) accounts for 29% and natural landscape (forested, grassland and wetland) account for the remaining 55% (Rothenberger et al. 2009). In addition, the NRE is a historically eutrophic system and has suffered from a range of extensive algal blooms over the past few decades (Paerl et al. 2006; Peierls et al. 2012). Regardless of the impact of land-use changes and eutrophication events on estuarine DOM fluorescence, our results suggest that CDOM within the shallow, microtidal NRE is strongly influenced by both riverine and internal sources. Furthermore, we conclude that degraded, ubiquitous terrestrial-like DOM fluorescence, as indicated by component C1, had the greatest contribution to total fluorescence and remained a constant background signal throughout the NRE (Fig. 2.4). Dixon et al. (submitted), also found that within the NRE mean C:N values indicated the predominantly terrestrial nature of DOM.

In addition to these findings, previous studies have noted the dominance of terrestrial-like components that account for the largest fraction of fluorescent DOM even though they these systems have experienced significant land use changes and eutrophication as well (Stedmon et al. 2006; Fellman et al. 2011; Asmala et al. 2013; Mendoza and Zika, 2013). For example, Fellman et al. (2011) stated that although the Swan-Canning estuary (in Australia)

has experienced harmful algal blooms; the legacy of the native landscape has persisted as a large source of terrestrial DOM to the river and estuary. Stedmon et al. (2006) observed two streams entering the Horsens Estuary (in Denmark) and noted that the primary source of DOM was likely composed of terrestrial plants and soils regardless of agricultural land cover and autochthonous production. In addition, Mednoza and Zika (2013) examined DOM dynamics on the south Florida Shelf and found that DOM fluorescence is dominated by terrestrial-like material even though the surrounding landscape (Florida Everglades) has experienced some conversion of natural lands to agricultural and urban areas.

Even though the majority of the DOM fluorescence within the NRE is derived from terrestrial sources, previous studies from the Neuse have shown that riverine inputs of nutrients support algal blooms and the production of planktonic DOM (Paerl et al. 2006; Osburn et al. 2012). For example, over the past several decades, the NRE has undergone nutrient driven eutrophication and suffered from a range of extensive algal blooms (Paerl et al. 2006; Peierls et al. 2012). In this study, this effect can be seen in the significant increases in planktonic-like C2 and protein-like C4, which were observed from NR0 to NR180 over all seasons and annually.

These findings are similar to Osburn et al. (2012), who also found protein-like fluorescence became more prominent during estuarine transport within the NRE. In addition, Fellman et al. (2011) observed changes in the composition of DOM fluorescence from humic-like OM in the upper and middle regions of the Swan-Canning estuary to protein-like fluorescence in the lower estuary over all sampling dates. Kowalzcuk et al. (2009) also observed increases in protein-like fluorescence transitioning from the Cape Fear River into

coastal waters of the South Atlantic Bight. Lastly, Murphy et al. (2008) examined fluorescent DOM collected on trans-oceanic cruises in the Pacific and Atlantic Oceans and found that protein-like fluorescence components dominate the fluorescent composition of surface water in the open ocean.

2.4.2 Terrestrial DOM Degradation in the NRE

Within the micro-tidal NRE, freshwater discharge influenced fluorescent DOM sources throughout the sampling year. These findings are similar to a previous study by Dixon et al. (submitted), which reported that increases in discharge resulted in increases in DOC, DON and CDOM concentrations within the NRE. Previous studies have also observed that the quality of DOM during periods of peak discharge is indicative of terrestrial sources (Mallin et al. 1993; Pinckney et al. 1999; Fellman et al. 2011).

In this study, terrestrial DOM fluorescence quality exhibited strong variability that coincides with increases in riverine discharge. Overall, increases in the relative fluorescence contributions of terrestrial-like OM (C1, C3 and C5) were apparent in the spring compared to the summer of 2010 ($P<0.05$) (Table 2.6, Fig. 2.5C, 2.5E). Additionally, the fluorescence contributions of less degraded terrestrial-like OM (soil fulvic-like C3 and soil leachate fulvic-like C5) appear to be more responsive to increases in discharge. In order to evaluate this further, the fluorescence contribution of C3 and C5 in surface waters was plotted against station location downstream of NR0 under high (April 2010) and low (July 2010) discharge (Fig. 2.6A-2.6B). It is apparent that both C3 and C5 are being added mid-estuary, roughly around station NR70, as discharge increases in April 2010 (Fig. 2.6A). DON and DOC concentrations in surface waters are also elevated during this time (Fig. 2.7A-2.7B). More

importantly, DOC concentrations in surface waters exhibit a peak at roughly the same location that C3 and C5 increase within the NRE (Fig. 2.7A). When discharge is reduced in July 2010, it is apparent that C3 exhibits little to no variation down estuary and C5 steadily decreases from the head of the NR towards the river mouth (Fig.2.6B). Additionally, both DOC and DON concentrations exhibited little variation progressing down estuary.

A possible source for the peak in DOC concentration and terrestrial fulvic acid-like OM within the NRE may be due to the Trent River (TR), which is a tributary of the NR estuary just below station NR30 (Fig. 2.1). Additionally, the DOM quality of the TR tends to be carbon rich compared to NR DOM (Paerl and Peierls, 2014). This is likely due to the fact that the TR watershed is made up of forest and wetlands, whereas the NR is a combination of natural landscapes as well as agricultural and urban areas (Deamer 2009; Paerl and Peierls, 2014). Previous studies have also noted that land-use change, such as conversion of the natural landscape to agricultural fields, can alter the chemical complexity and bioavailability of DOM (Stedmon et al. 2006; Wilson and Xenopoulos 2009; Williams et al. 2010; Massicotte and Frenette, 2011). Thus, we suggest that the difference in DOM quantity and quality during peaks in riverine discharge is due to the TR likely sourcing DOM and less degraded terrestrial fulvic-like OM into the NRE due to the unique land cover of the TR watershed compared to the NR watershed.

In order to elucidate more information on the differences in DOM quality during peaks in riverine discharge, a PCA was conducted on the FMax values of the fluorescent PARAFAC components from the NR-TR PARAFAC model and accounted for 96% of the variance in the data (Fig. 2.8). In addition to PARAFAC component loadings, sample scores

were also plotted. What is interesting is the clear separation between the NR and TR sample scores and the PARAFAC component loadings. For example, PARAFAC component loadings were as followed: planktonic- and protein-like components C3 and C5 covary together, terrestrial humic-like and soil fulvic-like components C1 and C2 covary together and terrestrial fresh fulvic-like component C4 does not covary with any other component, but is inversely related to terrestrial-like component C1 and C2. Specifically, component C4 of the TR-NR PARAFAC model appears to be exclusive to the TR, due to the loadings for component C4 falling near the TR sample scores. The remaining four NR-TR PARAFAC component loadings (C1, C2, C3, and C5) appear to be indicative of the NR since the loadings fall with the NR sample scores. These findings suggest that TR is sourcing fresh terrestrial fulvic-like DOM into the NR basin. It appears that our previous assumption that the TR may be solely sourcing terrestrial fulvic-like material into the NR basin may not be entirely correct. This is because component 2 in the NR-TR PARAFAC model, which has been characterized as terrestrial soil fulvic-like material, covaries with component C1, terrestrial humic-like material.

In addition to these findings, previous studies have also shown that within the NRE increases in autochthonous production throughout the estuary is further enhanced during periods of decreased discharge (Mallin et al. 1993; Paerl et al. 2006; Osburn et al. 2012). For instance, decreased discharge as seen in the summer of 2010, allowed for substantial autochthonous production of planktonic and protein-like fluorescent OM to occur. This was expressed in the significant increases in both planktonic-like C2 and protein-like C4 fluorescence contributions compared to spring values (Fig. 2.5B and 2.5D). Furthermore,

Dixon et al. (submitted) observed similar findings as expressed by increases in the mean slope ratio (S_R) and biological index (BIX) values, which reflected LMW DOM of autochthonous origin during the summer of 2010. Osburn et al. (2012) also states that during low discharge in the watershed it is not surprising to see strong mixing between autochthonous and terrestrial OM sources within the NRE. Increases in planktonic-like and protein-like DOM fluorescence within the NRE is likely due to (1) mixing of protein-rich marine water with humic-rich freshwater and (2) in-situ production along the river-estuarine continuum within the NR.

It is important to note that the fluorescence intensities of planktonic-like C2 and protein-like C4 were not strongly correlated with chlorophyll in the NRE. In a recent study by Osburn et al. (2012) a combined DOM-POM PARAFAC model also noted similar results for protein-like DOM within the NRE. Protein-like DOM fluorescence was poorly correlated to chl-a does not appear related to recent primary production of autochthonous OM. However, Osburn et al. (2012) did find that protein-like fluorescence in the particulate organic matter (POM) pool is a marker for recent autochthonous POM and likely sources of protein-like fluorescence in the DOM pool. Based on the results of this study and the findings of Osburn et al. (2012), we suggest that planktonic-like C2 and protein-like C4 are both markers for autochthonous production, albeit not recent production, within the NRE.

2.4.3 Contribution from Rainwater

Rainwater might be an overlooked allochthonous source of DOM within the NRE. Despite the potential importance of rainwater DOC to estuarine waters, there are few detailed studies on how it contributes to estuarine DOM quality. For example, rain events with more

continental influences had stable carbon isotope (δ^{13}C-DOC) values closer to the terrestrial sources, while rain events with stronger oceanic influences had δ^{13}C-DOC values shifting towards those typical of marine systems (Avery et al. 2006). Keiber et al. (2006) also suggest that elevated CDOM levels in continentally influenced rainwater, relative to marine dominated events, imply that anthropogenic and/or terrestrial sources are important contributors to CDOM levels in precipitation. Additionally, Keiber et al. (2006) and Miller et al. (2009) compared ^{1}H-NMR spectra from Cape Fear River (CFR) CDOM and rain CDOM and found that they are similar, with the exception that the CFR ^{1}H-NMR spectrum displays larger broader peaks, indicating a greater complexity of the CDOM in river water compared to rain water. In addition to these findings, Keiber et al. (2006) observed a unique fluorescent peak associated with CDOM in rain that occurs at roughly an excitation range of 275-325 nm and an emission range of 375-475 nm regardless of storm trajectory and CDOM concentration. This peak range is similar to the previously characterized fluorescent region of terrestrially derived humic and fulvic acids. In this study, our results illustrate that the greatest overlap with the rain CDOM peak occurs between terrestrial-like components C1 (terrestrial humic-like), C3 (soil fulvic-like) and C5 (soil leachate fulvic-like) (ex range- 240-335 and em range- 438-508) (Table 2.4). Therefore, the overlap between rain CDOM and terrestrial CDOM derived humic and fulvic-like material suggests that rain CDOM may be a potentially important contributor to estuarine CDOM signal within the NRE during precipitation events. Additional detailed analysis of the contribution of rain CDOM to the estuarine CDOM signal within the NRE is necessary in order to shed light on CDOM dynamics within this system.

2.4.4 Terrestrial DOM Degradation in the NRE

Terrestrial DOM is comprised primarily of humic acids (HA) and fulvic acids (FA), which reflect the precursor OM (Larsen et al. 2010; Asmala et al. 2013). Overall, the discrimination between HA and FA is based on the separation of both fractions via pH: the HA fraction precipitates completely at a pH of 1, whereas the FA fraction remains soluble (Senesi, 1990). In general, the molecular structure of both HA and FA can be described as consisting of a variously extended network of aromatic rings consisting of aliphatic components and chemically active functional groups (Senesi, 1990). Despite the compositional similarity between FA and HA, the HA fraction can be described as high molecular weight (HMW), highly aromatic and often containing of less oxygen-containing functional groups (Chen and Kenny, 2007). The FA fraction, on the other hand, is generally characterized by lower molecular weight (LMW), decreased aromaticity and higher oxygen containing functional groups (Senesi, 1990). The distinct interactive properties of HA and FA with organic chemicals are thought to play an important role in the bioavailability and biogeochemical cycling of OM (Senesi, 1990). These findings further suggest that the FA fraction is more chemically and physio-chemically active than the HA counterpart (Senesi, 1990a).

The overall fluorescence behavior of HA and FA will primarily depend on their molecular structure. Thus, any given change in molecular structure will likely induce a change in their overall fluorescent properties (Senesi, 1990; Boyd and Osburn 2004; Cory and McKnight 2005). For example, the optical properties commonly associated with terrestrial HA and FA primarily arise in part from intramolecular charge-transfer interactions

between hydroxyl-aromatic donors and quinoid acceptors formed through the partial oxidation of lignin, derived from vascular plant sources (Senesi, 1990a; Boyle et al. 2009). Due to this, HA and FA exhibit rather unique absorption and fluorescent characteristics. For example, absorption decreases with increasing wavelength in an exponential fashion and arises from the continuum of coupled states formed through charge transfer interactions of distinct chromophores (Senesi, 1990a; Del Vecchio and Blough, 2004; Boyle et al. 2009). Additionally, the fluorescence emission and excitation intensities decrease with increasing molecular weight. For example, as molecular weight increases a distinct red shift accompanied by a broadening of the emission peak has been observed (Senesi, 1990a; Boyle et al. 2009; Jug and Franko, 2013). These effects are attributed to the greater proximity of aromatic chromophores and the greater probability of deactivation of excited states due to fluorescence quenching and increased non-irradiative relaxation (Senesi, 1990a; Boyle et al. 2009; Coelho et al. 2010; Jug and Franko, 2013). On the other hand the LMW fraction exhibits enhanced fluorescence at lower wavelengths and a blue shift in the emission peak (Senesi, 1990a).

Within the NRE, significant decreases in the relative fluorescence contributions of soil fulvic-like C3 and soil leachate fulvic-like C5 occurred from station NR0 to NR180 and corresponded to stable relative fluorescence contributions of ubiquitous terrestrial humic-like C1 (Fig. 2.5A, 2.5C, 2.5E). Unique FA sources and their chemical variability produce unique spectral signatures. Specifically, the chemical structures of FA vary depending on their phase and origin, i.e., aquatic or terrestrial origin, and environmental parameters (vegetation, temperature and precipitation) (Bauer and Bianchi, 2011). The broad excitation spectrum of

C3 is consistent with a higher plant origin (sourced from vascular plants) and is likely due to overlapping chromophores, which is consistent with ground-state charge-transfer interactions (Senesi, 1990a; Del Vecchio and Blough, 2004; Boyle et al. 2009). Increases in molecular weight have likely caused the emission maximum red shift observed for C3. This probably reflects the greater proximity of aromatic chromophores, the greater probability fluorescence quenching and increased non-irradiative relaxation (Senesi, 1990a; Boyle et al. 2009; Coelho et al. 2010; Jug and Franko, 2013). Additionally, the emission maximum of C5 (em_{max}= 438nm) is blue shifted relative to C3 (em_{max}= 508nm) (Table 2.4). The blue shifted emission peak of C5 is indicative of lower molecular weight, less aromatic material and suggests C5 is likely derived from a less conjugated source compared to C3.

Furthermore, it appears that terrestrial humic-like OM is coupled to the disappearance of terrestrial fulvic-like OM within the NRE. A potential mechanism for the loss in fulvic acid-like material may be due to microbial communities within the NRE. Microbial communities within the estuary utilize lower molecular weight, less aromatic allochthonous DOM (i.e. soil fulvic-like C3 and soil leachate fulvic-like C5) because it is more chemically and physio-chemically active (Peierls and Paerl 2010). In addition to this, we suggest that there is a preference to the quality of fluorescent DOM that microbial communities utilize first within the NRE. For example, the first tier of fluorescent DOM utilization occurs as soil fulvic-like C3 and soil leachate fulvic acid-like C5 are preferentially utilized and transformed by microbial communities into terrestrial humic-like C1.

The microbial utilization of these components is not surprising within the NRE. Especially given that Peierls and Paerl (2010) found that both allochthonous and planktonic

DOM within the NRE are removed rapidly by bacterioplankton activity. Additionally, physiochemical changes occurring through the freshwater-marine continuum may also enhance the biolability of this allochthonous OM for microbial communities. For example, Boyd and Osburn (2004) found that within the San Francisco Bay and Chesapeake Bay variations in fluorescent DOM were dependent on the source of CDOM and the bacterial population present. Thus, allochthonous DOM may become more labile due to conformational changes (i.e. molecular structure) during estuarine mixing. Stepanaukas et al. (1999) also observed bacterial degradation of OM across the salinity gradient and noted that degradation was impacted by bacterial populations. Asmala et al. (2013) observed significant increases in humic-like fluorescence, which they attributed to bacteria selectively degrading the bioavailable DOM and in the process generating humic fluorescence. They suggested that this is evidence of bacterial communities adapting to degrade terrestrial OM since it is most abundantly available even though it is not the most favorable substrate for heterotrophic utilization. Overall, it appears that as water progresses down the estuary, soil fulvic-like C3 and soil leachate fulvic-like C5 significantly decrease ($P<0.05$) and may be utilized by bacterioplankton communities in the NRE (Fig. 2.4). It is not likely that photo-degradation is significantly contributing to this loss based on the finding so Dixon et al. (submitted). For example, Dixon et al. (submitted) state that within the NRE light is attenuated rapidly in the upper water column, which results in photo-degradation restricted to just below the surface. Thus, photo-degradation is not a primary removal mechanism of DOM and only affects a small portion of the estuary on a volume basis (Osburn et al. 2009; Dixon et al. (submitted)). Moreover, as this material is being degraded, it is possible that it is being transformed into

more degraded terrestrial humic-like material (C1), which does not significantly change down the length of the NRE.

2.4.5 Fluorescence Characteristics and DOC within the NRE

Fluorescence characteristics were also useful for distinguishing between sources and changes in the quality of DOM within the NRE. Many studies have found very strong correlations between terrestrial DOM fluorescent components modeled by PARAFAC and DOC concentrations (Fellman et al. 2009; Petrone et al. 2010; Kowalczuk et al. 2010). In contrast to these studies, when we grouped our results for the NRE annually and then by season, poor correlations were found between DOC concentrations and terrestrial-like fluorescent OM. This would appear to suggest that the fluorescent quality of terrestrial DOM within the NRE was mostly independent of DOC concentration. However, when select sampling cruises were considered, we observed improved correlations between DOC concentrations and terrestrial-like OM fluorescence (Table 2.7). We also grouped the data into correlations between DOC concentrations with fluorescent OM including NR0 and correlations between DOC concentrations with fluorescent OM excluding NR0 (Table 2.7). This was done to further assess the impact of the Trent River on terrestrial DOM dynamics within the NRE. This tributary may be sourcing and replenishing the terrestrial DOM pool down river of station NR0, which would result in variations in the correlation between DOC and fluorescent DOM within the NRE.

Overall it appears that by analyzing the data on a monthly time scale, regardless of the incorporation of station NR0, there are stronger correlations between DOC and DOM quality within the NRE. First, correlations between DOC concentrations and all three

terrestrial-like fluorescent OM components (C1, C3 and C5) where NR0 was included yielded R^2 values that ranged between 0.44 and 0.60 within the NRE. In general, these correlations are improved from the annual and seasonal correlations made initially, but overall they were sparse with only five being significant ($P<0.05$). On the other hand, correlations between DOC concentrations with terrestrial-like fluorescent OM where NR0 was excluded resulted in improved R^2 values and significantly more correlations were observed (Table 2.7). Specifically, a positive linear relationship between DOC concentrations and FMax values for each of the terrestrial-like components (C1, C3 and C5) was found and generally explained between 46 to 86% of the variation ($P<0.05$ for all; Table 2.7). Overall these findings suggest that the Trent River, which enters the NR below station NR30, plays an important role in the relationship between terrestrial fluorescent OM dynamics and DOC concentrations within the NRE.

Nevertheless, DOC concentrations and terrestrial FMax values were not significantly correlated during all sampling months. Jaffé et al. (2008) found that between diverse aquatic ecosystems in different biomes, there is not always an overall relationship between DOC concentration and DOM quality parameters. Although the Jaffé et al. (2008) comparison was not made with FMax values derived from PARAFAC components, that study illustrates that variations in DOM quality are not necessarily associated with DOC concentrations. Furthermore, Hood et al. (2006**)** examined DOM quality changes on hourly timescales and found that DOM quality can change on varying spatial scales and on both long- and short-term temporal scales. In terms of the NRE, these findings emphasize that DOM optical properties can be highly variable and can be impacted by different physical (hydrology),

chemical (photo-degradation/redox conditions) and biological (primary production/microbial degradation) processes.

2.4.6 DON within the NRE

Eutrophication, or the increase in OM production, is a widespread problem, which negatively affects the structure and function of many aquatic systems (Paerl and Peierls, 2014). It is often linked to both externally supplied (e.g. atmospheric deposition, river runoff, nitrogen fixation) and internally supplied (in situ regeneration and recycling) nutrients and DOM enrichment, especially nitrogen since it is the primary nutrient limiting algal production in the NRE (Paerl et al. 2006; Corbett 2010; Paerl and Peierls, 2014). The NRE has experienced nutrient- driven eutrophication and fish kills over the past several decades, which have led to a mandated 30% reduction in total nitrogen (TN) loading (Paerl et al. 2006; Paerl et al. 2010; Paerl and Peierls, 2014). This required 30% reduction in TN has not been achieved thus far, and recent trends suggest that this is due to increases in the organic form of nitrogen (DON or particulate organic nitrogen) (Paerl and Peierls, 2014). Moreover, DON in aquatic systems is made up of a wide array of compounds with varying reactivity, bioavailability and concentration (Bronk et al. 2007; Paerl and Peierls, 2014). DON chemical species range from highly labile, LMW compounds, such as amino acids and urea, to highly refractory, HMW compounds such as humic acids (Paerl and Peierls, 2014).

Given that DOM protein-like fluorescence within the NRE is associated with planktonic material and is dominated by fluorescent amino acids (tryptophan and tyrosine), strong correlations between DON and protein-like C4 fluorescence intensities might be expected. Surprisingly, a negative linear relationship between DON concentrations and

planktonic and protein-like OM fluorescence was observed within the NRE (Table 2.6). On the other hand, positive significant trends were observed between DON concentrations and terrestrial fluorescent OM (Table 2.6). Component C5 exhibited significant correlations for all seasons as well as the strongest correlation. Thus, despite a clear fluorescence signature indicating the presence of autochthonous DOM (planktonic and protein-like fluorescent OM), much of DON in the NRE appears to be bound in terrestrial humic-material (Table 2.6). It appears that DON within the NRE is highly associated with highly refractory, HMW compounds such as humic substances. Thus, our results suggest that most DON is terrestrially sourced within the NRE due to its relationship with terrestrial-like fluorescent OM.

The lack of correlation between DON concentrations and protein-like fluorescence has been observed in a range of aquatic environments (Stedmon et al. 2007; Fellman et al. 2011; Osburn et al. 2012). Specifically within the NRE Osburn et al. (2012) noted a negative relationship between DON concentration and protein-like DOM fluorescence in pre-Hurricane Irene DOM samples. Additionally, they found that terrestrial-like fluorescence in the region similar to peak C5 was a better indicator of DON concentrations before and after Hurricane Irene, therefore concluding that DON in the NRE is primarily sourced from the terrestrial environment. The findings of this study corroborate those of Osburn et al. (2012) and further suggest that terrestrially derived DON is a major source of N to the NRE due to its strong relationship with terrestrial-like fluorescent OM.

2.5 Conclusions

Overall, our study demonstrates that fluorescent DOM within the shallow, microtidal NRE is influenced by both riverine and internal sources. The major conclusions of this study are as follows:

1. The degraded, terrestrial-like C1 component had the greatest contribution to total fluorescence and remained a constant background signal within the NRE throughout the year. Additionally, within the NRE, terrestrial DOM fluorescence quality exhibited strong variability that coincides with increases in discharge.
2. We suggest that during peaks in riverine discharge the TR is likely supplying terrestrial-like OM (component C4 from the NR-TR PARAFAC model) to the NRE. Upon entering the NRE, this C4 component of the NR-TR PARAFAC model is then altered and may be contributing to the source of component C5 in the NR PARAFAC model.
3. Within the NRE, it appears that terrestrial humic-like OM is coupled to the disappearance of terrestrial fulvic-like OM. Moreover, based on our PCA results, terrestrial humic-like C1 is more degraded than terrestrial fulvic-like components C3 and C5. These results indicate that bacterial utilization of more labile allochthonous DOM (i.e. soil fulvic-like C3 and soil leachate fulvic-like C5) is likely occurring down the length the NRE.
4. Overall, correlation between DOC concentrations and terrestrial fluorescent OM suggest that DOM quality changes can occur on varying spatial scales and on both long- and short-term temporal scales. In terms of the NRE, these findings emphasize

that DOM optical properties can be highly variable and can be impacted by different physical (hydrology), chemical (photodegradation/redox conditions) and biological (primary production/microbial degradation) processes.

5. Despite a clear fluorescence signature indicating the presence of autochthonous DOM (planktonic and protein-like fluorescent OM), much of DON was associated with terrestrial humic-material.
6. Planktonic-like and protein-like DOM fluorescence increased from station NR0 to station NR180. These results are likely due to: (1) mixing of protein rich marine water with humic rich freshwater; and (2) *in-situ* production within the NRE.

2.6 References

Asmala, E., Autio, R., Kaartokallio, H., Pikanen, L., Stedmon, C.A., and Thomas, D.N., 2013. Bioavailability of riverine dissolved organic matter in three Baltic Sea estuaries and the effect of catchment land use. Biogeosciences, 10: 6969-6986.

Avery Jr., G.B., Willey, J.D., and Kieber, R.J., 2006. Carbon isotopic characterization of dissolved organic carbon in rainwater: Terrestrial and marine influences. Atmospheric Environment, 40: 7539-7545.

Bauer J.E. and Bianchi T.S., 2011. Dissolved Organic Carbon Cycling and Transformation. In: Wolanski E and McLusky DS (eds.) Treatise on Estuarine and Coastal Science, Vol 5, pp. 7–67. Waltham: Academic Press.

Benner, R. and Strom, M. 1993. A critical evaluation of the analytical black associated with DOC measurements by high-temperature catalytic oxidation. Marine Chemistry, 41(1-3): 153-160.

Boyd, T.J., and Osburn, C.L., 2004. Changes in CDOM fluorescence from allochthonous and autochthonous sources during tidal mixing and bacterial degradation in two coastal estuaries. Marine Chemistry, 89(1-4): 189-210.

Boyd, T. J., Barham, B. P., Hall, G. J. and Osburn, C. L., 2010. Variation in ultrafiltered and LMW organic matter fluorescence properties under simulated estuarine mixing transects: 1. Mixing alone. Journal of Geophysical Research–Biogeosciences 115: G00F13. doi: 10.1029/2009JG000992.

Boyle, E.S., Guerriero, N., Thiallet, A., Del Vecchio, R., and Blough, N.V., 2009. Optical Properties of Humic Substances and CDOM: Relation to Structure. Environmental

Science and Technology, 43: 2262-2268

Bronk, D., J. See, P. Bradley, and L. Killberg. 2007. DON as a source of bioavailable nitrogen for phytoplankton. Biogeosciences 4: 283–296.

Brookshire, E.N.J., Valett, H.M., Thomas, S.A., and Webster, J.R., 2005. Coupled Cycling of Dissolved Organic Nitrogen and Carbon in a Forest Stream. Ecology, 86(9): 2487-2496.

Burkholder, J.M. et al., 2006. Comprehensive trend analysis of nutrients and related variables in a large eutrophic estuary: A decadal study of anthropogenic and climatic influences. Limnology and Oceanography, 51(1): 463-487.

Cawley, K.M., Yamashita, Y., Maie, N., and Jaffé, R. 2013. Using Optical Properties to Quantify Fringe Mangrove Inputs to the Dissolved Organic Matter (COM) Pool in a Subtropical Estuary. Estuaries and Coast. DOI 10.1007/s12237-013-9681-5.

Chen, H., Zheng, B., Song, Y., and Qin, Y., 2011. Correlation between molecular absorption spectral slope ratios and fluorescence humification indices in characterizing CDOM. Aquatic Sciences, 73(1): 103-112.

Chen, H., and Zheng, B., 2012. Characterizing natural dissolved organic matter in a freshly submerged catchment (Three Gorges Dam, China) using UV absorption, fluorescence spectroscopy and PARAFAC. Water Science and Technology, 65.5: 962-969.

Christian, R.R., Boyer, J.N. and Stanley, D.W., 1991. Multiyear distribution patterns of nutrients within the Neuse River Estuary, North Carolina. Marine Ecology Progress Series, 71(3): 259-274.

Coble, P. G. 1996. Characterization of marine and terrestrial DOM in seawater using excitation-emission matrix spectros- copy. Mar. Chem. 51: 325–346.

Coelho, C., G. Guyot, A. ter Halle, L. Cavani, C. Ciavatta and C. Richard. 2010. Photoreactivity of humic substances: relationship between fluorescence and singlet oxygen production. Environ. Chem. Lett. 2010:1–5.

Corbett, D.R., 2010. Resuspension and estuarine nutrient cycling: insights from the Neuse River Estuary. Biogeosciences, 7(10): 3289-3300.

Cory, R.M., and McKnight, D.M., Fluorescence spectroscopy reveals ubiquitous presence of oxidizes and reduced quinones in dissolved organic matter. Environmental Science and Technology, 39: 8142-8149.

Crosswell, J. R., M. S. Wetz, B. Hales, and Paerl., H. W., 2012. Air-water CO_2 fluxes in the microtidal Neuse River Estuary, North Carolina, Journal Geophysical Research, 117, C08017, doi:10.1029/2012JC007925.

Deamer, N. 2009. Neuse River Basinwide Water Quality Plan. North Carolina Department of Environment and Natural Resources - Division of Water Quality.

Del Vecchio, R. and N. V. Blough. 2004. On the origin of the optical properties of humic substances. Env. Sci. Technol. 38(14):3885– 3891.

Dixon, J.L., Osburn, C.L., Paerl, H.W., and Peierls, B.L., 2014. Seasonal changes in estuarine dissolved organic matter due to variable flushing time and wind-driven mixing events. Estuarine, Coastal and Shelf Science, Manuscript submitted for publication.

Fellman, J.B., Miller, M.P., Cory, R.M., D'Amore, D.V., and White, D., 2009. Characterizing Dissolved Organic Matter Using PARAFAC Modeling of Fluorescence Spectroscopy: A Comparison of Two Models. Environmental Science and Technology, 43: 6228-6234.

Fellman, J.B., Petrone, K.C. and Grierson, P.F., 2011. Source, biogeochemical cycling, and fluorescence characteristics of dissolved organic matter in an agro-urban estuary. Limnology and Oceanography, 56(1): 243-256.

Ferrari, G.M., Dowell, M.D., Grossi, S., and Targa, C., 1996. Relationship between the optical properties of chromophoric dissolved organic matter and total concentration of dissolved organic carbon in the southern Baltic Sea region. Marine Chemistry, 55: 299-316.

Graeber, D., Gelbrecht, J., Pusch, M., Anlanger, C. & von Schiller, D., 2012. Agriculture has changed the amount and composition of dissolved organic matter in Central European headwater streams. Science of The Total Environment,438,435-446.

Hood, E., M. N. Gooseff, and Johnson, S. L., 2006. Changes in the character of stream water dissolved organic carbon during flushing in three small watersheds, Oregon, J. Geophys. Res., 111, G01007, doi:10.1029/2005JG000082.

Hulatt, C. J., Kaartokallio, H., Asmala, E., Autio, R. A., Stedmon, C. A., Sonninen, E., Oinonen, M., and Thomas, D. N., 2013. Microbial Degradation of Dissolved Organic Matter (DOM) from a northern peat dominated catchment, Aquatic Sciences, in press.

Jaffé, R., J.N. Boyer, X. Lu, N. Maie, C. Yang, N.M. Scully, and S. Mock. 2004. Source characterization of dissolved organic matter in a subtropical mangrove-dominated estuary by fluorescence analysis. Marine Chemistry, 84: 195–210.

Jaffé, R., McKnight, D, Maie, N., Cory, R., McDowell, W.H., and Campbell, J.L., 2008. Spatial and temporal variations in DOM composition in ecosystems: The importance of long-term monitoring of optical properties. Journal of Geophysical Research, 113: G04032.

Jorgensen, L., Stedmon, C.A., Kragh, T., Markager, S., Middelboe, M., Sondergaard, M., 2011. Global trends in the fluorescence characteristics and distribution of marine dissolved organic matter. Marine Chemistry, 126: 138-148.

Jug, T., and Franko, M., 2013. Fluorescence quenching as an indicator of the conformational change of humic acids. Emirates Journal of Food and Agriculture, 25(12): 994-1001.

Kieber, R.J., Willey, J.D., Whitehead, R.F., and Reid, S.N., 2007. Photobleaching of chromophoric dissolved organic matter (CDOM) in rainwater. Journal of Atmospheric Chemistry. 58: 219-235.

Kirk, J. T. O., 1994. Light and Photosynthesis in Aquatic Ecosystem. Cambridge University Press.

Kothawala, D.N., von Wachenfeldt, E., Koehler, B., Tranvik, L.J., 2012. Selective loss and preservation of lake water dissolved organic matter fluorescence during long-term dark incubations. Science of the Total Environment, 433:238-246.

Kowalczuk, P., Durako, M.J., Young, H., Kahn, A.E., Cooper, W.J., and Gonsior, M., 2009. Characterization of dissolved organic matter fluorescence in the South Atlantic Bight

with use of PARAFAC model: interannual variability. Marine Chemistry, 113: 182-196.

Kowalczuk, P., Cooper, W.J., Durako, M.J., Kahn, A.E., Gonsior, M., and Young, H., 2010. Characterization of dissolved organic matter fluorescence in the South Atlantic Bight with use of PARAFAC model: Relationship between fluorescence and its components, absorption coefficients and organic carbon concentrations. Marine Chemistry, 118:22-36.

Kowalczuk, P., Zablocka, M., Sagan, S., and Kulinski, K., 2010a. Fluorescence measured in situ as a proxy of CDOM absorption and DOC concentration in the Baltic Sea. Oceanologia, 52(3): 431-471.

Larsen, L. G., Aiken, G. R., Harvey, J. W., Noe, G. B., and Crimaldi, J. P., 2010. Using fluorescence spectroscopy to trace seasonal DOM dynamics, disturbance effects, and hydrologic transport in the Florida Everglades, J. Geophys. Res., 115, G03001, doi:10.1029/2009JG001140.

Lawaetz, A.J. and Stedmon, C.A., 2009. Fluorescence Intensity Calibration Using the Raman Scatter Peak of Water. Applied Spectroscopy, 63(8): 936-940.

Lochmuller, C. H., and S. S. Saavedra. 1986. Conformational changes in a soil fulvic acid measured by time dependent fluo- rescence depolarization. Analyt. Chem. 38**:** 1978–1981.

Luettich, R. A. J., S. D. Carr, J. V. Reynolds-Fleming, C. W. Fulcher, and J. E. Mcninch. 2002. Semi-diurnal seiching in a shallow, micro-tidal lagoonal estuary. Continental Shelf Research, 22: 1669–1681.

Maie, N., Scully, N. M., Pisani, O., Jaffé, R., 2007. Composition of a protein-like fluorophore of dissolved organic matter in coastal wetland and estuarine ecosystems. Water Res. 41 (3), 563−570.

Mallin, M.A., Paerl, H.W., Rudek, J. and Bates, P.W., 1993. Regulation of estuarine primary production by watershed rainfall and river flow. Marine Ecology-Progress Series, 93(1- 2): 199203.

Mannino A., Russ M. E., Hooker S. B., 2008, Algorithm development and validation for satellite-derived distributions of DOC and CDOM in the U.S. Middle Atlantic Bight, J. Geophys. Res., 113, C07051, doi:10.1029/2007JC004493.

Markager, S., Stedmon, C.A. and Sondergaard, M., 2011. Seasonal dynamics and conservative mixing of dissolved organic matter in the temperate eutrophic estuary Horsens Fjord. Estuarine Coastal and Shelf Science, 92(3): 376-388.

Massicotte, P., and Frenette, J-J., 2011. Spatial connectivity in a large river system: resolving the sources and fate of dissolved organic matter. Ecological Applications, 2(17): 2600-2617.

McKnight, D. M.; Boyer, E. W.; Westerhoff, P. K.; Doran, P. T.; Kulbe, T.; Andersen, D. T., 2001. Spectrofluorometric characterization of dissolved organic matter for indication of precursor organic material and aromaticity. Limnolology and Oceanography 46: 38-48.

Mendoza, W.G., and Zike, R.G., 2014. On the temporal variation of DOM fluorescence on the southwest Florida continental shelf. Progress in Oceanography, 120: 189-204.

Miller, C., Gordon, K.G., Kieber, R.J., Willey, J.D., and Seaton, P.J., 2009. Chemical characteristic of chromophoric dissolved organic matter in rainwater. Atmospheric Environment, 43:2497-2502.

Murphy, K.R., Stedmon, C.A., Waite, T.D., and Ruiz, G.M., 2008. Distinguishing between terrestrial and autochthonous organic matter sources in marine environments using fluorescence spectroscopy. Marine Chemistry, 108: 40-58.

Murphy, K.R., Hambly, A., Singh, A., Henderson, R.K., Baker, A., Stuetz, R., and Khan, S.J., 2011. Organic Matter Fluorescence in Municipal Water Recycling Schemes: Toward a Unified PARAFAC Model. Environmental Science and Technology, 45: 2909-2916.

Murphy, K.R., Stedmon, C.A., Graeber, D., and Bro, R., 2013, Fluorescence spectroscopy and multi-way techniques. PARAFAC. Analytical Methods, 5, 6557-6566.

Murphy, K.R., Stedmon, C.A., Wenig, P., and Bro, R., 2014. OpenFluor- an online spectral library of auto-fluorescence by organic compounds in the environment. Analytical Methods, 6: 658-661.

Murphy, K.R., Bro, R., Stedmon, C.A., 2014a, Chemometric analysis of organic matter fluorescence. in: Coble, P., Baker, A., Lead, J., Reynolds, D., Spencer, R. (Eds.). Aquatic organic matter fluorescence. Cambridge University Press, New York.

Null, K.A., Corbett, D.R., DeMaster, D.J., Burkholder, J.M., Thomas, C.J., and Reed, R.E. 2011. Porewater advection of ammonium into the Neuse River Estuary, North Carolina, USA. Estuarine, Coastal and Shelf Science, 95: 314-325.

Ohno, T., and Bro, R. 2006. Dissolved organic matter characterization using multiway

spectral decomposition of fluorescence landscapes. Soil Sci. Soc. Am. J., 70 (6), 2028−2037.

Osburn C.L., Handsel L.T., Mikan M.P., Paerl H.W., and Montgomery M.T., 2012. Fluorescence tracking of dissolved and particulate organic matter quality in a river-dominated estuary. Environ. Sci. Technol. 46,8628-36.

Pace, M. L., Reche, I., Cole, J. J., Fernandez-Barbero, A., Mazuecos, I. P. and Prairie, Y. T. 2012. pH change induces shifts in the size and light absorption of dissolved organic matter. Biogeochemistry 108:109-18.

Paerl, H.W., Pinckney, J.L., Fear, J.M. and Peierls, B.L., 1998. Ecosystem responses to internal and watershed organic matter loading: consequences for hypoxia in the eutrophying Neuse river estuary, North Carolina, USA. Marine Ecology-Progress Series, 166: 17-25.

Paerl, H.W.,Valdes, L.M., Peierls, B.L., Adolf, J.E., Harding Jr., L.W., 2006. Anthropogenic and climatic influences on the eutrophication of large estuarine ecosystems. Limnology and Oceanography, 51(1, part2): 448-462.

Paerl, H.W., Rossignol, K.L., Hall, N.S., Peierls, B.L., and Wetz, M.S., 2010. Phytoplankton Community Indicators of Short- and Long- term Ecological Change in the Anthropogenically and Climatically Impacted Neuse River Estuary, North Carolina, USA, 33: 485-497.

Paerl, H.W. and Peierls, B.L., 2014. Bioavailability and fate of organic nitrogen loading to Neuse River Estuary phytoplankton. Report No. 440 at WRRI Annual Conference, 21 March, Raleigh, NC.

Peierls, B. L., and H. W. Paerl. 1997. Bioavailability of atmospheric organic nitrogen deposition to coastal phytoplankton. Limnol. Ocean. 42: 1819–1823.

Peierls, B.L., and Paerl, H.W., 2010. Temperature, organic matter, and the control of bacterioplankton in the Neuse River and Pamlico Sound estuarine system. Aquatic Microbial Ecology, 60(2): 139-149.

Peierls, B.L., Hall, N.S., and Paerl, H.W., 2012. Non-monotonic Responses of Phytoplankton Biomass Accumulation to Hydrologic Variability: A Comparison of Two Coastal Plain North Carolina Estuaries, 35: 1376-1392.

Petrone, K., Fellman, J., Donn, M., Hood, E.,, and Grierson, P., 2010. Quantifying and managing organic matter-derived nutrients in coastal catchments and estuaries. CSIRO: Water for a Healthy Country National Research Flagship. ISSN: 1835-095X.

Pincknet, J.L., Paerl, H.W., and Harrington, M.B., 1999. Responses of the phytoplankton community growth rate to nutrient pulses in variable estuarine environements. Journal of Phycology, 35(6): 1455-1463.

Premuzic, E.T., Benkovitz, C.M., Gaffney, J.S., and Walsh, J.J., 1982. The nature and distribution of organic matter in the surface sediments of world oceans and seas. Org. Geochem., 4:63-77.

Reed, R.E., Glasgow, H.B., Burkholder, J.M. and Brownie, C., 2004. Seasonal physical-chemical structure and acoustic Doppler current profiler flow patterns over multiple years in a shallow, stratified estuary, with implications for lateral variability. Estuarine Coastal and Shelf Science, 60(4): 549-566.

Rochelle-Newall, E. J., and Fisher, T. R., 2002. Chromophoric dissolved organic matter and dissolved organic carbon in Chesapeake Bay. Marine Chemistry, 77, 23–41.

Rothenberger, M.B., Burkholder, J.M, and Brownie, C., 2009. Long-term effects of changing land use practices on surface water quality in a coastal river and lagoonal estuary. Environmental Management, 44:505-523.

Senesi, N., 1990. Molecular and quantitative aspects of the chemistry of fulvic acid and its interaction with metal ions and organic compounds. Part I. The fluorescence approach. Analytica Chimica Acta, 232: 51-75.

Senesi, N., 1990. Molecular and quantitative aspects of the chemistry of fulvic acid and its interaction with metal ions and organic compounds. Part II. The fluorescence approach. Analytica Chimica Acta, 232: 77-106.

Spencer R.G.M., Baker A., Ahad J.M.E., Cowie G.L., Ganeshram R., Upstill-Goddard R.C., and Uher G., 2007. Discriminatory classification of natural and anthropogenic waters in two UK estuaries. Sci Total Environ 373:305–323.

Stedmon, C. A., Markager, S., and Bro, R., 2003. Tracing dissolved organic matter in aquatic environments using a new approach to fluorescence spectroscopy. Marine Chemistry, 82 (3−4): 239−254.

Stedmon, C.A. and Markager, S., 2003. Behaviour of the optical properties of coloured dissolved organic matter under conservative mixing. Estuarine Coastal and Shelf Science, 57(5-6): 973-979.

Stedmon, C. A., and S. Markager (2005), Resolving the variability in dissolved organic matter fluorescence in temperate estuary and its catchment using PARAFAC analysis, Limnol. Oceanogr., 50(2), 686 – 697.

Stedmon, C.A., Markager, S., Tranvik, L., Kronberg, L., Slatis, T., and Martinsen, W., 2007. Photochemical production of ammonium and transformation of dissolved organic matter in the Baltic Sea. Marine Chemistry, 104: 227-240.

Stedmon, C.A., Thomas, D.N., Granskog, M., Kaartokallio, H., Papadimitriou, S. and Kuosa, H., 2007a. Characteristics of dissolved organic matter in Baltic Coastal sea ice: Allochthonous or Autochthonous. Environmental Science and Technology, 41: 7273-7279.

Stedmon, C. A., and Bro, R., 2008. Characterizing dissolved organic matter fluorescence with parallel factor analysis: a tutorial. Limnology and Oceanography Methods, 6: 572−579.

Steel, J. 1991. Albemarle-Pamlico estuarine system: technical analysis of status and trends. Albemarle-Pamlico Estuarine Study Report No. 91-01. N.C. Department of Environment, Health, and Natural Resources, Albemarle-Pamlico Estuarine Study, Raleigh, NC.

Stepanauskas, R., Edling, H., Tranvik, L.J., 1999. Differential dissolved organic nitrogen availability and bacterial aminopeptidase activity in limnic and marine waters. Microbial Ecology 38, 264e272.

Walker, S. A., R. M. W. Amon, C. Stedmon, S. Duan, and P. Louchouarn (2009), The use of PARAFAC modeling to trace terrestrial dissolved organic matter and fingerprint

water masses in coastal Canadian Arctic surface waters, J. Geophys. Res., 114, G00F06, doi:10.1029/2009JG000990.

Williams, C.J., Yamashita, Y., Wilson, H.F., Jaffé, R., and Xenopoulos, M.A., 2010. Unraveling the role of land use and microbial activity in shaping dissolved organic matter charasteristics in stream ecosystems. Limnology and Oceanography, 55(3): 1159-1171.

Willey, J. D., R. J. Kieber, M. S. Eyman, and G. B. Avery Jr., Rainwater dissolved organic carbon: Concentrations and global flux, Global Biogeochem. Cycles, 14, 139–148, 2000.

Wilson, H.F., and Xenopoulos, M.A., 2008. Effects of agricultural land use on the composition of fluvial dissolved organic matter. Nature Geoscience, DOI:10.1038/NGEO391.

Yamashita, Y., N. Maie, H. Briceño, and R. Jaffé., 2010. Optical characterization of dissolved organic matter in tropical rivers of the Guayana Shield, Venezuela, J. Geophys. Res., 115, G00F10, doi:10.1029/2009JG000987.

2.7 Tables and Figures

Table 2.1: Mean monthly discharge measured at Fort Barnwell, NC (USGS site #02091814), which is 24 km upstream of station NR0. Discharge data was divided by the ratio of gauged to total watershed area (0.69 for the NRE) as a correction for un-gauged watershed discharge (Peierls et al. 2012).

Date	Discharge ($m^3 s^{-1}$)
March 2010	183.7
April 2010	123.7
May 2010	51.4
June 2010	65.6
July 2010	17.3
August 2010	31.3
September 2010	26.4
October 2010	168.9
November 2010	34.3
December 2010	39.0
January 2011	42.5
February 2011	70.6

Table 2.2: Monthly mean, minimum and maximum FMax values for PARAFAC fluorescence and water quality data (DO- mg L^{-1} and Chl-mg L^{-1}) at station NR0, NR70 and NR180.

Season	Station		**C1**	**C2**	**C3**	**C4**	**C5**	**DO**	**pH**	**Chl**
Spring	NR0	Max	34.9	18.2	8.5	3.8	9.9	11.1	7.3	6.8
		Min	32.4	15.3	4.2	1.8	2.7	5.5	6.2	3.0
		Mean	33.3	16.4	6.1	2.8	5.2	7.5	6.7	4.9
Summer	NR0	Max	32.6	19.9	4.6	4.6	3.0	7.7	7.5	11.6
		Min	30.3	17.6	3.6	3.5	2.5	4.3	6.8	2.1
		Mean	31.6	18.9	4.1	4.0	2.7	6.2	7.2	5.4
Autumn	NR0	Max	33.8	19.3	6.6	4.3	6.8	8.7	8.0	4.6
		Min	31.4	15.5	3.7	2.5	2.7	4.1	6.9	3.7
		Mean	33.0	17.1	5.4	3.0	4.7	6.5	7.4	4.3
Winter	NR0	Max	33.0	17.6	5.6	4.1	3.8	12.5	9.2	9.6
		Min	31.3	14.9	4.3	3.2	3.4	10.4	7.8	4.5
		Mean	32.0	16.4	4.9	3.7	3.6	11.7	8.4	7.0
Spring	NR70	Max	34.1	18.5	8.0	4.7	9.6	12.2	7.8	24.2
		Min	31.4	15.9	3.6	2.1	1.2	3.8	6.6	7.0
		Mean	32.8	16.9	5.1	3.2	3.6	8.4	7.4	12.9
Summer	NR70	Max	32.2	23.8	4.0	5.7	1.8	8.0	8.4	13.5
		Min	30.4	19.5	3.4	3.5	0.5	3.5	7.3	5.6
		Mean	31.3	21.1	3.8	4.6	0.9	6.1	7.9	9.3
Autumn	NR70	Max	33.5	24.2	6.7	6.1	4.7	10.5	8.2	13.7
		Min	31.0	16.9	3.8	2.7	0.3	2.5	7.2	5.0
		Mean	32.0	20.3	4.7	4.8	1.7	7.7	7.8	9.5
Winter	NR70	Max	32.5	21.9	5.3	5.4	2.5	14.2	8.5	76.8
		Min	30.1	16.3	2.7	4.1	1.1	10.0	7.6	8.7
		Mean	31.7	19.7	4.2	4.6	1.7	12.3	8.0	32.6
Spring	NR180	Max	33.1	21.3	4.5	4.9	1.5	12.5	8.1	28.1
		Min	30.3	18.5	3.6	3.9	0.7	6.9	7.5	4.7
		Mean	32.1	19.8	4.1	4.3	1.1	9.7	7.8	10.4
Summer	NR180	Max	31.5	24.2	4.3	6.5	0.4	8.2	8.1	7.7
		Min	29.5	21.5	3.6	4.8	0.0	0.4	7.4	2.4
		Mean	30.5	23.3	3.9	5.6	0.2	5.9	7.9	5.1
Autumn	NR180	Max	32.6	25.8	5.4	9.9	1.7	9.5	8.2	12.9
		Min	26.9	18.4	3.2	4.3	0.0	2.6	7.6	4.6
		Mean	30.8	21.6	4.3	6.1	0.8	7.3	7.9	7.9
Winter	NR180	Max	32.3	23.4	4.1	8.8	0.6	12.1	8.2	18.1
		Min	29.7	21.9	3.5	5.2	0.2	10.9	7.4	4.6
		Mean	31.1	22.6	3.8	6.5	0.4	11.5	7.8	9.8

Table 2.3: Monthly mean, minimum and maximum FMax values for PARAFAC fluorescence and water quality data (DO- mg L^{-1} and Chl-mg L^{-1}) within the NRE.

Season	**Month**		**C1**	**C2**	**C3**	**C4**	**C5**	**DO**	**pH**	**Chl**
Spring	March	Max	33.4	18.6	5.7	4.7	3.6	12.5	8.1	28.1
		Min	31.4	15.3	4.2	2.9	1.4	10.8	7.0	4.6
		Mean	32.6	16.9	4.9	3.6	2.5	11.6	7.6	13.0
		N=6								
Spring	April	Max	34.9	20.2	8.5	4.3	9.9	11.0	7.9	15.7
		Min	31.7	15.3	4.0	1.8	1.2	3.8	6.2	4.7
		Mean	33.5	17.3	6.3	2.8	5.6	7.0	7.1	8.5
		N=6								
Spring	May	Max	32.6	21.3	4.3	4.9	2.8	8.2	7.9	7.0
		Min	30.3	18.1	3.6	3.3	0.7	5.7	6.6	3.0
		Mean	31.9	19.4	3.9	4.0	1.6	6.6	7.2	5.4
		N=5								
Summer	June	Max	32.6	23.3	4.6	5.3	3.0	7.7	8.1	11.8
		Min	30.1	17.6	3.4	3.5	0.3	4.9	7.0	3.4
		Mean	31.6	20.0	3.9	4.1	1.4	6.1	7.7	7.3
		N=6								
Summer	July	Max	31.5	24.2	3.9	6.5	2.5	8.2	8.0	13.5
		Min	29.5	19.1	3.6	4.4	0.1	3.5	7.2	2.1
		Mean	30.6	21.6	3.7	5.1	1.1	6.8	7.7	5.5
		N=6								
Summer	August	Max	32.2	24.0	4.6	6.3	2.9	7.7	8.4	11.6
		Min	29.8	19.2	3.8	3.8	0.0	0.4	6.8	4.1
		Mean	31.3	21.6	4.1	5.0	1.3	5.2	7.7	7.0
		N=6								
Autumn	September	Max	33.2	25.8	4.4	9.9	2.9	8.3	8.2	9.1
		Min	26.9	18.2	3.2	3.4	0.0	4.1	6.9	3.7
		Mean	31.0	22.3	3.8	5.9	1.3	6.3	7.7	6.5
		N=6								
Autumn	October	Max	33.8	22.5	6.7	6.7	6.7	8.9	8.1	13.2
		Min	31.1	15.5	4.2	2.5	0.6	2.5	6.9	4.3
		Mean	32.7	18.0	5.5	3.9	3.0	5.8	7.5	7.4
		N=6								
Autumn	November	Max	33.5	21.4	6.6	4.8	6.8	10.5	8.2	13.7
		Min	31.0	16.2	4.2	2.5	0.8	8.6	7.7	4.5
		Mean	32.1	18.8	5.0	4.0	2.9	9.4	7.9	7.5
		N=6								

Table 2.3 Continued

Winter	December	Max	33.0	23.2	4.8	7.1	3.8	12.5	8.6	13.7
		Min	30.1	16.6	2.7	3.6	0.5	11.5	7.6	4.9
		Mean	31.5	20.1	4.0	4.8	2.0	12.0	8.0	8.1
		N=6								
Winter	January	Max	32.5	22.4	4.4	6.5	3.5	14.2	9.2	61.7
		Min	30.6	16.8	3.6	3.8	0.3	11.1	7.4	4.5
		Mean	31.8	19.8	4.2	4.9	1.7	12.4	8.1	18.7
		N=6								
Winter	February	Max	32.3	23.4	5.6	8.8	3.5	12.7	8.5	76.8
		Min	29.7	14.9	3.5	3.2	0.2	10.0	7.8	5.5
		Mean	31.5	18.7	4.8	5.1	1.8	11.0	8.1	22.6
		N=6								

Table 2.4: Composition of excitation/emission peak maxima in DOM fluorescence of NRE along with peak maxima and PARAFAC model components. OpenFluor identified similar spectra as having Tucker congruence (θ) exceeding 0.95 on the excitation and emission simultaneously.

Component	Ex. λ (nm)	Em. λ (nm)	%Fmax Range	OpenFluor Correlation (P<0.05)	Source	Potential Source
C1	<240	440	44.5-57.7	4	Terrestrial; Humic acid	Ubiquitous terrestrial humic acid-like
C2	<240	386	24.7-42.7	6	Planktonic	Microbial humic-like, M-Peak, Wastewater/nutrient enrichment tracer
C3	270	508 (312)	4.5-14.1	8	Soil fulvic-like	Terrestrial soil fulvic-like, reduced semi-quinone-like
C4	240	336 (492)	3.0-16.4	1	Protein-like	Protein-like; ubiquitous tryptophan; recent biological production, T-Peak
C5	335	438	0.0-16.4	0	Soil leachate Fulvic-like	Terrestrial fulvic acid-like, constituents of tannins (gallic acid)

*Secondary peaks are noted in parenthesis

Table 2.5: Seasonal and annual R^2 values for FMax values vs. DOC concentrations and FMax values vs. DON concentration ($P<0.05$, n.s.- not significant).

DOM pool	R^2 value per season	**C1**	**C2**	**C3**	**C4**	**C5**
DOC	All seasons	0.20	0.17	0.28	0.21	0.23
	Autumn	n.s.	n.s.	n.s.	n.s.	n.s.
	Spring	n.s.	n.s.	0.24	0.29	0.25
	Summer	0.39	0.26	n.s.	0.36	n.s.
	Winter	n.s.	n.s.	n.s.	n.s.	n.s.
DON	All seasons	n.s.	0.16	0.29	0.24	0.37
	Autumn	0.35	0.67	0.59	0.55	0.70
	Spring	0.18	0.17	0.40	0.58	0.52
	Summer	0.40	0.58	n.s.	0.57	0.36
	Winter	n.s.	0.27	n.s.	0.47	0.28

Table 2.6: Monthly R^2 values for DOC concentrations versus FMax values with NR0 and without NR0 in the NRE ($P<0.05$, n.s.- not significant).

All Data	C1	C2	C3	C4	C5
March	n.s.	n.s.	n.s.	n.s.	n.s.
April	n.s.	n.s.	n.s.	n.s.	n.s.
May	n.s.	n.s	n.s.	n.s	n.s.
June	n.s	n.s	n.s.	0.58	n.s.
July	n.s	n.s.	n.s.	n.s.	n.s.
August	0.44	n.s.	n.s.	n.s	n.s.
September	n.s.	n.s	0.55	n.s	n.s.
October	n.s.	n.s.	n.s.	n.s.	n.s.
November	n.s.	n.s	0.60	n.s	0.58
December	n.s.	n.s.	n.s.	n.s.	n.s.
January	n.s	n.s.	n.s.	n.s.	n.s
February	n.s.	n.s	n.s	n.s.	n.s.

Data (without NR0)	C1	C2	C3	C4	C5
March	n.s.	n.s.	n.s.	n.s.	n.s.
April	n.s.	n.s.	n.s.	n.s.	n.s.
May	n.s.	0.86	n.s.	0.67	0.59
June	0.50	0.79	n.s.	0.66	0.75
July	n.s.	0.54	n.s.	n.s.	0.86
August	0.54	n.s.	n.s.	0.70	n.s
September	n.s	0.69	0.53	0.46	0.72
October	0.49	n.s	n.s	n.s.	n.s
November	n.s.	n.s.	0.50	n.s.	0.50
December	n.s.	n.s.	n.s.	n.s	n.s
January	0.46	n.s	n.s	n.s.	n.s.
February	n.s.	0.78	0.76	n.s	0.47

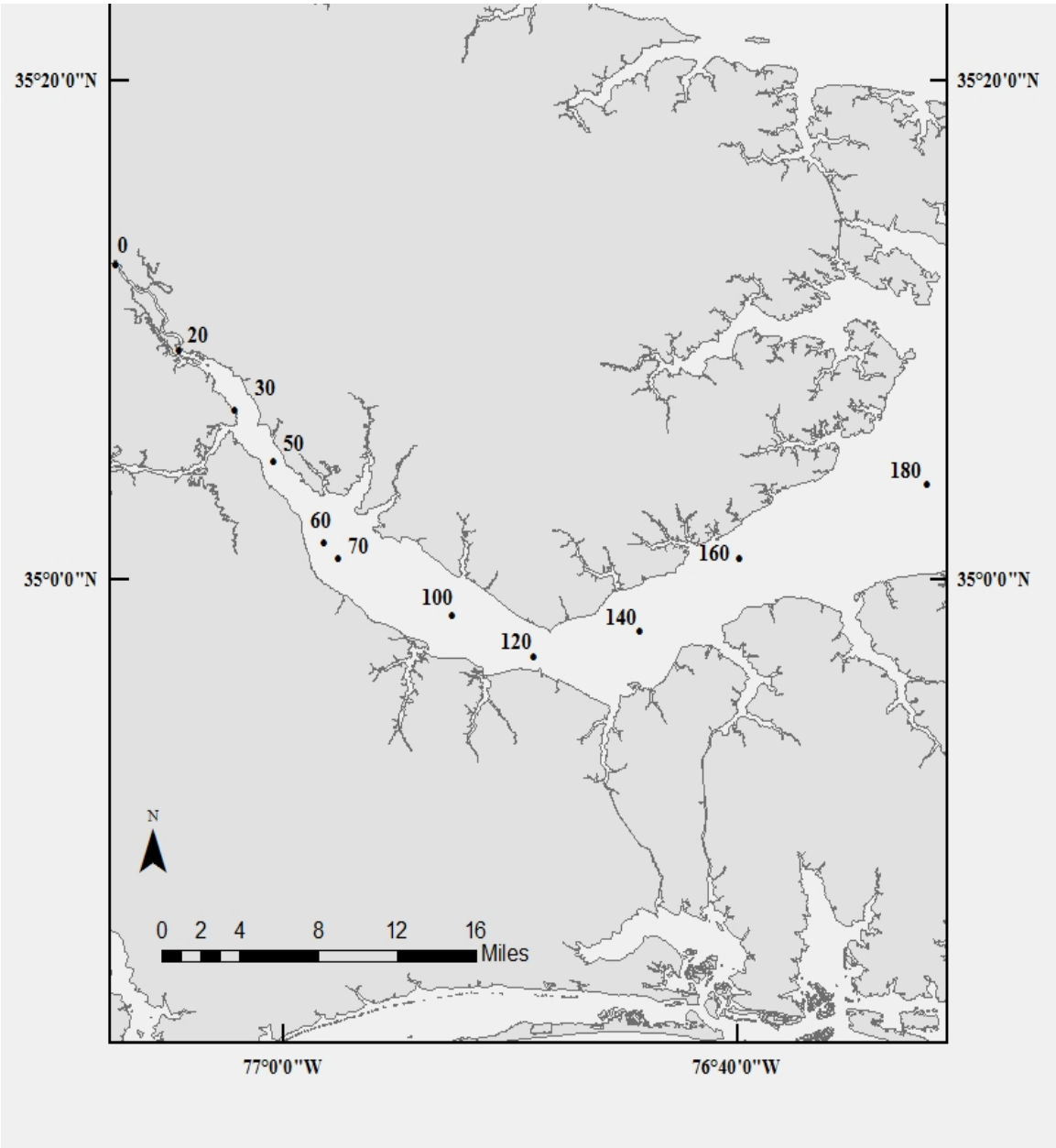

Figure 2.1: Map of Neuse River Estuary including ModMon sampling sites (courtesy of Lauren Handsell).

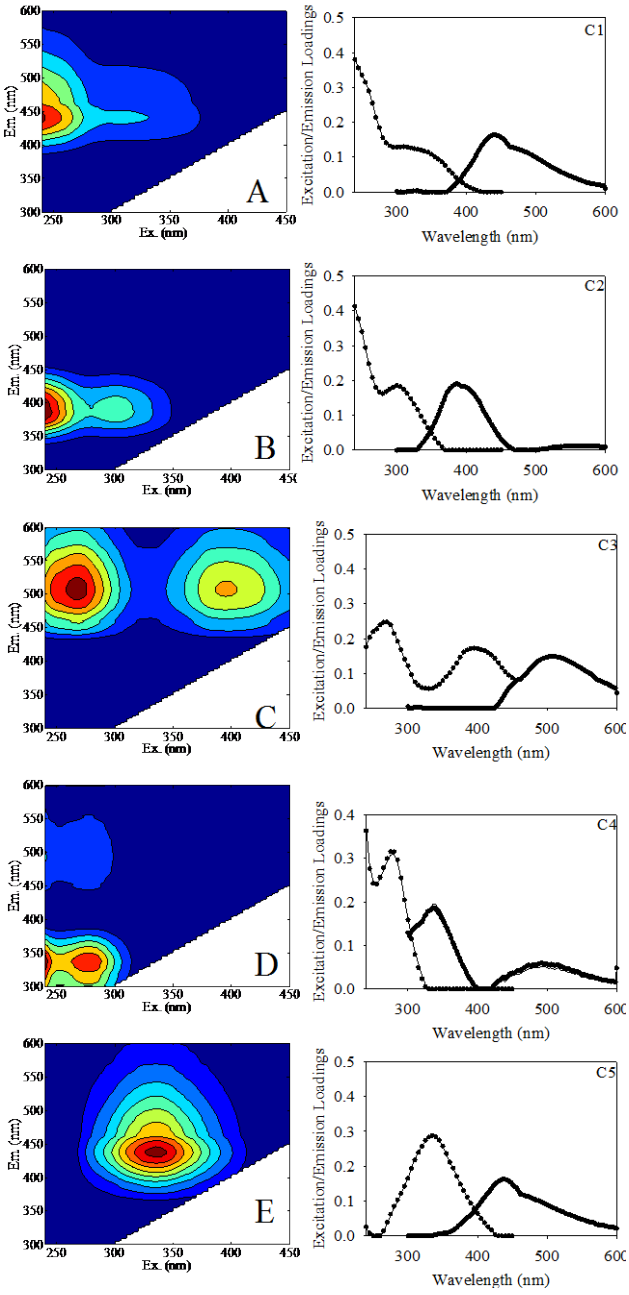

Figure 2.2: Five split half validated fluorescent components calculated from a PARAFAC model fit to DOM EEMs from the NRE between March 2010 and February 2011. The individual excitation and emission loadings are shown (solid line) for comparison to previous studies and the split-half validation results also are indicated (dotted line).

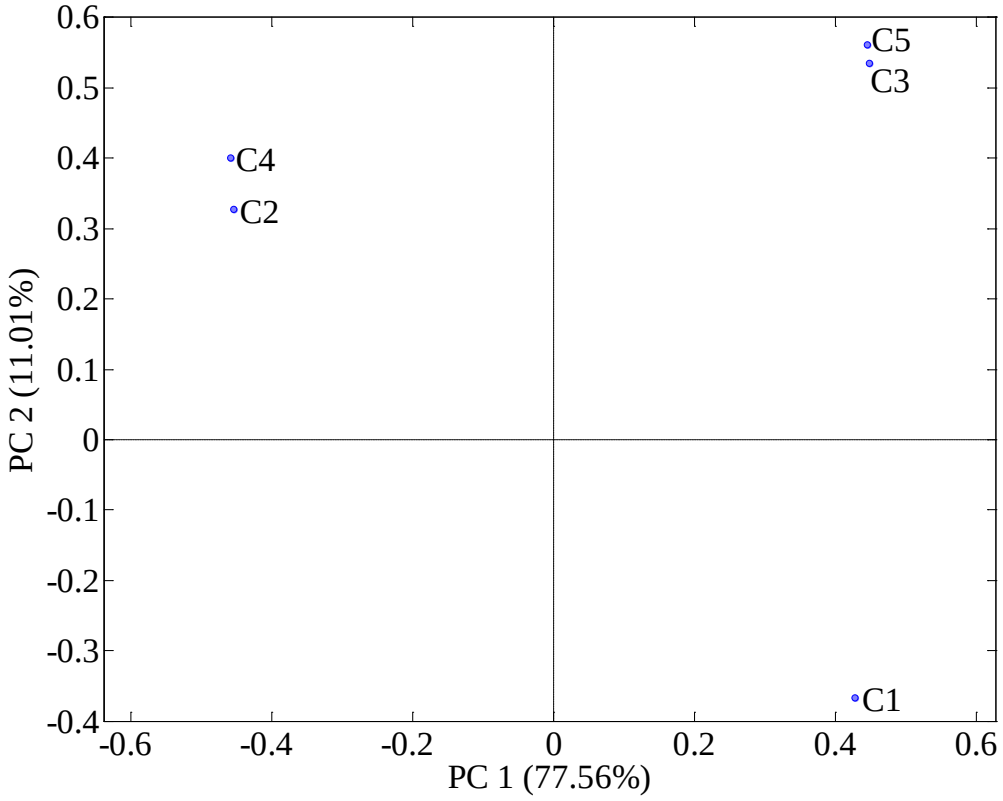

Figure 2.3: Plots of loadings (variables) from a principle component analysis of PARAFAC components. The main trend in loadings along PC1 is representative of OM source while the main trend in loadings along PC2 is representative of OM degradation processes.

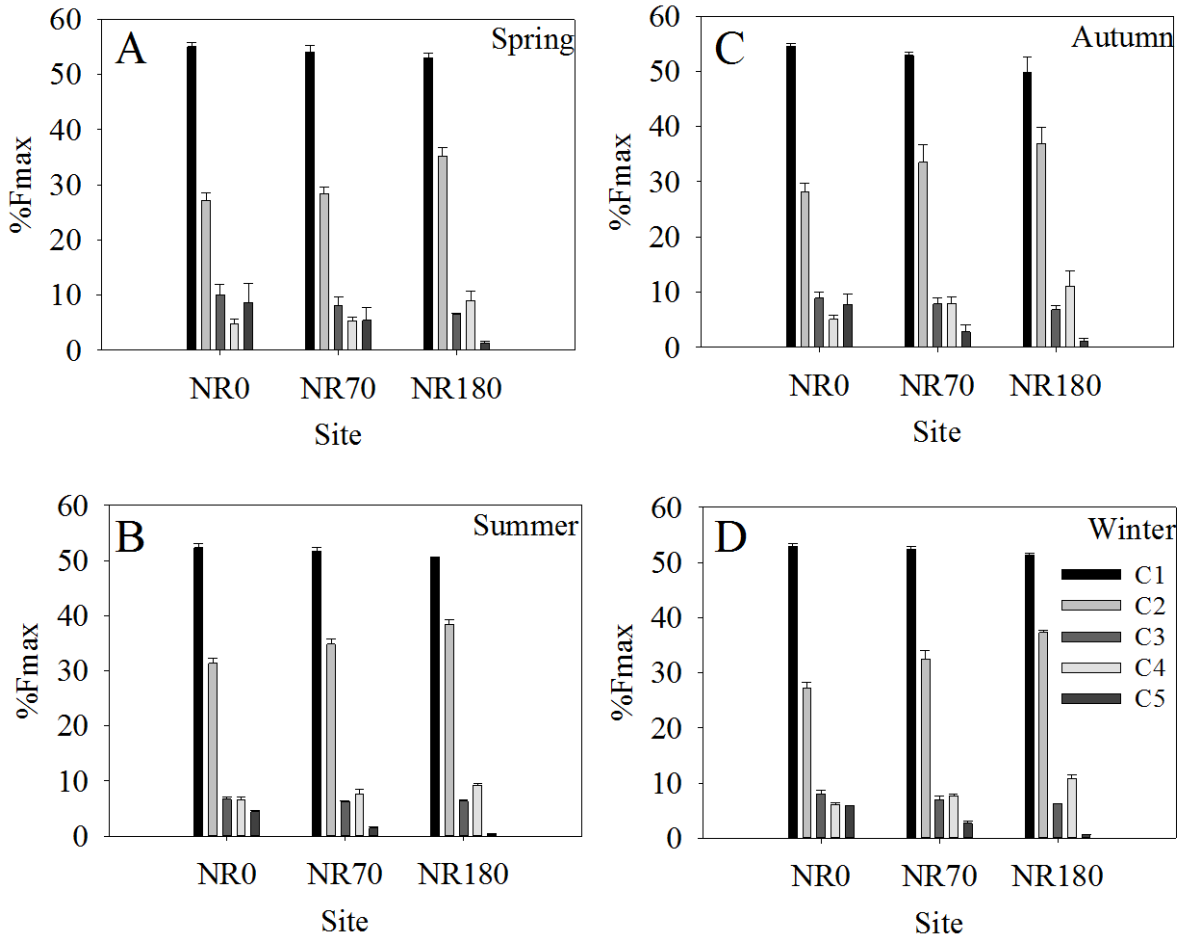

Figure 2.4: Spatial and seasonal trends in PARAFAC mean %Fmax values at stations NR0, NR70 and NR180 during the spring (A), summer (B), autumn (C) and winter (D).

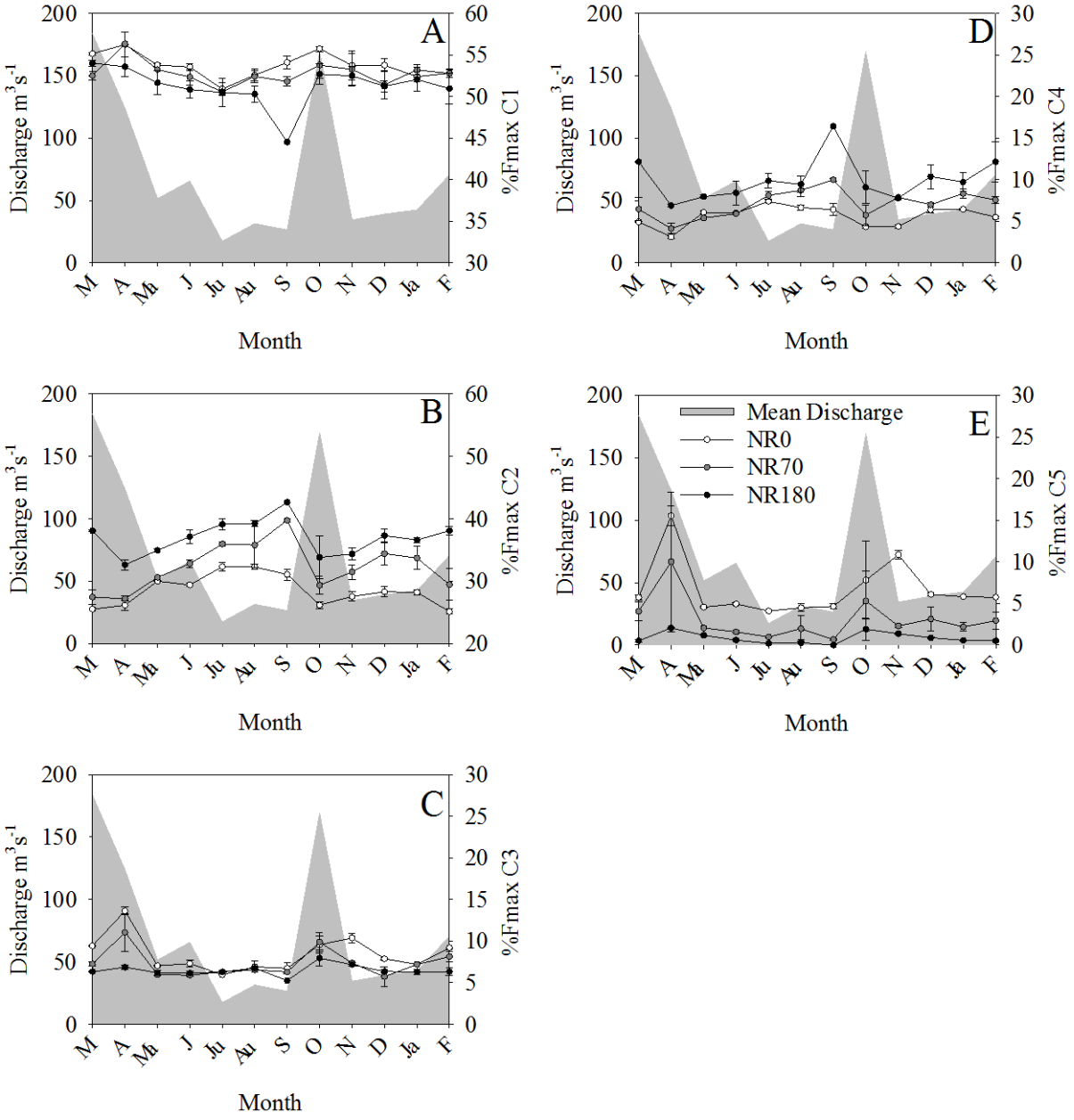

Figure 2.5: %Fmax abundance of PARAFAC components at site NR0, NR70 and NR180 with monthly mean discharge in the Neuse River Estuary, 2010-2011. Note variability in the scale for %FMax values on right y-axes.

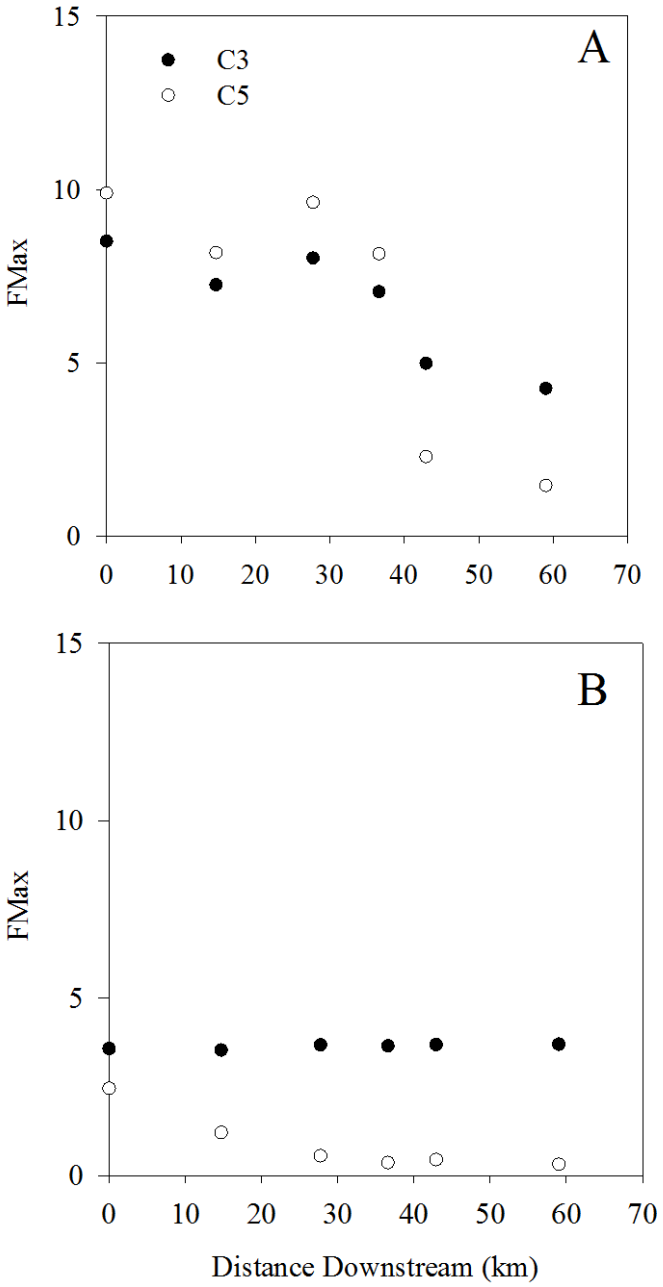

Figure 2.6: Surface water FMax abundance values for soil-fulvic like C3 and terrestrial fulvic-like C5 in (A) April 2010 (discharge 123.7 $m^3 s^{-1}$) and (B) July 2010 (discharge 17.3 $m^3 s^{-1}$) compared against the distance downstream from NR0 in the Neuse River Estuary. Note variability in the scale for %FMax values on the y-axes.

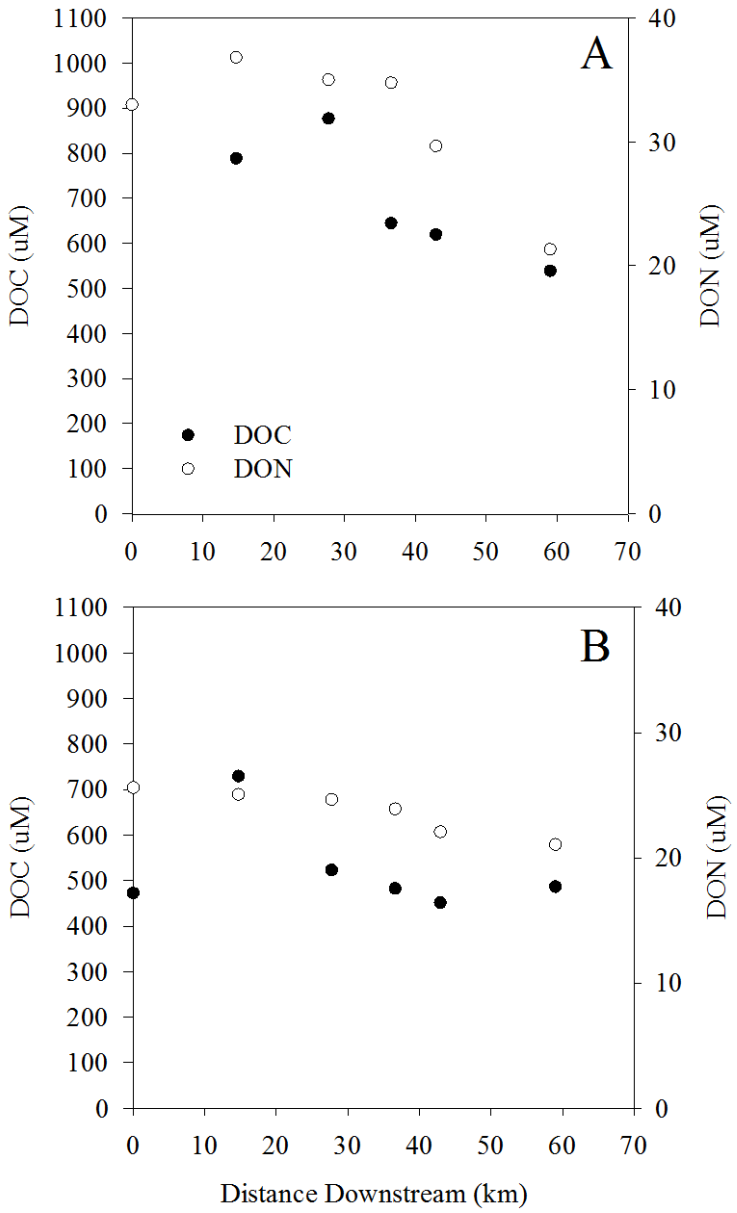

Figure 2.7: Surface water DOC and DON values in (A) April 2010 (discharge 123.7 $m^3 s^{-1}$) and (B) July 2010 (discharge 17.3 $m^3 s^{-1}$) compared against the distance downstream from NR0 in the Neuse River Estuary. Note variability in the scale for %FMax values on the y-axes.

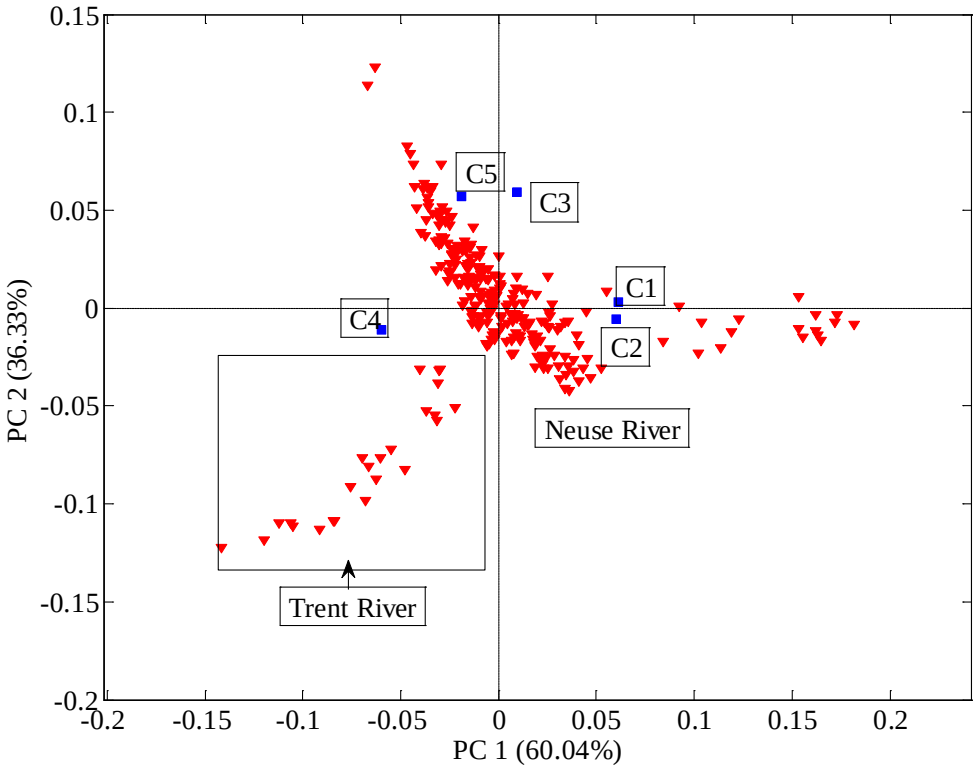

Figure 2.8: Plots of loadings (variables) from a principle component analysis of NR-TR PARAFAC components.

Chapter 3: A biogeochemical study of the Neuse River Estuary: Linking lignin phenols, δ^{13}C-DOM and optical properties of dissolved organic matter.

3.1 Introduction

Dissolved organic matter (DOM) is a heterogeneous mixture of aromatic and aliphatic compounds that remains largely uncharacterized, yet plays an active role in the biogeochemistry of the carbon cycle on a global scale (Walker et al. 2009; Bauer and Bianchi, 2011). The flux of terrigenous DOM through highly productive estuarine and coastal waters represents a major pathway between terrestrial and marine environments. Within these waters the quantity and quality of DOM is controlled by seasonal cycles in riverine loading, mixing, primary productivity, and biotic/abiotic turnover, photochemical reactions and remineralization (Walker et al. 2009; Bauer and Bianchi, 2011). By analyzing the spatial and temporal variability of DOM within estuaries, information pertaining to OM source and fate across the freshwater-marine continuum can be obtained.

The highly productive, eutrophic waters of the Neuse River Estuary (NRE), in eastern North Carolina, USA, serve as such a transition zone for terrigenous DOM between the head of the Neuse River and Pamlico Sound. Previous studies have determined that the NRE is dominated by inputs from riverine discharge, yet very clear shifts in DOM quality are apparent as discharge varied (Paerl et al. 1998; Osburn et al. 2012; Dixon et al. accepted). Furthermore, flushing times within the NRE will aid in determining whether DOM is primarily autochthonous or allochthonous and if it is processed internally or transported unaltered downstream to the Pamlico Sound (Paerl et al. 1998; Mari et al. 2007, Peierls et al.

2012). Thus, the main sources of DOM, its composition and quantity can change throughout an estuary depending on the hydrodynamic conditions.

Chromophoric dissolved organic matter (CDOM) represents the light absorbing fraction of DOM in natural waters and absorbs light in the ultraviolet and visible wavelength range Coble, 2007). The optical properties of CDOM provide quantitative and qualitative information on DOM quantity (i.e., predict DOC concentrations) and quality (i.e., compositional characteristics between marine and terrestrial sources) (Bricaud et al. 1981; Coble 1996; Coble, 2007). CDOM is measured using optical methods such as UV-visible absorbance and fluorescence spectroscopy (e.g. Coble, 1996; Stedmon and Markager, 2003). Over the past decade, it has become common practice to use a combination of spectroscopic fluorescence excitation and emission matrices (EEMs) with Parallel Factor analysis (PARAFAC) to decompose EEM datasets mathematically into components corresponding to a chemical analyte or group of strongly covarying analytes (Ohno and Bro 2006; Stedmon et al. 2003; Stedmon and Bro, 2008; Murphy et al. 2013). These methods offer an inexpensive, non-destructive means for obtaining sensitive measurements with the ability to differentiate and trace sources of CDOM.

Chemical biomarkers, such as carbon stable isotopes ($\delta^{13}C$) and lignin phenols, are also routinely used to identify DOM sources in coastal waters (Benner and Opsahl, 2001; Harvey and Mannino, 2001; Bauer, 2002). For example, $\delta^{13}C$ values for marine DOM derived from phytoplankton typically have $\delta^{13}C$ values that range from −20 to −22‰, while terrestrial DOM derived from C3 land plants typically has $\delta^{13}C$ values that range from −26 to −28‰ (Bauer, 2002). Additionally, lignin is a unique geochemical biomarker of vascular

plants and can be used to trace the fate of terrestrial DOM in coastal seawater (e.g., Hernes and Benner, 2003; Walker et al. 2009; Osburn and Stedmon, 2011). Further, the ratios of the different lignin phenolic compounds derived from the oxidation of lignin can be used to distinguish between plant sources (e.g. angiosperm vs. gymnosperm or woody vs. non-woody tissue) and the extent of degradation (Hedges et al. 1988).

Previous studies on DOM within the NRE have shown that it is dominated by inputs from riverine discharge, yet very clear shifts in DOM quality are apparent as discharge has varied (Paerl et al. 1998; Osburn et al. 2012). The focus of this study was to test the previous DOM findings with biogeochemical measurements such as $\delta^{13}C$ values and lignin phenols. We suggest that both $\delta^{13}C$ values and lignin phenols will reflect terrestrial material and increased lignin concentrations as discharge increases within the NRE. In addition, we hypothesize that $\delta^{13}C$ values and lignin phenols will correlate with shifts in DOM quality and quantity from the head of the NR to the river mouth. Furthermore, using lignin to characterize DOM is a long and expensive process, often involving large sample volumes and many time-consuming steps of sample preparation and analysis. Since the chemical nature of CDOM defines its optical properties, the absorbance and fluorescence properties of DOM have become a much more convenient proxy of DOM in a variety of aquatic systems (Walker et al. 2009; Osburn and Stedmon, 2011). Thus, we aim to examine the relationships between the optical and chemical characteristics so that future work on tracing carbon flow in this region can gain information from the relatively rapid and cheap optical measurements, which can be carried out extensively.

3.2 Methods

3.2.1 Study Site

The NRE is a drowned river valley and a major tributary of the second largest estuarine/lagoonal complex in the United States, the Albemarle-Pamlico Sound (Steel, 1991) (Fig. 3.1). Regional land cover changes, within the NR basin, caused by timber, naval stores (storage of tar, pitch, and turpentine) and free-range livestock industries can be dated back to the early eighteenth (Frost 1993). However, much of the natural landscape in the NR basin consists of longleaf pine (*Pinus palustris*) and bald cypress (*Taxodium distichum*) swamps, which dominate the river upstream of the estuary, above New Bern, NC (Vahatalo et al. 2005; Elam et al. 2009). The watershed is approximately 16,108 km^2. The estuary has an average surface area of 455 km^2 and an average depth of 2.7 m (Paerl et al. 2010). River discharge rates range from 50 to 1000 m^3s^{-1} resulting in flushing times that range from 20 to 200 days (Luettich et al. 2002; Crosswell et al. 2012). The limited oceanic exchange of the NRE contributes to the long residence and slower flushing times, which aid in extensive recycling of nutrients in the water column (Christian et al. 1991; Steel, 1991). Furthermore, over the past few decades, accelerated eutrophication and OM loading driven by urban development and expanding agricultural operations in the NRE watershed has resulted in annual fish kills, harmful algal blooms, and poor water quality in the NRE (Paerl et al. 1998, 2010; Burkholder et al., 2006). The flow regime of the mesohaline estuary is surface outflow and bottom-water inflow with minimal tidal influence (Reed et al., 2004; Null et al. 2011). Winds are an important mixing force in this shallow system and play a significant role in sediment resuspension, influencing OM concentrations, dissolved oxygen distributions, and

nutrient release from the benthic environment (Reed et al., 2004; Corbett, 2010; Null et al. 2011).

3.2.2 Sample Collection

Monthly samples were collected between March 2010 and February 2011 during the NRE modeling and monitoring (ModMon: see; http://www.unc.edu/ims/neuse/modmon/) sampling cruises, which spanned the main axis of the estuary (Fig. 3.1). At each site, water samples were collected near the water surface and at roughly 0.5 meters above the bottom, transferred to acid-cleaned 1 liter HDPE bottles, and kept cool and shaded during transport to the laboratory. All samples were stored in the dark at 4 °C until shipped to N.C. State University, where they were vacuum-filtered through Sterivex-GP 0.22 μm filters into pre-cleaned glass vials with Teflon coated lids. All glassware in contact with samples was soaked in a detergent solution for a minimum of six hours, rinsed with ultrapure (18.2 MΩ resistivity) water, air-dried, and then combusted in an oven at 550°C for at least six hours.

3.2.3 C:N Values

Dissolved organic C:N values, the molar ratio of dissolved organic carbon (DOC) to dissolved organic nitrogen (DON), were calculated and used as an indicator of DOM source, e.g., terrestrial or vascular plant derived C:N values are generally greater than 15 and C:N values less than 8 favor marine (or more broadly autochthonous) sources of DOM (Premuzic et al. 1982). The Institute of Marine Science (UNC-IMS) provided the DOC and DON data that were used to calculate C:N values. DOC and DON samples were transported in carboys to UNC-IMS and either refrigerated before filtration or immediately pressure filtered through a pre-combusted, 142 mm Whatman GF/F filter and a 142 mm Millipore Express Plus 0.22

μm effective pore size polyethersulfone membrane filter arranged in series. DOC measurements were made using high temperature combustion techniques on a Shimadzu model TOC5000, equipped with an ASI-5000A autosampler (Benner & Strom 1993). Acidified (HCl, pH < 2) samples were sparged for 8 min with air to drive off DIC. Background checks revealed complete removal of DIC by this treatment. Reported values represent the average of 3 injections. DON was calculated as the difference between total dissolved N (TDN) and total dissolved inorganic N (DIN: sum of nitrite, nitrate, and ammonium) measured on a Lachat QuikChem 8000 flow injection analyzer (Lachat, Milwaukee,WI, USA

3.2.4 Optical Properties of DOM

CDOM absorbance was measured from 240 to 800 nm using a 1-cm quartz cell (relative to air) on a Varian 300 UV spectrophotometer. They were blank-corrected by subtracting the absorbance of Milli-Q water from each sample. CDOM samples were allowed to warm to room temperature prior to optical measurements. Absorbance spectra and blank-corrected absorbance values were converted to Napierian absorption coefficients (a_λ, m^{-1}) at each wavelength (λ):

$$a_\lambda = 2.303 / A_\lambda * l$$

where A_λ is the blank corrected spectrophotometer absorbance reading at wavelength λ and l is the optical pathlength in meters (Kirk 1994). CDOM was quantified as the absorption coefficient at 350 nm (a350). The spectral slope ratio, S_R, is defined as the ratio of the slope of the shorter wavelength interval (275–295 nm) to that of the longer wavelength interval

(350–400 nm) (Helms et al. 2008). S_R values were used to characterize DOM source and molecular weight (Helms et al. 2008).

DOM excitation and emission matrix (EEM) fluorescence was measured on a Varian Eclipse spectrofluorometer using a 1 cm quartz cuvette. EEMs for each sample were obtained by collecting a series of emission (Em) wavelengths ranging from 300 to 600 nm (2 nm increments) at excitation (Ex) wavelengths ranging from 240 to 450 (5-nm increments). EEM fluorescence intensities were corrected for Rayleigh and Raman (natural scattering properties of pure water after it absorbs light) scattering by Milli-Q water blank subtraction and for instrument bias prior to correction for any inner-filtering effect (Stedmon and Bro 2008). Finally, the instrument measured fluorescence intensity in arbitrary units (A.U.), which were converted to quinine sulfate equivalents (ppb QSE) (Laewetz and Stedmon 2009). HIX is a fluorescence index used to determine the degree of DOM humification and recalcitrance within a natural system and was calculated as the ratio of the integrated emission from 435–480 nm to the integrated emission from 300–345 nm at 255 nm. (Zsolnay et al.1999; Huguet et al. 2009). PARAFAC modeling of EEM fluorescence was done in Matlab using the DOMFluor toolbox (Stedmon and Bro, 2008). The number of components was determined by using split half validation and assessed with random initialization fits and residual analysis according to the approach described in Stedmon and Bro (2008).

3.2.5 Dissolved Organic Carbon (DOC) and Stable Carbon Isotopes ($\delta^{13}C$)

Dissolved organic carbon (DOC) and carbon stable isotope ($\delta^{13}C$) samples were filtered into pre-combusted (550 °C, 6 h minimum) 40 mL glass vials capped with Teflon-lined septa and acidified to pH 2 to 3 with reagent grade 85% H_3PO_4 (Fisher Scientific).

These samples were stored at 4 °C for in the dark prior to analysis. DOC concentration and $\delta^{13}C$ values were analyzed in continuous flow mode on a modified analytical system that coupled an OI-1010 TOC wet chemical oxidation carbon analyzer to a Thermo Delta PlusXP isotope ratio mass spectrometer (WCO- IRMS; Osburn and St-Jean, 2007).

DOC measurements were made on 2 mL samples after presparging with UHP He for 10 min to remove inorganic C prior to analysis. The CO_2 evolved after heated persulfate oxidation was then sparged from solution and swept past a nondispersive infrared detector (NDIR) to quantify DOC concentrations, and then swept in a stream of ultra high purity (UHP) helium to the IRMS for $\delta^{13}C$ measurements. Calibration of carbon concentrations was achieved with the response of potassium hydrogen phthalate (KHP) solutions of known concentration (0 – 25 mgC L^{-1}). Carbon stable isotope values of DOC are reported as $\delta^{13}C$ in per mil units (‰):

$$\delta^{13}C = \left[\frac{R_{Sample}}{R_{std}} - 1\right] * 1000$$

where R_{sample} is the ratio of $^{13}C/^{12}C$ for the sample, R_{std} is the ratio of $^{13}C/^{12}C$ in the CO_2 reference gas and carbon isotope values were normalized to the Vienna Pee Dee Belemnite international scale using solutions of oxalic acid (-18.3‰) and L-glutamic acid (-26.2‰).

3.2.6 Lignin Phenol Method

Lignin phenols were used as biomarkers for vascular plant contribution to DOM within the NRE. Roughly 500 to 1000 mL of 0.2 μm filtrates was acidified to pH 2 to 3 with reagent grade 85% H_3PO_4 (Fisher Scientific) and extracted onto C_{18} resin following Louchouarn et al. (2000). The extracts were eluted from columns in the laboratory using high

purity methanol into 40 mL combusted glass vials and evaporated to dryness in a Zymark Turbovap under a constant stream (10-12 psi) of compressed nitrogen (Airgas NP300). 150 mL Teflon reaction vessels containing samples were then hydrolyzed in 2 M NaOH via microwave-assisted CuO oxidation (Goni and Montgomery 2000; Osburn and Stedmon 2011). Trans-cinnamic acid was added as a recovery standard and lignin oxidation products were quantified on a five-point calibration of eight individual phenol standards (Hernes and Benner, 2002). Separation of lignin phenols was performed on a Varian 431-GC gas chromatograph and detection was performed using a Varian 220-MS ion-trap mass spectrometer. The mass spectrometer was operated in the electron ionization (EI) mode using ms-ms (tandem mass spectrometer).

Lignin was quantified as the sum of eight vanillyl (vanillin (VAL), acetovanillone (VON), vanillic acid (VAD)), syringyl (syringaldehyde (SAL), acetosyringone (SON), syringic acid (SAD)) and cinnamyl (p-coumaric acid (CAD), and ferulic acid (FAD)) phenols ($\Sigma 8$) and was normalized to DOC concentrations ($\Lambda 8$). The ratios of syringyl to vanillyl phenols (S:V) and cinnamyl to vanillyl phenols (C:V) were used to indicate vascular plant tissue type. The ratio of acid to aldehyde phenols in the vanillyl group $(Ad:Al)_V$ was used to indicate oxidative degradation.

3.2.7 Statistical Analysis

Monthly sample analyses, combining data from surface and bottom waters, were performed on samples from March 2010 to February 2011. All statistical tests were performed using Matlab v.R2009a software. Nonparametric tests were applied when assumptions of parametric tests could not be met with either non-transformed or transformed

data. A one-way analysis of variance (ANOVA) or a Kruskal-Wallis test was used to examine the individual effects of season and spatial location on physical and chemical variables at a 95% confidence interval (i.e., $P<0.05$) unless otherwise specified. Significant differences between seasons and spatial location were determined using either a Tukey or Dunn post-hoc test. Data were limited in March, June and July and therefore statistical analysis could not be made.

A parallel factor analysis (PARAFAC) model was built using the DOMFluor and N-way toolbox and 231samples (Stedmon and Bro, 2008). PARAFAC statistically decomposes multi-way data into a set of three linear terms and a residual array to produce robust, non-biased models. The number of components was determined by using split half validation and assessed with random initialization fits and residual analysis according to the approach described in Stedmon and Bro (2008). Five components, referred to as C1 through C5, were split-half validated from the data set under non-negativity constraints. A single EEM was identified as an outlier and removed.

3.3 Results

3.3.1 Physical Mixing Patterns

Regional climate trends for the area can be described as a wet period occurring in the late fall of 2009 and extending through April 2010 (Peierls et al. 2012). In addition, the remnants of Tropical Storm Nicole combined with a stationary low pressure system produced record rainfall over the region in late September/early October 2010 (National Climatic Data Center 2010). Daily discharge values at Fort Barnwell ranged from of 16.0 $m^3 s^{-1}$ to 218.6 $m^3 s^{-1}$ between March 2010 to February 2011 (Table 3.1). Furthermore, increases in discharge

within the NRE correspond to increases in precipitation. This result was similar to previous findings that illustrate how overland flow and discharge are responsive to precipitation events and influence the transport of dissolved materials via runoff into the NRE (Mallin et al. 1993; Paerl et al. 1998).

3.3.2 DOC Concentrations

Within the NRE, DOC concentrations ranged from 4.61 to 17.2 mg L^{-1} between stations NR0 to NR180. Overall, a poor negative relationship was observed between DOC concentrations and salinity ($P>0.05$, $R^2=0.11$). The data were further examined monthly in order to explore trends over shorter temporal scales (Table 3.2). Overall, significant correlations were seen in August, October, November and December 2010 ($P<0.05$) (Table 3.2). Upon excluding NR0 from the dataset the overall correlation between DOC concentration and salinity increased to an $R^2=0.41$ ($P<0.05$).

3.3.3 Spatial and Seasonal Carbon Stable Isotope and Lignin Phenol Concentrations in the NRE

The chemical markers, carbon stable isotope (δ^{13}C-DOM) and lignin values, were used to evaluate spatial and seasonal trends in DOM source within the NRE. A summary of these data can be found in Table 3.2. Our aim was to determine if δ^{13}C-DOM and lignin phenol concentrations (Σ_8 values) (1) varied seasonally and (2) changed between the head of the NR0 (head of the NRE) and NR180 (mouth of the NRE).

Spatial analysis of these two parameters on the other hand yielded different results. δ^{13}C-DOM values increased from station NR0 and NR180 ($P<0.05$) (Fig. 3.2A). In addition, δ^{13}C-DOM values in the NRE increased with salinity and ranged from -31 to -18‰ ($P<0.05$)

(Table 3.3, Fig. 3.2A). There was no significant difference between lignin phenol concentrations (Σ_8 values) at station NR0 and NR30, but Σ_8 values did decrease from the headwaters of the NRE to station NR180 ($P<0.05$) (Fig. 3.2B). When the entire dataset was analyzed, a negative linear relationship between Σ_8 values and salinity was observed, explaining roughly 50% of the variability in the data ($R^2=0.47$, $P<0.05$) (Fig. 3.2B). Furthermore, Σ_8 values and salinity were examined monthly within the NRE and resulted in improved correlations and unique trends (Table 3.4). Overall, the highest R^2 values observed within the NRE were observed in April ($R^2=0.96$), September ($R^2=0.73$) and October ($R^2=0.99$), each explained roughly 75 to 99% of the variation in the data ($P<0.05$, Table 3.2). Increases in Σ_8 values were closely associated with runoff events, which were most commonly observed as discharge increased within the NRE.

In addition to using the Σ_8 values, the carbon-normalized yields of dissolved lignin phenols (Λ_8) were used to estimate the relative contributions of vascular plant material to DOC. Significant spatial differences between in Λ_8 values were observed between stations NR0 to NR180. For example, there was no significant difference between Λ_8 values between station NR0 and NR30, but Λ_8 values did decrease from the headwaters of the NRE to NR180 ($P<0.05$) (Fig. 3.2C). Overall, lower yields indicate a smaller proportion of vascular plant material. Upon analyzing the entire dataset, Λ_8 values exhibited a negative relationship with salinity ($P<0.05$, $R^2=0.41$) and ranged from ranged from 0.12 to 0.84 mg 100 mg OC^{-1} (Table 3.3). Λ_8 values were examined monthly versus salinity and resulted in increased correlations during select sampling months. Specifically, the correlation between Λ_8 values

and salinity was highest in April (R^2=0.79), September (R^2=0.88) and October (R^2=0.92) (Table 3.2). The remaining significant monthly trends explained roughly ca. 50% of the variability between salinity and Λ_8 values.

3.3.4 Carbon Stable Isotope and C:N Values Within The NRE

For a subset of the data (N=44) representing the NRE at stations NR0, NR30, NR70 and NR120 δ^{13}C-DOM values were compared against C:N values, the molar ratio of DOC to DON, in order to further distinguish between allochthonous and autochthonous OM sources. Station NR180 was not included because DON values were not obtained at this location. Overall, C:N values ranged between 14.3 and 33.6, and reflected the primarily terrestrial nature of DOM in the NRE (Table 3.3). All samples clustered together inside the region typical of OM derived from C3 land plants (Fig. 3.3A). Upon examining the data by station and sample depth, variations in OM source emerged (Fig. 3.3B). Specifically, it appears that samples collected in surface and bottom waters at stations NR0, NR30 and NR70 all exhibit relatively consistent δ^{13}C-DOM values over a broad range of C:N values (Fig. 3.3). However, station NR120 exhibited the largest variation in δ^{13}C-DOM values (-31.4 to -19.8‰) over a similar range of C:N values compared to the other stations.

3.3.5 C:V and S:V Values in the NRE

Individual phenolic families can also yield pertinent information on terrestrial OM sources. Syringyl phenols, S, are unique indicators of angiosperm tissues, cinnamyl phenols, C, are unique indicators of nonwoody tissues, whereas vanillyl phenols, V, are present in all lignin. Therefore, plots of syringyl to vanillyl phenol ratios (S:V) and cinnamyl to vanillyl phenol ratios (C:V) can be used to distinguish between woody and non-woody angiosperm

and gymnosperms tissue in terrigenous OM (Hedges and Mann, 1979; Hernes and Benner, 2003; Bianchi et al. 2009). The majority of the NRE samples were fairly tightly clustered above the woody and nonwoody gymnosperm region of the plot (Fig. 3.4), indicating a rather uniform source. It is important to note that the a few samples from station NR120 and NR180 fall close to the non-woody angiosperm region of the plot (Fig. 3.4).

3.3.6 DOC and Lignin Fluxes through the NRE

We used DOC concentrations and Σ_8 values to compute seasonal DOM export out of the NRE based on seasonal discharge at Fort Barnwell, NC. Surface water flux out of the NRE at station NR0 ranged from 2.2 x 10^{12} to 5.5 x 10^{12} L $year^{-1}$. The values in Table 3.4 correspond to a maximum seasonal DOC fluxes into the NRE at station NR0 in the spring of 6.9 x 10^{13} g $year^{-1}$ and in the autumn of 3.1 x 10^{13} g $year^{-1}$. In addition, a seasonal maximum Σ_8 flux out of the NRE in the spring of 2.1 x10^8 g $year^{-1}$ and in the autumn of 1.23 x10^8 g $year^{-1}$ was also observed. Furthermore, the minimum seasonal DOC and Σ8 flux out of the NRE occurred in summer and winter, when seasonal discharge was the lowest reported (Table 3.4). The flux of terrigenous dissolved OM out of the NRE at station NR180 was also reported (Table 3.4). The trends observed at station NR180 are similar to those reported for station NR0. Specifically, maximum seasonal DOC fluxes out of the NRE at station NR180 in the spring were 5.2 x 10^{13} g $year^{-1}$ and in the autumn of 2.4 x 10^{13} g $year^{-1}$. While the seasonal maximum Σ_8 flux out of the NRE in the spring of 1.0 x10^8 g $year^{-1}$ and in the autumn of 2.4 x10^7 g $year^{-1}$. This comparison was made to evaluate the difference in terrestrial DOM entering the NRE from station NR0 versus terrestrial DOM entering the Pamlico Sound from station NR180.

3.3.5 Characterization of DOM fluorescence

DOM fluorescence was modeled by PARAFAC on a larger set of samples (N=231) collected from March 2010 to February 2011 over all ModMon sampling stations in the NRE (Dixon et al. accepted). Our PARAFAC model produced five spectral components (Table 3.5, Fig. 3.5). Three of the components (C1, C3 and C5) resembled terrestrial fluorescent material; specifically C1 was characterized as the ubiquitous terrestrial humic-like material, C3 resembled soil fulvic-like material and C5 represented terrestrial fulvic-like material. The remaining two components represented autochthonous-like fluorescent material. C2 resembled planktonic-like fluorescent material and component C4 resembled that of the protein-like fluorescent material, such as the amino acid tryptophan (Dixon et al. (accepted) and sources therein). In addition to their sources, fluorescent DOM exhibited varying degrees of degradation and lability. For example, C1, likely represents a fraction of degraded DOM comprised of humic acids. Furthermore, soil fulvic-like C3 and terrestrial fulvic-like C5 are indicative of less degraded OM (Senesi, 1990). Lastly, planktonic and protein-like components C2 and C4 are related to *in situ* production.

3.3.6 Relationship between CDOM and lignin

CDOM optical indices and lignin parameters were used to determine overall trends in terrestrial DOM distributions within the NRE. This comparison revealed several key findings between fluorescent DOM, CDOM, and lignin within the NRE (Table 3.6). First, there was an overall positive relationship between $a350$ and Σ_8 values, which resulted in an R^2=0.40 ($P<0.05$). Second, comparison of terrestrial fluorescent DOM components (C1, C3 and C5) and Σ_8 values all exhibited positive linear relationships ($P<0.05$). For instance, soil fulvic-like

C3 (R^2=0.45) and terrestrial fulvic-like C5 (R^2=0.49) described roughly 50% of the variation in the data (P<0.05) (Table 3.5). The R^2 value for Σ_8 and terrestrial humic-like C1 was much lower (R^2=0.24) and accounted for less than 30% of the variability in the data. Additionally, the FMax values of both planktonic-like C2 (R^2=0.40) and protein-like C4 (R^2=0.40) exhibited negative linear relationships with lignin concentrations (P<0.05).

Exploring the data on a monthly basis resulted in improved correlations and unique trends in select months (Table 3.6). For example, the correlation between fluorescent DOM and Σ_8 values exhibited significant trends in select months. Overall, Σ_8 values and terrestrial humic-like C1 exhibited significant positive correlations (P<0.05) that ranged from 0.48 to 0.65 in April, September and October (Table 3.6). Soil fulvic-like C3 and Σ_8 values correlations ranged from 0.56 to 0.93 and exhibited significant positive correlations (P<0.05) in April, September and February. Lastly in April, September and February terrestrial fulvic-like C5 was positively correlated with Σ_8 values, and explained roughly 57 to 95% of the data (P<0.05, Table 3.6). On the other hand, both planktonic- and protein-like fluorescent DOM were negatively correlated with Σ_8 values in April, September, October and February and correlations ranged between 0.67 to 0.98 (P<0.05, Table 3.6).

Lastly, Σ_8 values were examined with S_R and HIX values to determine lignin quality within the NRE. Overall Σ_8 values increased with decreasing S_R values (Fig. 3.6). The lowest S_R values of 0.7 corresponded to a higher Σ_8 value of 55.0 ug L^{-1} at station NR0. Additionally, the highest S_R values reported was 1.2 and corresponded to a Σ_8 value of 13.2 ug L^{-1} at station NR120. Σ_8 values increased with increasing HIX values within the NRE

(Fig. 3.6). The highest HIX value reported was 16.2, which corresponded to a Σ_8 value of 60.7 ug L^{-1} at station NR0, while the lowest HIX values observed was 5.8 and corresponded to a Σ_8 value of 12.2 ug L^{-1} at station NR120.

3.4 Discussion

3.4.1 Lignin Phenols in the NRE

Overall, lignin phenol concentrations significantly decreased from the head of the NR at station NR0 to the mouth of the NR at station NR180. A number of previous studies have also observed significant decreases along the river-estuarine continuum in various aquatic environments such as the Mississippi River, Yukon River, Sacramento River, Willow Slough and Big Pine Creek (Hernes and Benner, 2003; Dalzell et al. 2007; Spencer et al. 2008; Hernes et al. 2008). Decreases in the abundance of lignin in estuarine/coastal systems may involve losses from in situ microbial breakdown, flocculation, sorption/desorption processes with resuspended sediments, photochemical alterations and dilution by low lignin marine waters (Bauer and Bianchi, 2011).

A main objective of this study is to discuss the types of vascular plant material found in the NRE. To begin, the compositional trend in S:V and C:V values corresponds closely to woody gymnosperms and non-woody angiosperms material. These findings are sensible given that the vegetation in the Neuse's watershed consists of deciduous trees and grasses (grasslands and saltwater marshes) (Deamer 2009). Many other studies have used these ratios to provide useful qualitative information on the relative importance of angiosperm versus gymnosperm and woody versus non-woody sources within aquatic systems. For example, previous work by Hedges et al. (1984) observed S:V and C:V ratios in the following

tributaries of the Columbia River: Crab Creek, Willamette River and Methow River. Hedges et al. (1984) found that Crab Creek reflects a mixture of non-woody angiosperm material, which coincides with the dominance of grasses and herbaceous plants. In contrast, the S:V and C:V values of the Willamette and Methow Rivers drain primarily coniferous forests and reflect primarily woody gymnosperm material (Hedges et al. 1984). Mitra et al. (2000) found that S:V ratios in the Chesapeake Bay and Middle Atlantic Bight indicate DOM either originating from gymnosperm sources or that there is a significant amount of degradation occurring. Additionally, they suggest that lower S:V ratios and evenly distributed sources of angiosperms and gymnosperms throughout the watershed seem to indicate that lignin may be fairly degraded. Lastly, Hernes et al. (2008) results suggest that within the Willow Sough. S:V and C:V values indicated a fairly uniform non-woody angiosperm source. Their results were not unexpected, given that the entire watershed is dominated by non-woody angiosperm vegetation, whether natural or as crops.

3.4.2 $\delta^{13}C$ and C:N values in the NRE

The relationship between δ^{13}C-DOM and C:N values were used to assess the relative contributions of terrestrial and planktonic sources within the NRE. Marine DOM specifically derived from phytoplankton typically reflect $\delta^{13}C$ values that range from -20‰ to -22‰ (Bauer, 2002). On the other hand, terrestrial DOM derived from C3 plants typically have $\delta^{13}C$ values that range from -28‰ to -25‰ (Onstad et al. 2000; Bauer, 2002), whereas C4 plants (corn and grasses) have δ^{13}C-DOM values that range from -14‰ to -10‰ (Onstad et al. 2000). Within the NRE δ^{13}C-DOM values fell between -31.5‰ and -18.8‰ and increased from station NR0 to NR180. Additionally, this pattern of $\delta^{13}C$ values in estuarine waters,

reflecting terrestrial and marine source material, has been observed in a number of other studies. For example, Otero et al. (2003) and Hernes et al. (2008), illustrate that OM composition is continuously evolving during downstream transit through rivers and estuaries, where there is continuous integration of (1) soil OM from the surrounding landscape and (2) autochthonous OM from in situ production.

Although a shift in $\delta^{13}C$ values was observed in the NRE from NR0 to NR120, our C:N values reflect terrestrial DOM sources and further indicate that the majority of DOM above NR120 is composed of C3 land plants (Fig. 3.3). A possible mechanism for the shift in $\delta^{13}C$ within the lower regions of the NRE could be due to (1) bald cypress swamps and (2) saltwater wetlands that are dominated by C4 plants (*spartina alterniflora*) (Matson et al. 1983; Deamer 2009). For example, Smith and Epstein (1971) and Troughton et al. (1974**)** took direct measurements of cypress (*Cypressus* spp.) plants and found $\delta^{13}C$-DOM that ranged between -12.1‰ to -15.9‰. In addition, Benner et al. (1987) found that *spartina alterniflora* leaf material exhibited $\delta^{13}C$-DOM values that ranged from -12.6‰ to -13.1‰. Thus, the prevalence of these ecosystems could result in the $\delta^{13}C$ shift and the terrestrial signature of C:N values in NRE DOM.

3.4.3 Lignin and CDOM in the NRE

Lignin biomarkers are an invaluable tool for studying carbon cycling in both freshwater and marine environments due to the unambiguous information that they can provide about sources and diagenesis. However, making lignin measurements can often be time consuming and expensive, therefore making it hard to achieve the spatial and temporal resolution that is required to adequately characterize aquatic systems. One method of

extending lignin coverage is to develop optical proxies for lignin concentrations and compositions. For example, previous work by Hernes and Benner (2003), Hernes et al. (2008) and Fichot and Benner (2012) have observed a strong relationship between the absorption coefficient at 350 nm, *a*350, and lignin concentrations in the Mississippi River Plume, the Willow Slough and surface waters of the Mississippi and Atchafalaya Rivers. Furthermore, Hernes et al. (2009) also found strong and consistent trends between fluorescence and chemical functional groups. Specifically, they discuss how the fluorescence intensity at any given excitation-emission wavelength pairing depends on the concentration of fluorescing functional groups. Thus, concentrations of fluorescing compounds like lignin should be strongly related to fluorescence intensity.

Monthly correlations of Σ_8 values and fluorescent DOM and *a*350 values resulted in similar trends between the two CDOM pools. For example, *a*350, soil fulvic-like C3 and terrestrial fulvic-like C5 were highly correlated with Σ_8 values in April, September and October (Table 3.6). The April results coincide with increases in daily riverine discharge at Fort Barnwell. Daily discharge in September and October 2010 was not as high in comparison to daily spring discharge conditions. It is important to note that in September and October record rainfall over the region was reported and resulted in increases in the mean monthly discharge. Our daily discharge data likely missed this rainfall event. Therefore, increases in *a*350, soil fulvic-like C3 and terrestrial fulvic-like C5 in September and October are associated with increased discharge, even though it is not apparent in the daily discharge data. The remaining months exhibited correlations that were not significant ($P>0.05$). Overall, these results suggest that during times of prolonged reduced discharge lignin,

CDOM and fluorescent DOM are uncoupled in the NRE.

Additionally, Σ_8 values also were compared to S_R and HIX values in order to interpret lignin humification and molecular weight. For example, S_R values less than 1.0 have been reported for fresh and estuarine waters and are indicative of predominantly terrestrial OM that is of a high molecular weight (HMW) while S_R values greater than 1.0 have been reported for coastal and open ocean water and are indicative autochthonous OM of low molecular weight (LMW) (Helms et al. 2008). Overall, it appears that higher Σ_8 values correspond to lower S_R values (R^2=0.22, P<0.05). These findings suggest that higher concentrations of lignin are indicative of HMW vascular plant material. Furthermore, HIX is a fluorescence index used to determine the degree of DOM humification and recalcitrance within a natural system (Zsolnay et al.1999; Huguet et al. 2009). Highly humified OM is resistant to degradation and often persists in environments longer than OM with a lower degree of humification. Low HIX values (<5) represent fresh OM and high values of HIX (10–16) represent the presence of condensed humic OM usually of terrestrial origin. Within the NRE, increases in Σ_8 values correspond to increases in HIX values (R^2=0.41, P<0.05). These findings suggest that high concentrations of lignin within the NRE reflect a greater degree of humification.

3.4.4 Terrestrial DOM Flux Out of the NRE

Another main objective of this study was to examine the abundance of terrigenous material sourced from vascular plant derived material within the NRE. In addition, we wanted to address whether the distributional patterns reflect variations in hydrological

conditions at Fort Barnwell, NC. In order to evaluate this further, δ^{13}C-DOC and Σ_8 value were examined against monthly discharge in surface waters of NR0. First, δ^{13}C-DOC values decreased with increases in discharge at Fort Barnwell (Fig. 3.7A). These findings suggest that as discharge increases δ^{13}C-DOC appear more terrestrial and reflect C3 plant sources. Second, increases in discharge at Fort Barnwell, NC resulted in increased concentrations of lignin phenols at station NR0 ($P<0.05$) (Fig. 3.7B). Additionally, the greatest Σ_8 value was 62.5 $\mu g\ L^{-1}$ occurred as monthly discharge increased to 179 m^3s^{-1} in April 2010 and the lowest Σ_8 value observed was 16 $\mu g\ L^{-1}$ and it occurred in December 2010, when monthly discharge was 56.6 m^3s^{-1}.

3.4.5 DOC Mass Balance in the NRE

In order to evaluate the annual loading of DOC into the NRE, we examined the annual DOC contributions from four sources within the basin: the head of the NR (represented by station NR0), the Trent River (TR), submarine groundwater discharge (SGD) and rainwater. It is important to note that for the purposes of this study we have chosen to focus on the four contributors mentioned previously, but there are additional sources that may contribute to the annual DOC loading into the NRE, such as local creeks (i.e. Slocum Creek) and additional tributaries (i.e. South River).

To begin, NR0 was chosen as the main source of DOC for the NR component because it is the most riverine site in our study. Multiple samples were taken within the TR and the average DOC concentration was used as the main source of DOC for this component. Discharge was obtained at Fort Barnwell, NC. Discharge for the TR was collected at USGS station 02092500**.** SGD DOC concentrations have not been documented within the NRE, but

Moore et al. (2010) reported SGD DOC concentrations of 250 μM for Long Bay in eastern North Carolina. This value will be used to represent the NRE because the sampling locations are in the same region and are likely similar. In addition to this, Null et al. (2011) calculated the average SGD for three sites that covered the length the NRE. The average rainfall at four sampling locations (Kinston, New Bern, Cherry Point and Piney Island) within the NR basin was used because it accounts for the average amount of rain entering the basin down the length of the NR. Additionally, the mean concentration of DOC from Hurricane Irene rainwater at Greenville, North Carolina, was 2.3 mgC L^{-1} (Mitra et al. 2013). This value is slightly higher than typical rainwater DOC concentrations reported globally for coastal and marine systems (Willey et al. 2000). Additionally it is also higher than the volume-weighted annual average at the Wilmington, North Carolina rainwater collection site (116 μM) (Willey et al. 2000; Avery et al. 2003). The concentration of 2.3 mgC L^{-1} value will be used to represent the contribution of average rain DOC entering the NRE.

The average annual flow rate for the NR is 3.5 x 10^9 m^3 yr^{-1} and in addition to this the TR provides 1.8 x 10^8 m^3 yr^{-1}. Using the average DOC concentration for the NR (NR0: 9.2 mgC L^{-1}) and the average DOC concentration for the TR (12.2 mgC L^{-1}) combined with the annual flow rate above, we calculate a total carbon flux of 3.2 x 10^{13} mg C yr^{-1} for the NR and 2.2 x 10^{12} mg C yr^{-1} for the TR. The average concentration of DOC in rainwater of Hurricane Irene is 2.3 mg L^{-1}, combined with an average annual rainfall over the sampling year (March 2010 to February 2011) of .11 m, and the surface area of NRE, we calculate a total rainwater DOC flux of 1.2 x 10^{11} mgC yr^{-1}. Lastly, the average SGD of 3.7 x 10^4 m^3 yr^{-1}

combined with the SGD DOC concentration of Long Bay of 250 μM, results in a total SGD DOC flux of 1.1 x 10^8 mgC yr^{-1}.

Overall, both the NR and TR supply the highest amount of DOC entering the NRE basin, while SGD and rain supply smaller contributions. Specifically, in terms of the total DOC entering the basin the NR supplies 93.4%, the TR supplies 6.3%, and lastly rainwater supplies 0.3% and groundwater supplies 0%. Therefore the riverine supply of DOC by the NR is 15 times greater than the TR, which appears to be due to differences in discharge. Additionally, DOC sourced from the NR is 278 times greater than the rainwater supply.

Understanding the quantity and quality of DOC for both components is needed to obtain more precise information on DOC loading within the NRE from rainfall and SGD. Although the SGD and rainfall calculations are limited, they are informative and suggest that both components are likely negligible contributors to DOC flux in the NRE. Furthermore, our findings suggest that more work is needed to simultaneously quantify SGD and rainfall DOC concentrations, spatially and temporally, within the NRE. In conclusion, the NR dominates the flux of DOC to the NRE with the TR being a secondary contributor.

3.5 Conclusions

Overall, the findings of this study demonstrate that terrestrial DOM within the shallow, microtidal NRE is influenced by riverine discharge at Fort Barnwell. The major conclusions of this study are as follows:

1. Overall, lignin phenol concentrations decrease (by dilution or removal) from NR0 to NR180 and appear to be related to increases in discharge at Fort Barnwell.
2. Furthermore, the composition of lignin within the NRE, based on S:V and C:V

values, corresponds closely to woody gymnosperms and non-woody angiosperms material. These findings are reasonable given that the vegetation in the NRE watershed consists of deciduous trees and saltwater marshes.

3. Within the NRE δ^{13}C-DOM and C:N values in NRE DOM reflect terrestrial sources, which are depleted in nitrogen when compared to planktonic material. Therefore, in the NRE, δ^{13}C-DOM values are likely a reflection of the relative contributions of (1) C3 plants (specifically the introduction of cypress OM) and/or (2) C4 plants from saltwater marshes (specifically *spartina*).
4. It appears that trends between Σ_8 values and *a*350, soil fulvic-like C3 and terrestrial fulvic-like C5 were all highly correlated in April, September and October as discharge increased at Fort Barnwell, NC.
5. Higher Σ_8 values correspond to lower S_R values and high HIX values within the NRE. These findings suggest that high concentrations of lignin within the NRE reflect a high molecular weight material that is highly humified.
6. As discharge increases at NR0 δ^{13}C-DOC values appear more terrestrial and reflect C3 plant sources. Additionally, increases in discharge resulted in increased concentrations of lignin phenols at station NR0.

3.6 References

Avery Jr., G.B., Willey, J.D., Kieber, R.J., Shank, C.G., and Whitehead, R.F., 2003. Flux and bioavailability of Cape Fear River and rainwater dissolved organic carbon to Long Bay, southeastern United States. Global Biogeochemical Cycles, 17(2): 1042, doi:10.1029/ 2002GB001964, 2003

Bauer J.E. and Bianchi T.S., 2011. Dissolved Organic Carbon Cycling and Transformation. In: Wolanski E and McLusky DS (eds.) Treatise on Estuarine and Coastal Science, Vol 5, pp. 7–67. Waltham: Academic Press.

Benner, R., Fogel, M.L., Sprague, E.K., and Hodson, R.E., 1987. Depletion of ^{13}C in lignin and its implications for stable carbon isotope studies. Nature, 329(6141): 708-710.

Benner, R., Opsahl, S., 2001. Molecular indicators of the sources and transformations of dissolved organic matter in the Mississippi river plume. Organic Geochemistry 32 (4), 597–611.

Bianchi, T.S., DiMarco, S.F., Smith, R.W., and Schreiner, K.M., 2009. A gradient of dissolved organic carbon and lignin from Terrebonne-Timbalier Bay estuary to the Louisiana shelf (USA). Marine Chemistry, 117: 32-41.

Bricuad, A., Morel, A., and Prieur, L., 1981. Absorption by dissolved organic matter of the sea (yellow substance) in the UV and visible domains. Limnology and Oceanography, 26: 43-53.

Burkholder, J.M. et al., 2006. Comprehensive trend analysis of nutrients and related variables in a large eutrophic estuary: A decadal study of anthropogenic and climatic influences. Limnology and Oceanography, 51(1): 463-487.

Christian, R.R., Boyer, J.N. and Stanley, D.W., 1991. Multiyear distribution patterns of nutrients within the Neuse River Estuary, North Carolina. Marine Ecology Progress Series, 71(3): 259-274.

Coble, P.G., 1996. Characterization of marine and terrestrial DOM in seawater using excitation emission matrix spectroscopy. Marine Chemistry, 51(4): 325-346.

Corbett, D.R., 2010. Resuspension and estuarine nutrient cycling: insights from the Neuse River Estuary. Biogeosciences, 7(10): 3289-3300.

Crosswell, J. R., M. S. Wetz, B. Hales, and Paerl., H. W., 2012. Air-water CO2 fluxes in the microtidal Neuse River Estuary, North Carolina, Journal Geophysical Research, 117, C08017, doi:10.1029/2012JC007925.

Dalzell B. J., Filley T. R. and Harbor J. M., 200,) The role of hydrology in annual organic carbon loads and terrestrial organic matter export from a midwestern agricultural watershed. Geochim. Cosmochim. Acta,71, 1448–1462.

Deamer, N. 2009. Neuse River Basinwide Water Quality Plan. North Carolina Department of Environment and Natural Resources - Division of Water Quality.

Elam, C.E., Stucky, J.M., Wentworth, T.R., and Gregory, J.D., 2009. Vascular Flora, Plant Communities, and Soils of Significant Natural Area in the Middle Atlantic Coastal Plant (Craven County, North Carolina). Southern Appalachian Botanical Society, 74(1): 53-77.

Fichot, C.G., and Benner, R., 2012. The spectral slope coefficient of chromophoric dissolved organic matter ($S_{275-295}$) as a tracer of terrigenous dissolved organic carbon in river-influenced ocean margins. Limnology and Oceanography, 57(5): 1453-1466.

Frost, C.C., 1993. Four centuries of changing landscape patterns in the longleaf pine ecosystem. North Carolina Plant Conservation Program, Plant Industry Division, NC Department of Agriculture, Raleigh, NC.

Goni, M.A., Montgomery, S., 2000. Alkaline CuO oxidation with a microwave digestion system: lignin analyses of geochemical samples. Analytical Chemistry 72 (14), 3116–3121.

Harvey, H.R., Mannino, A., 2001. The chemical composition and cycling of particulate and macromolecular dissolved organic matter in temperate estuaries as revealed by molecular organic tracers. Organic Geochemistry 32 (4), 527–542.

Hedges, J.I., Mann, D.C., 1979. Characterization of plant-tissues by their lignin oxidation-products. Geochimica Et Cosmochimica Acta 43 (11), 1803–1807.

Hedges, J.I., Clark, W.A., Cowie, G.L., 1988. Fluxes and reactivities of organic matter in a coastal marine bay. Limnology and Oceanography 33, 1137–1152.

Helms, J.R., Stubbins, A., Ritchie, J.D., Minor, E.C., Kieber, D.J., and Mopper, K. 2008. Absorption spectral slopes and slope ratios as indicators of molecular weight, source, and photobleaching of chromophoric dissolved organic matter. Limnology and Oceanography, 53(3): 955-969.

Hernes, P.J., Benner, R., 2002. Transport and diagenesis of dissolved and particulate terrigenous organic matter in the North Pacific Ocean. Deep-Sea Research Part I—Oceanographic Research Papers 49 (12), 2119–2132.

Hernes, P.J., Benner, R., 2003. Photochemical and microbial degradation of dissolved lignin phenols: implications for the fate of terrigenous dissolved organic matter in marine environments. Journal of Geophysical Research—Oceans 108 (C9).

Hernes, P.J., Spencer, R.G.M., Dyda, R.Y., Pellerin, B.A., Bachand, P.A.M., and Bergamaschi, B.A., 2008. The role of hydrologic regimes on dissolved organic carbon composition in an agricultural watershed. Geochimica et Cosmochimica Acta, 72: 5266-5277.

Huguet, A., Vacher, L., Relexans, S., Saubusse, S., Froidefond, J.M., and Parlanti, E. 2009. Properties of fluorescent dissolved organic matter in the Gironde Estuary. Organic Geochemistry, 40(6): 706-719.

Kirk, J. T. O., 1994. Light and Photosynthesis in Aquatic Ecosystem. Cambridge University Press.

Lawaetz, A.J. and Stedmon, C.A., 2009. Fluorescence Intensity Calibration Using the Raman Scatter Peak of Water. Applied Spectroscopy, 63(8): 936-940.

Louchouarn, P., Opsahl, S., Benner, R., 2000. Isolation and quantification of dissolved lignin from natural waters using solid-phase extraction and GC/MS. Analytical Chemistry 72 (13), 2780–2787.

Luettich, R. A. J., S. D. Carr, J. V. Reynolds-Fleming, C. W. Fulcher, and J. E. Mcninch. 2002. Semi-diurnal seiching in a shallow, micro-tidal lagoonal estuary. Continental Shelf Research, 22: 1669–1681.

Mallin, M.A., Paerl, H.W., Rudek, J. and Bates, P.W., 1993. Regulation of estuarine primary production by watershed rainfall and river flow. Marine Ecology-Progress Series, 93(1-2): 199-203.

Mari, X., Rochelle-Newall, E., Torréton, J.P., Pringault, O., Jouon, A., and Migon, C., 2007. Water residence time: A regulatory factor of the DOM to POM transfer efficiency. Limnology and Oceanography, 52(2): 808-819.

Matson, E.A., and Brinson, M.M., 1990. Stable carbon isotopes and the C:N ratio in the estuaries of the Pamlico and Neuse Rivers, North Carolina. Limnology and Oceanography, 35(6): 1290-1300.

Meyers. P.A., 1994. Preservation of elemental and isotopic source identification of sedimentary organic matter. Chemical Geology, 114: 289-302.

Mitra, S., Bianchi, T.S., Guo, L., and Santschi, P.H., 2000. Terrestrially derived dissolved organic matter in the Chesapeake Bay and the Middle Atlantic Bight. Geochimica et Cosmochimica Acta, 63(20): 3547-3557.

Moore, W.S., 2010. The Effect of Submarine Groundwater Discharge on the Ocean. Annual Review of Marine Science, 2:59:88.

Murphy, K.R., Stedmon, C.A., Graeber, D., and Bro, R., 2013, Fluorescence spectroscopy and multi-way techniques. PARAFAC. Analytical Methods, 5, 6557-6566.

Null, K.A., Corbett, D.R., DeMaster, D.J., Burkholder, J.M., Thomas, C.J., and Reed, R.E. 2011. Porewater advection of ammonium into the Neuse River Estuary, North Carolina, USA. Estuarine, Coastal and Shelf Science, 95: 314-325.

Ohno, T., and Bro, R. 2006. Dissolved organic matter characterization using multiway spectral decomposition of fluorescence landscapes. Soil Sci. Soc. Am. J., 70 (6), 2028−2037.

Osburn, C.L. and St-Jean, G., 2007. The use of wet chemical oxidation with high amplification isotope ratio mass spectrometry (WCO-IRMS) to measure stable isotope values of dissolved organic carbon in seawater. Limnology and Oceanography Methods, 5:296.308.

Osburn, C.L. and Stedmon, C.A., 2011. Linking the chemical and optical properties of dissolved organic matter in the Baltic-North Sea transition zone to differentiate three allochthonous inputs. Marine Chemistry, 126(1): 281-294.

Paerl, H.W., Pinckney, J.L., Fear, J.M. and Peierls, B.L., 1998. Ecosystem responses to internal and watershed organic matter loading: consequences for hypoxia in the eutrophying Neuse river estuary, North Carolina, USA. Marine Ecology-Progress Series, 166: 17-25.

Paerl, H.W., Rossignol, K.L., Hall, N.S., Peierls, B.L., and Wetz, M.S., 2010. Phytoplankton Community Indicators of Short- and Long- term Ecological Change in the Anthropogenically and Climatically Impacted Neuse River Estuary, North Carolina, USA, 33: 485-497.

Peierls, B.L., Hall, N.S., and Paerl, H.W., 2012. Non-monotonic Responses of Phytoplankton Biomass Accumulation to Hydrologic Variability: A Comparison of Two Coastal Plain North Carolina Estuaries, 35: 1376-1392.

Premuzic, E.T., Benkovitz, C.M., Gaffney, J.S., and Walsh, J.J., 1982. The nature and distribution of organic matter in the surface sediments of world oceans and seas. Org. Geochem., 4:63-77.

Reed, R.E., Glasgow, H.B., Burkholder, J.M. and Brownie, C., 2004. Seasonal physical-chemical structure and acoustic Doppler current profiler flow patterns over multiple years in a shallow, stratified estuary, with implications for lateral variability. Estuarine Coastal and Shelf Science, 60(4): 549-566.

Senesi, N., 1990. Molecular and quantitative aspects of the chemistry of fulvic acid and its interaction with metal ions and organic compounds. Part II. The fluorescence approach. Analytica Chimica Acta, 232: 77-106.

Smith, B.N., and Epstein, S., 1971. Two categories of $^{13}C/^{12}C$ ratios for higher plants. Plant Physiology, 47: 380-384.

Spencer, R.G.M., Aiken, G.R., Butler, K.D., Dornblaser, M.M., Striegl, R.G., and Hernes, P.J., 2008. Utilizing chromophoric dissolved organic matter measurements to derive export and reactivity of dissolved organic carbon exported to the Arctic Ocean: A case study of the Yukon River, Alaska. Geophysical Research Letters, 36.

Spencer, R.G.M., Hernes, P.J., Ruf, R., Baker, A., Dyda, R.Y., Stubbins, A., and Six, J., 2010. Temporal controls on dissolved organic matter and lignin biogeochemistry in a pristine tropical river, Democratic Republic of Congo. Journal of Geophysical Research-Biogeosciences, 115.

Stedmon, C.A. and Markager, S., 2003. Behaviour of the optical properties of coloured dissolved organic matter under conservative mixing. Estuarine Coastal and Shelf Science, 57(5-6): 973-979.

Stedmon, C.A., Markager, S. and Bro, R., 2003. Tracing dissolved organic matter in aquatic environments using a new approach to fluorescence spectroscopy. Marine Chemistry, 82(3-4): 239-254.

Stedmon, C. A., and Bro, R., 2008. Characterizing dissolved organic matter fluorescence with parallel factor analysis: a tutorial. Limnology and Oceanography Methods, 6: 572−579.

Steel, J. 1991. Albemarle-Pamlico estuarine system: technical analysis of status and trends. Albemarle-Pamlico Estuarine Study Report No. 91-01. N.C. Department of Environment, Health, and Natural Resources, Albemarle-Pamlico Estuarine Study, Raleigh, NC.

Troughton, J.H., Card, K.A., and Hendy, C.H., 1974. Photosynthetic pathways and carbon isotope discrimination by plants. Carnegie Inst Yearbook, 73: 768-779.

Vähätalo. A.V., Wetzel, R.G., and Paerl, H.W., 2005. Light absorption by phytoplankton and chromophoric dissolved organic matter in the drainage basin and estuary of the Neuse River, North Carolina (U.S.A). Freshwater Biology, 50, 477-493.

Walker, S.A., Amon, R.M.W., Stedmon, C., Duan, S., and Louchouarn, P., 2009. The use of PARAFAC modeling to trace terrestrial dissolved organic matter and fingerprint water masses in coastal Canadian Arctic surface waters. Journal of Geophysical Research, 114: G00F06.

Willey, J. D., R. J. Kieber, M. S. Eyman, and G. B. Avery Jr., 2000. Rainwater dissolved organic carbon: Concentrations and global flux, Global Biogeochemical Cycles, 14: 139–148.

Zsolnay, A., Baigar, E., Jimenez, M., Steinweg, B. and Saccomandi, F., 1999. Differentiating with fluorescence spectroscopy the sources of dissolved organic matter in soils subjected to drying. Chemosphere, 38(1): 45-50.

3.7 Tables and Figures

Table 3.1- Daily discharge measured at Fort Barnwell, NC (USGS site #02091814), which is 24 km upstream of station NR0. Discharge data was divided by the ratio of gauged to total watershed area (0.69 for the NRE) as a correction for un-gauged watershed discharge (Peierls et al. 2012).

Date	$m^3 s^{-1}$
3/1/10	218.6
4/12/10	119.8
5/27/10	103.9
6/21/10	33.1
8/17/10	16.0
9/14/10	13.4
10/18/10	45.3
11/9/10	42.8
12/16/10	40.2
1/19/11	44.5
2/7/11	94.6

Table 3.2: Monthly R^2 values of Σ_8 (ng L^{-1}), Λ_8 (mg 100 mg OC^{-1}) and DOC (mg L^{-1}) against salinity within the NRE ($P<0.05$, n.a.- not applicable/data unavailable, n.s.- not significant).

Month	Year	Σ_8	Λ_8	DOC
March	2010	n.a.	n.a.	n.a.
April	2010	0.96	0.79	n.s.
May	2010	0.47	0.48	n.s.
June	2010	n.a.	n.a.	n.a.
July	2010	n.a.	n.a.	n.a.
August	2010	0.49	0.58	0.54
September	2010	0.73	0.88	n.s.
October	2010	0.99	0.92	0.71
November	2010	n.s.	n.s.	0.86
December	2010	n.s.	n.s.	n.s.
January	2011	n.s.	0.51	0.60
February	2011	0.63	n.s.	n.s.

Table 3.3: Minimum, maximum and average values of lignin phenols (ng L^{-1}), Σ_8 (ng L^{-1}) carbon-normalized lignin phenol yields (Λ_8) (mg 100 mg OC^{-1}), $S^{13}C$ values (‰), DOC concentration (mg L^{-1}), C:N values and PARAFAC fluorescent component Fmax values.

	Minimum	**Maximum**	**Average**
Salinity	0.05	20.12	6.81
Von	0.51	8.50	3.09
Val	1.00	14.61	5.33
Vad	0.76	15.85	6.04
Son	0.58	7.20	2.62
Sal	0.50	14.37	4.06
Sad	0.35	8.11	3.51
Fad	0.83	6.65	2.68
Cad	0.45	3.82	1.56
Σ_8	5.33	63.96	28.88
V	2.40	37.35	14.46
S	1.44	25.92	10.19
C	1.49	10.47	4.24
C:V	0.11	0.97	0.37
S:V	0.38	1.09	0.71
Ad:Al($_V$)	0.18	2.83	1.37
Λ_8	0.12	0.84	0.34
DOC	4.61	17.20	8.48
δ^{13}C-DOM	-31.45	-18.81	-25.00
C:N	14.43	33.69	21.94
C1	26.90	34.90	32.03
C2	14.90	25.80	19.18
C3	2.70	8.50	4.70
C4	1.80	9.90	4.22
C5	0.00	9.90	2.57

Table 3.4: The seasonal flux of terrigenous dissolved OM out of the NRE at NR0 and NR180 as expressed by Σ_8 and DOC fluxes was based on discharge at Fort Barnwell, NC.

		Ave. Discharge	**Σ_8** ng L-1	**DOC** mg L-1	**Σ_8** (g yr^{-1})	**DOC** (g yr^{-1})
NR0	**Spring**	$5.5x10^{12}$	38.3	12.6	$2.1\ x10^{8}$	$6.9\ x10^{13}$
	Summer	$2.2\ x10^{12}$	25.6	6.2	$1.4\ x10^{8}$	$1.4\ x10^{13}$
	Autumn	$3.5\ x10^{12}$	36.4	8.9	$2.0\ x10^{8}$	$3.1\ x10^{13}$
	Winter	$2.3\ x10^{12}$	21.0	8.1	$1.1\ x10^{8}$	$1.2\ x10^{13}$
NR180	**Spring**	$5.5\ x10^{12}$	18.4	9.5	$1.0\ x10^{8}$	$5.2\ x10^{13}$
	Summer	$2.2\ x10^{12}$	5.3	5.7	$1.3\ x10^{7}$	$1.3\ x10^{13}$
	Autumn	$3.5\ x10^{12}$	14.8	6.9	$2.4\ x10^{7}$	$2.4\ x10^{13}$
	Winter	$2.3\ x10^{12}$	8.4	7.7	$1.8\ x10^{7}$	$1.8\ x10^{13}$

Table 3.5- Composition of excitation/emission peak maxima in DOM fluorescence of NRE along with peak maxima and PARAFAC model components. OpenFluor identified similar spectra as having Tucker congruence (θ) exceeding 0.95 on the excitation and emission simultaneously.

Component	Ex. λ (nm)	Em. λ (nm)	%Fmax Range	OpenFluor Correlation (P<0.05)	Source	Potential Source
C1	<240	440	44.5-57.7	4	Terrestrial; Humic acid	Ubiquitous terrestrial humic acid-like
C2	<240	386	24.7-42.7	6	Planktonic	Microbial humic-like, M-Peak, Wastewater/nutrient enrichment tracer
C3	270	508 (312)	4.5-14.1	8	Soil fulvic-like	Terrestrial soil fulvic-like, reduced semi-quinone-like
C4	240	336 (492)	3.0-16.4	1	Protein-like	Protein-like; ubiquitous tryptophan; recent biological production, T-Peak
C5	335	438	0.0-16.4	0	Soil leachate Fulvic-like	Terrestrial fulvic acid-like, constituents of tannins (gallic acid)

*Secondary peaks are noted in parenthesis

Table 3.6- Correlation coefficients of PARAFAC component fluorescent intensities (FMax values) and absorption coefficients versus lignin phenol concentrations (Σ_8) (ng L^{-1}), (n.s. – not significant).

	C1	C2	C3	C4	C5	a350
March	n.s.	n.s.	n.s.	n.s.	n.s.	n.s.
April	0.48	0.93	0.93	0.98	0.95	0.89
May	n.s.	n.s.	n.s.	n.s.	n.s.	n.s.
June	n.s.	n.s.	n.s.	n.s.	n.s.	n.s.
July	n.s.	n.s.	n.s.	n.s.	n.s.	n.s.
August	n.s	n.s.	n.s.	n.s.	n.s.	n.s.
September	0.51	0.85	0.67	0.67	0.73	0.80
October	0.65	0.73	n.s.	0.68	n.s.	0.40
November	n.s.	n.s.	n.s.	n.s.	n.s.	n.s.
December	n.s.	0.62	n.s.	0.62	n.s.	n.s.
January	n.s.	n.s.	n.s.	n.s.	n.s.	n.s.
February	n.s.	0.68	0.56	0.48	0.57	n.s.

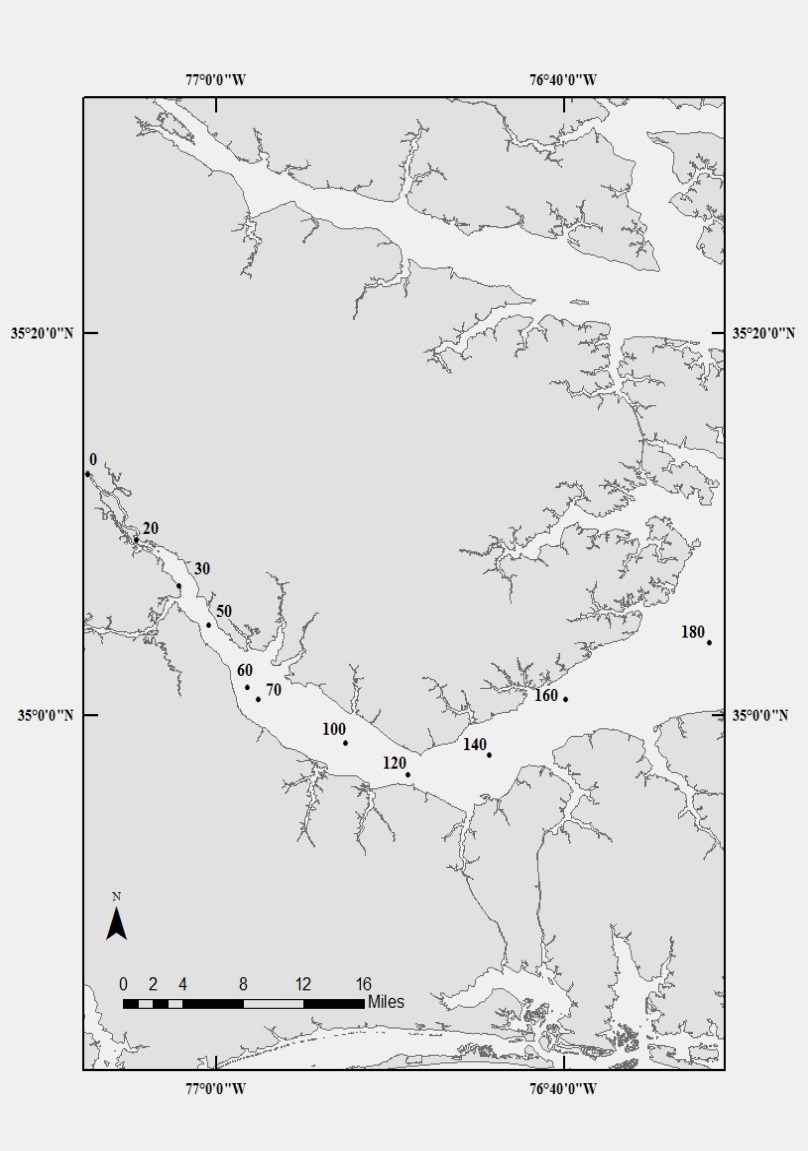

Figure 3.1: Map of Neuse River Estuary including ModMon sampling sites (courtesy of Lauren Handsell).

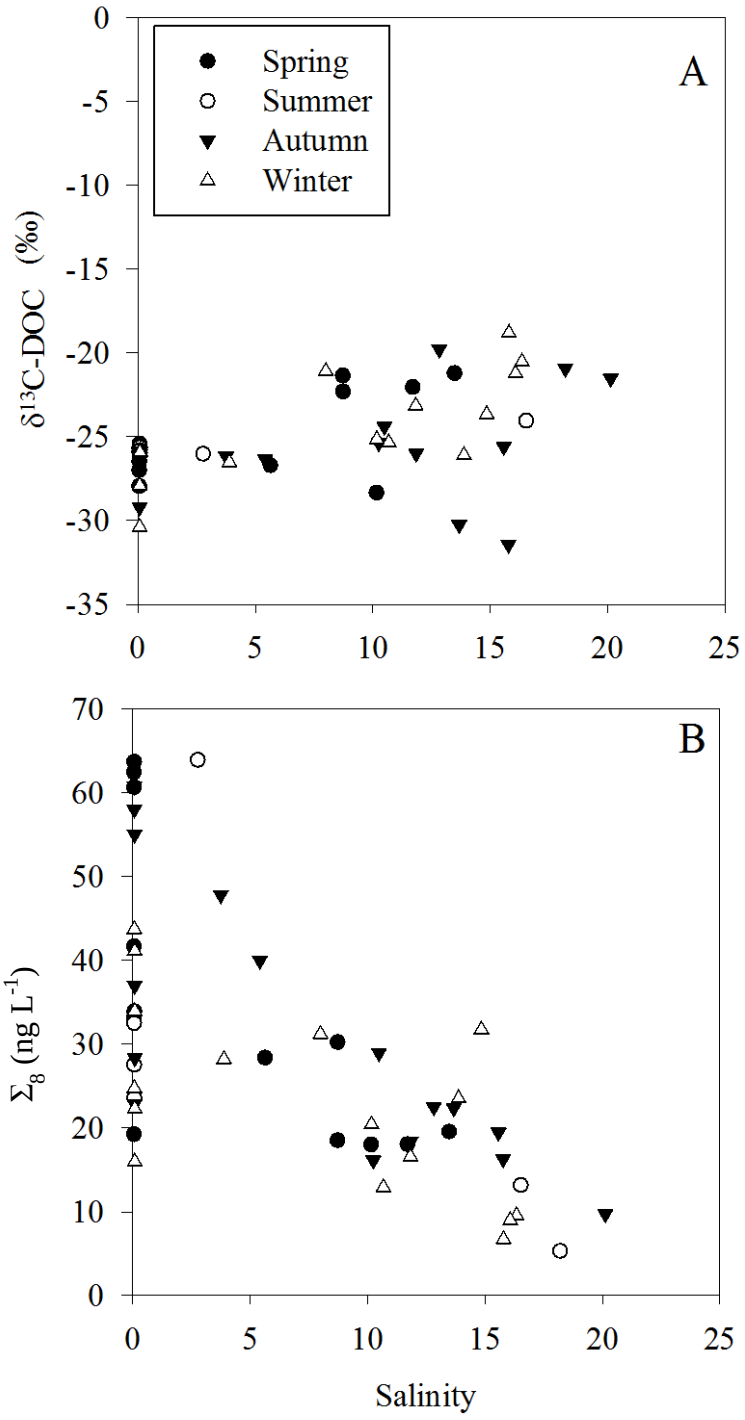

Figure 3.2: Seasonal (A) $S^{13}C$ values and (B) Σ_8 values (ng L^{-1}) versus salinity within the NRE.

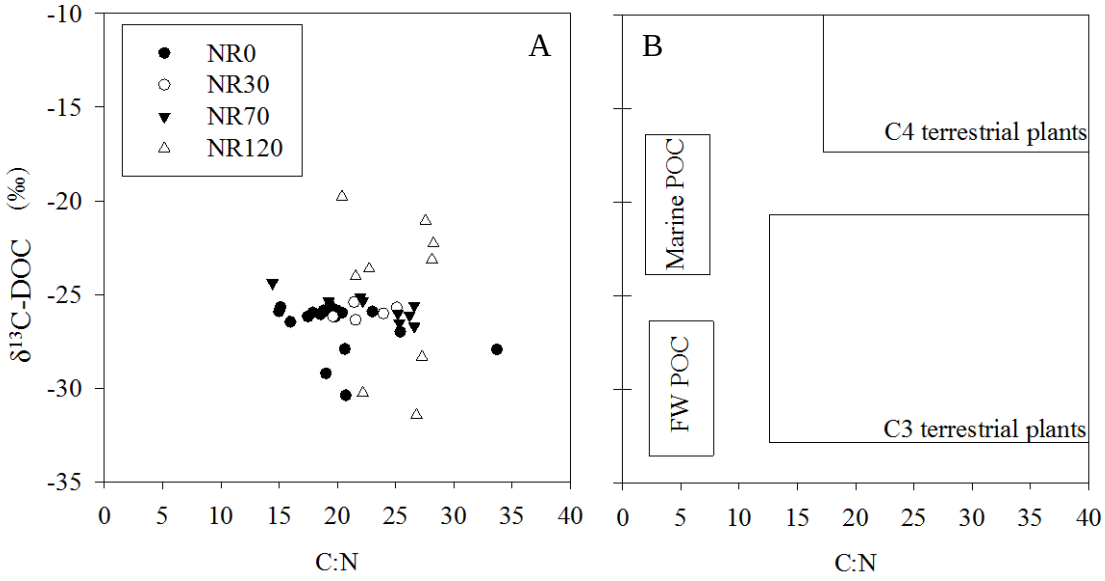

Figure 3.3: Station specific (A) $\delta^{13}C$ values versus C:N within the NRE and (B) distinct source combination regions of atomic C:N ratios and organic $\delta^{13}C$ values (Meyers, 1994).

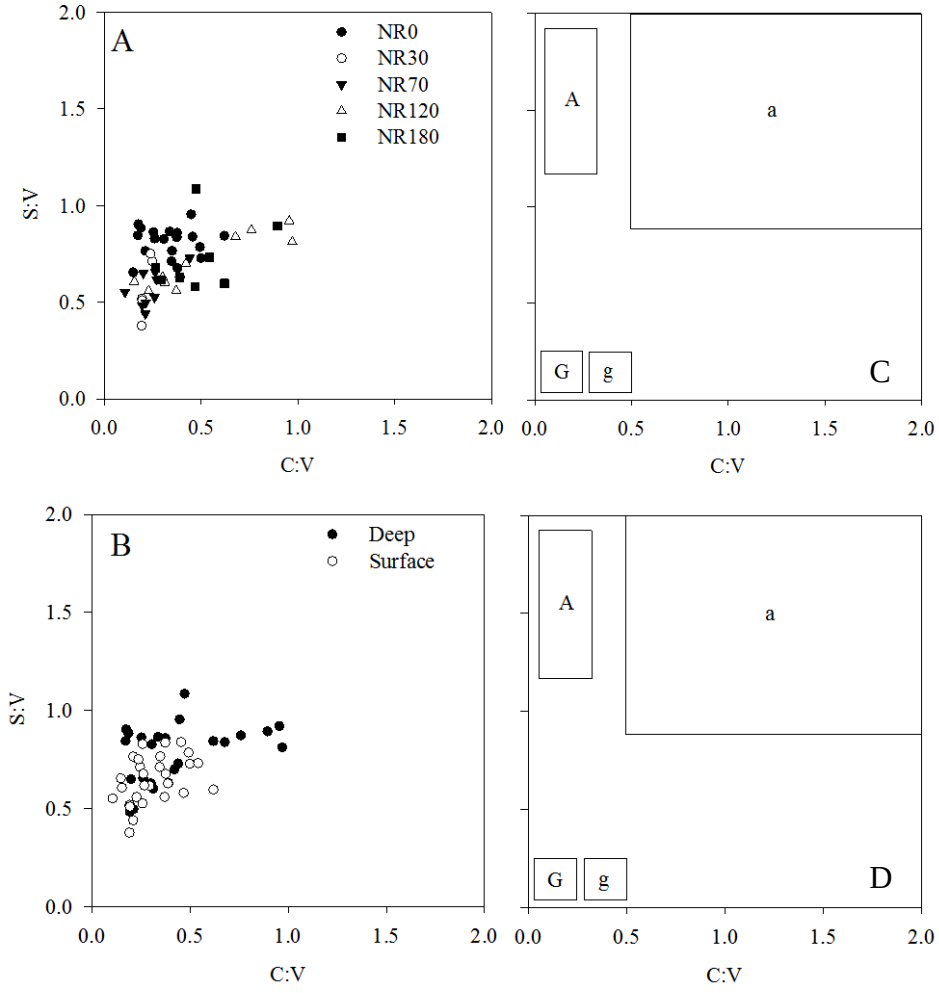

Figure 3.4: S:V and C:V comparison in the NRE at each sampling station (A) and in bottom and (B) surface waters. S:V and C:V ratios in panel C and D have been modified from Bianchi et al. 2009.

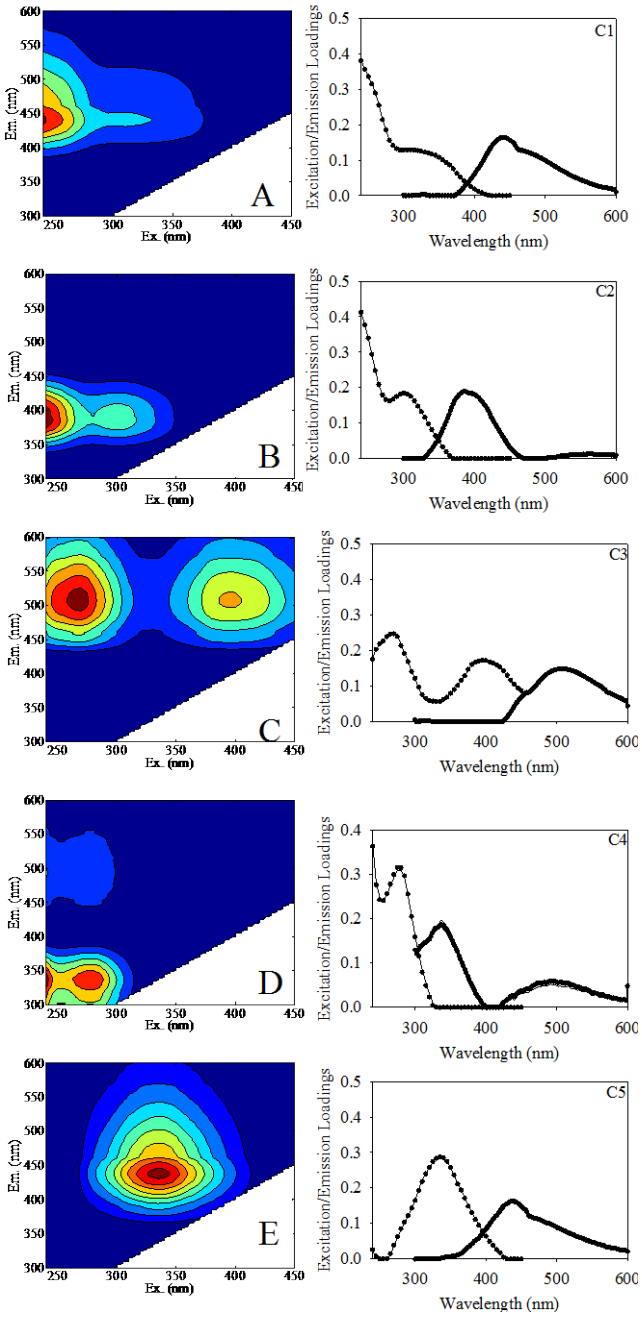

Figure 3.5: Five split half validated fluorescent components calculated from a PARAFAC model fit to DOM EEMs from the NRE between March 2010 and February 2011. The individual excitation and emission loadings are shown (solid line) for comparison to previous studies and the split-half validation results also are indicated (dotted line).

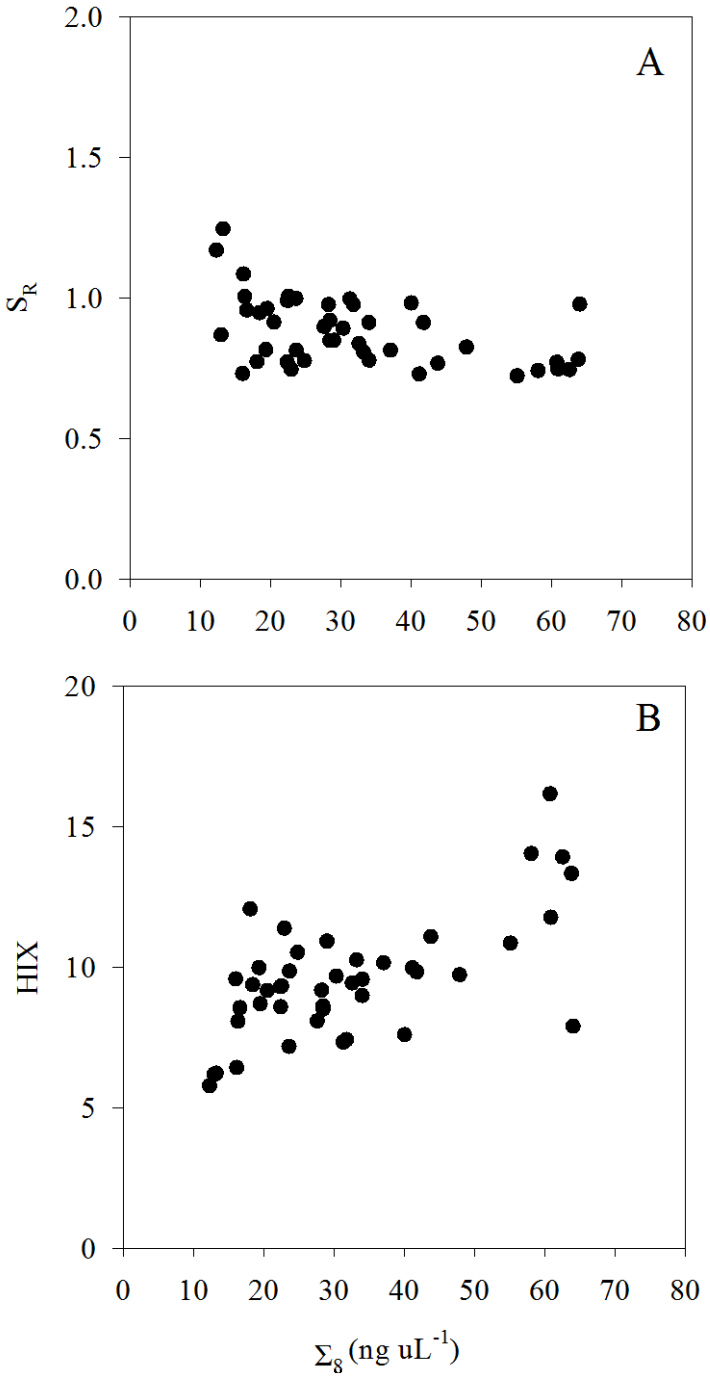

Figure 3.6: Σ_8 concentrations versus (A) S_R values and (B) HIX values.

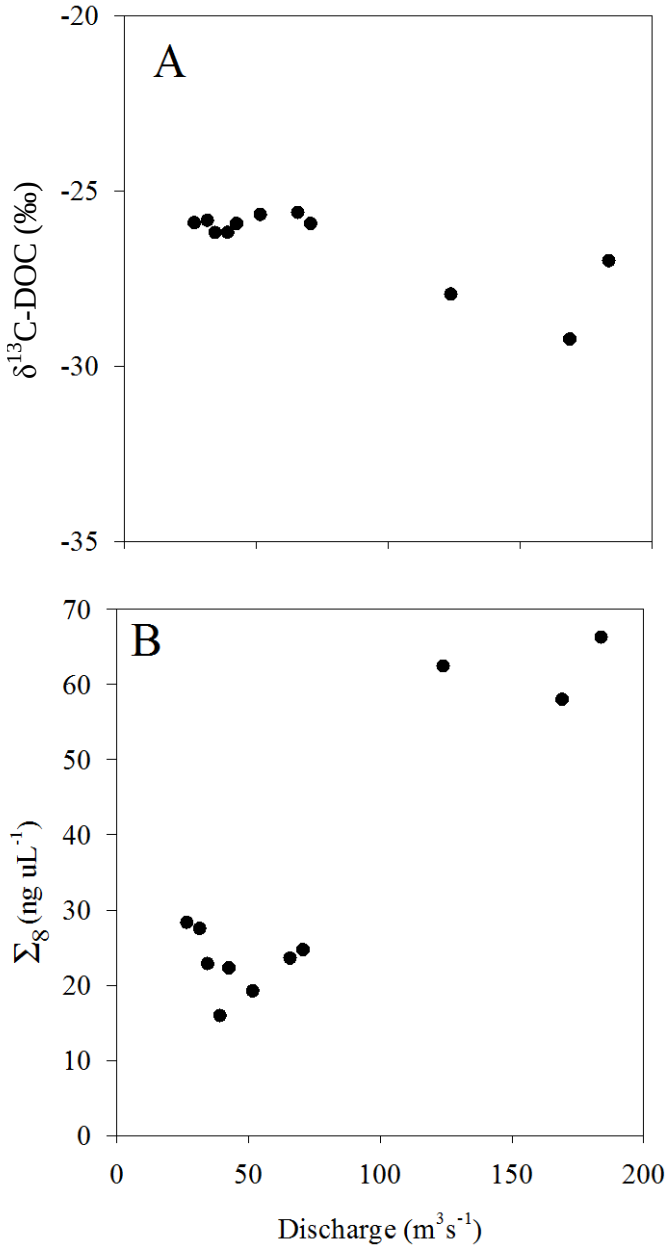

Figure 3.7: (A) δ^{13}C-DOC values and (B) Σ_8 values (ng L^{-1}) in surface waters at station NR0 versus mean monthly discharge at Fort Barnwell, NC.

Conclusions

The results of this study examined the spatial and temporal variability of dissolved organic matter (DOM) and chromorphoric dissolved organic matter (CDOM) sources and transformations within the Neuse River estuary (NRE) in eastern North Carolina between March 2010 and February 2011. During this time, monthly samples were collected in surface and bottom waters along the longitudinal axis of the NRE, ranging from freshwater to mesohaline segments.

To begin, in chapter one, we found that DOM and CDOM quality in the NRE is controlled by a combination of discharge, wind speed, and wind direction. DOM quality within the NRE was assessed with the following water quality parameters; C:N ratios, specific ultraviolet absorption at 254 nm ($SUVA_{254}$), absorption spectral slope ratio (S_R), and the humification (HIX) and biological (BIX) indices from fluorescence. Overall, the NRE reflects allochthonous sources when discharge and flushing are elevated at which times $SUVA_{254}$ and HIX increased relative to base flow. During periods of reduced discharge and long flushing times in the estuary, extensive autochthonous production modifies the quality of the DOM pool in the NRE. This was evidenced by falling C:N values, and higher BIX and S_R values. Lastly, by examining the data on a monthly scale we determined that a combination of increased wind speed and shifts in wind direction resulted in benthic resuspension events of heavily reworked, algal derived OM. Thus, the mean DOM characteristics in this shallow micro-tidal estuary can be rapidly altered during episodic mixing events on timescales of a few weeks.

In chapter two, DOM fluorescence was combined with our DOM quality data in order to further characterize how the quality and source of CDOM within the NRE. To begin, our PARAFAC-DOM model produced five spectral components of allochthonous and autochthonous OM origin. Specifically, component C1 was identified as a ubiquitous terrestrial humic-like component, component C2 was related to planktonic-like material, component C3 was related to soil fulvic-like material, component C4 was identified as ubiquitous protein-like material and lastly component C5 was identified as terrestrial fulvic-like material. In addition to these findings our PCA results distinguished varying degrees of OM degradation. For example, terrestrial humic-like C1 represented degraded DOM, while components C2-C5 were indicative of less degraded DOM. More specifically, our PCA results revealed the presence of multiple pools of allochthonous and autochthonous DOM. For instance, two distinct pools of terrestrial DOM appear to exist within the NRE. One pool consists of degraded terrestrial humic-like material (C1) and the other consists of fresh terrestrial fulvic-like material (C3 and C5). Additionally, the autochthonous DOM pool consists of both planktonic-like material and protein-like material that can be characterized as fresh OM.

Furthermore, the spatial trends in fluorescent DOM from station NR0 to NR180 exhibited an apparent shift in DOM quality from allochthonous-like material at the head of the Neuse to autochthonous-like material at the river mouth. We observed the following component specific trends progressing from NR0 to NR180: (1) a degraded terrestrial humic-like DOM (C1) was a constant background signal within the NRE, (2) fresh terrestrial and soil fulvic-like DOM abundance (C3 and C5) decreases from NR0 to NR180 and (3) fresh

planktonic- and protein-like DOM abundance (C2 and C4) increases from NR0 to NR180**.** Overall, the NRE reflects allochthonous sources when discharge is elevated relative to base flow. During periods of reduced discharge, extensive autochthonous production modifies the quality of the DOM pool in the NRE. This was evidenced by the increased fluorescence contribution of planktonic-like C2 and protein-like C4 in the summer.

Lastly, in chapter three, the relationships between CDOM, dissolved organic carbon (DOC), lignin and carbon stable isotope values ($\delta^{13}C$) of DOM were used to evaluate DOM sources. The composition of lignin within the NRE, based on S:V and C:V values, corresponds closely to woody gymnosperm material and non-woody gymnosperm material. Furthermore, $\delta^{13}C$ and C:N values within the NRE reflect the primarily terrestrial signature of DOM. The discrepancy between our geochemical and fluorescence results may be due to the pool of organic carbon that was analyzed in this study. Specifically, particulate organic carbon may be more indicative of autochthonous sources (i.e. chla) in the NRE based on Osburn et al. 2012. Therefore the lack of an autochthonous signature in the geochemical data is likely due to the fact that we focused solely on the dissolved fraction of the organic matter pool.

The major conclusions of this study demonstrate that DOM within the shallow, microtidal NRE is impacted by both allochthonous and autochthonous sources. This was apparent based on the allochthonous signal of the NRE as discharge increased. In addition to this, as discharge was reduced within the NRE the system reflected autochthonous-like material. Overall, the quality and reactivity of DOM will play a key role in NRE water quality. For example, DOM that is bioavailable or autochthonous-like is likely to be

remineralized as CO_2, while DOM that is recalcitrant or allochthonous-like will likely pass through the system unused. The hydrodynamics of the NRE will play a key role in this, for example, (1) increases in discharge will essentially transport DOM out of the estuary unaltered while (2) decreases in discharge will allow degradation processes and *in-situ* production to occur. Understanding DOM quality and varying flow regimes in shallow estuaries will be critical to understanding the impacts and fate of DOM and nutrient inputs within these systems. Future work within the NRE should examine (1) the impact of land-use change within the basin (agricultural vs. natural landscapes), (2) variability at the riverine end-member (station NR0) and how the quantity and quality of DOM at this station impacts down estuary trends and (3) the quantity and quality of DOM within the Pamlico Sound.